NUREG-1824
Draft for Comment

EPRI 1011999
Preliminary Report

Verification and Validation of Selected Fire Models for Nuclear Power Plant Applications

Volume 2:
Fire Dynamics Tools (FDT^{S})

January 2006

U.S. Nuclear Regulatory Commission
Office of Nuclear Regulatory Research
Washington, DC 20555-0001

Electric Power Research Institute
3412 Hillview Avenue
Palo Alto, CA 94303

Verification & Validation of Selected Fire Models for Nuclear Power Plant Applications

Volume 2: Fire Dynamics Tools (FDTs)

NUREG-1824 **EPRI 1011999**

January 2005

U.S. Nuclear Regulatory Commission
Office of Nuclear Regulatory Research (RES)
Division of Risk Analysis and Applications
Two White Flint North, 11545 Rockville Pike
Rockville, MD 20852-2738

U.S. NRC-RES Project Manager
M. H. Salley

Electric Power Research Institute (EPRI)
3412 Hillview Avenue
Palo Alto, CA 94303

EPRI Project Manager
R. P. Kassawara

DISCLAIMER OF WARRANTIES AND LIMITATION OF LIABILITIES

ORGANIZATION(S) THAT PREPARED THIS DOCUMENT:

U.S. Nuclear Regulatory Commission, Office of Nuclear Regulatory Research

Science Applications International Corporation

National Institute of Standards and Technology

ORDERING INFORMATION

Requests for copies of this report should be directed to EPRI Orders and Conferences, 1355 Willow Way, Suite 278, Concord, CA 94520, (800) 313-3774, press 2 or internally x5379, (925) 609-9169, (925) 609-1310 (fax).

COMMENTS ON DRAFT NUREG-1824 REPORT

This report is being published jointly by the U.S. Nuclear Regulatory Commission (NRC) and the Electric Power Research Institute (EPRI). Any interested party may submit comments on this report for consideration by the NRC and EPRI staffs. Comments may be accompanied by additional relevant information or supporting data. Please specify both the report number (Draft NUREG-1824) and the volume number in your comments, and send them by March 31, 2006, to the following address:

Chief Rules Review and Directives Branch
U.S. Nuclear Regulatory Commission
Mail Stop T-6D59
Washington, DC 20555-0001

For any questions about the material in this report, please contact:

Mark Henry Salley
Mail Stop T-10E50
U.S. Nuclear Regulatory Commission
Washington, DC 20555-0001
Phone: (301) 415-2840
Email: MXS3@nrc.gov

If EPRI members also wish to provide comments to EPRI, they may send them to the following address:

R.P. Kassawara
Electric Power Research Institute
3412 Hillview Avenue
Palo Alto, CA 94304
Phone: (650) 855-2775
Email: RKASSAWA@epri.com

CITATIONS

This report was prepared by

U.S. Nuclear Regulatory Commission,
Office of Nuclear Regulatory Research (RES)
Two White Flint North, 11545 Rockville Pike
Rockville, MD 20852-2738

Principal Investigators:
K. Hill
J. Dreisbach

Electric Power Research Institute (EPRI)
3412 Hillview Avenue
Palo Alto, CA 94303

Science Applications International Corp (SAIC)
4920 El Camino Real
Los Altos, CA 94022

Principal Investigators:
F. Joglar
B. Najafi

National Institute of Standards and Technology
Building Fire Research Laboratory (BFRL)
100 Bureau Drive, Stop 8600
Gaithersburg, MD 20899-8600

Principal Investigators:
K McGrattan
R. Peacock
A. Hamins

Volume 1, Main Report: B. Najafi, M.H. Salley, F. Joglar, J. Dreisbach
Volume 2, FDT^S: K. Hill, J. Dreisbach
Volume 3, FIVE-REV. 1: F. Joglar
Volume 4, CFAST: R. Peacock, J. Dreisbach, P. Reneke (NIST)
Volume 5, MAGIC: F. Joglar, B. Guatier (EdF), L. Gay (EdF), J. Texeraud (EdF)
Volume 6, FDS: K. McGrattan, J. Dreisbach
Volume 7, Experimental Uncertainty: A. Hamins, K. McGrattan

This report describes research sponsored jointly by U.S. Nuclear Regulatory Commission, Office of Nuclear Regulatory Research (RES) and Electric Power Research Institute (EPRI).

The report is a corporate document that should be cited in the literature in the following manner:

Verification and Validation of Selected Fire Models for Nuclear Power Plant Applications, Volume 2: Fire Dynamics Tools (FDT^S), U.S. Nuclear Regulatory Commission, Office of Nuclear Regulatory Research (RES), Rockville, MD: 2005 and Electric Power Research Institute (EPRI), Palo Alto, CA. NUREG-1824 and EPRI 1011999.

ABSTRACT

There is a movement to introduce risk- and performance-based analyses into fire protection engineering practice, both domestically and worldwide. This movement exists in the general fire protection community, as well as the nuclear power plant (NPP) fire protection community.

In 2002, the National Fire Protection Association (NFPA) developed NFPA 805, *Performance-Based Standard for Fire Protection for Light-Water Reactor Electric Generating Plants, 2001 Edition.* In July 2004, the U.S. Nuclear Regulatory Commission (NRC) amended its fire protection requirements in Title 10, Section 50.48, of the *Code of Federal Regulations* (10 CFR 50.48) to permit existing reactor licensees to voluntarily adopt fire protection requirements contained in NFPA 805 as an alternative to the existing deterministic fire protection requirements. In addition, the nuclear fire protection community wants to use risk-informed, performance-based (RI/PB) approaches and insights to support fire protection decision-making in general.

One key tool needed to support RI/PB fire protection is the availability of verified and validated fire models that can reliably predict the consequences of fires. Section 2.4.1.2 of NFPA 805 requires that only fire models acceptable to the Authority Having Jurisdiction (AHJ) shall be used in fire modeling calculations. Further, Sections 2.4.1.2.2 and 2.4.1.2.3 of NFPA 805 state that fire models shall only be applied within the limitations of the given model, and shall be verified and validated.

This report is the first effort to document the verification and validation (V&V) of five fire models that are commonly used in NPP applications. The project was performed in accordance with the guidelines that the American Society for Testing and Materials (ASTM) set forth in *Standard E1355-04, "Evaluating the Predictive Capability of Deterministic Fire Models."* The results of this V&V are reported in the form of ranges of accuracies for the fire model predictions.

CONTENTS

FIGURES

TABLES

REPORT SUMMARY

This report documents the verification and validation (V&V) of five selected fire models commonly used in support of risk-informed and performance-based (RI/PB) fire protection at nuclear power plants (NPPs).

Background

Over the past decade, there has been a considerable movement in the nuclear power industry to transition from prescriptive rules and practices towards the use of risk information to supplement decision-making. In the area of fire protection, this movement is evidenced by numerous initiatives by the U.S. Nuclear Regulatory Commission (NRC) and the nuclear community worldwide. In 2001, the National Fire Protection Association (NFPA) completed the development of NFPA Standard 805, "Performance-Based Standard for Fire Protection for Light Water Reactor Electric Generating Plants 2001 Edition." Effective July, 16, 2004, the NRC amended its fire protection requirements in 10 CFR 50.48(c) to permit existing reactor licensees to voluntarily adopt fire protection requirements contained in NFPA 805 as an alternative to the existing deterministic fire protection requirements. RI/PB fire protection relies on fire modeling for determining the consequence of fires. NFPA 805 requires that the "fire models shall be verified and validated," and "only fire models that are acceptable to the Authority Having Jurisdiction (AHJ) shall be used in fire modeling calculations."

Objectives

The objective of this project is to examine the predictive capabilities of selected fire models. These models may be used to demonstrate compliance with the requirements of 10 CFR 50.48(c) and the referenced NFPA 805, or support other performance-based evaluations in NPP fire protection applications. In addition to NFPA 805 requiring that only verified and validated fire models acceptable to the AHJ be used, the standard also requires that fire models only be applied within their limitations. The V&V of specific models is important in establishing acceptable uses and limitations of fire models. Specific objectives of this project are:

- Perform V&V study of selected fire models using a consistent methodology (ASTM E1355) and issue a report to be prepared by U.S. Nuclear Regulatory Commission Office of Nuclear Regulatory Research (RES) and Electric Power Research Institute (EPRI).
- Investigate the specific fire modeling issues of interest to the NPP fire protection applications.
- Quantify fire model predictive capabilities to the extent that can be supported by comparison with selected and available experimental data.

The following fire models were selected for this evaluation: (i) NRC's NUREG-1805 Fire Dynamics Tools (FDT^s), (ii) EPRI's Fire-Induced Vulnerability Evaluation Revision 1 (FIVE-Rev. 1), (iii) National Institute of Standards and Technology's (NIST) Consolidated Model of Fire Growth and Smoke Transport (CFAST), (iv) Electricite de France's (EdF) MAGIC, and (v) NIST's Fire Dynamics Simulator (FDS).

Approach

This program is based on the guidelines of the ASTM E1355, "Evaluating the Predictive Capability of Deterministic Fire Models," for verification and validation of the selected fire models. The guide provides four areas of evaluation:

- Defining the model and scenarios for which the evaluation is to be conducted,
- Assessing the appropriateness of the theoretical basis and assumptions used in the model,
- Assessing the mathematical and numerical robustness of the model, and
- Validating a model by quantifying the accuracy of the model results in predicting the course of events for specific fire scenarios.

Traditionally, a V&V study reports the comparison of model results with experimental data, and therefore, the V&V of the fire model is for the specific fire scenarios of the test series. While V&V studies for the selected fire models exist, it is necessary to ensure that technical issues specific to the use of these fire models in NPP applications are investigated. The approach below was followed to fulfill this objective.

1. A set of fire scenarios were developed. These fire scenarios establish the "ranges of conditions" for which fire models will be applied in NPPs.
2. The next step summarizes the same attributes or "range of conditions" of the "fire scenarios" in test series available for fire model benchmarking and validation exercises.
3. Once the above two pieces of information were available, the validation test series, or tests within a series, that represent the "range of conditions" was mapped for the fire scenarios developed in Step 1. The range of uncertainties in the output variable of interest as predicted by the model for a specific "range of conditions" or "fire scenario" are calculated and reported.

The scope of this V&V study is limited to the capabilities of the selected fire models. There are potential fire scenarios in NPP fire modeling applications that do not fall within the capabilities of these fire models and therefore are not covered by this V&V study.

Results

The results of this study are presented in the form of relative differences between fire model predictions and experimental data for fire modeling attributes important to NPP fire modeling applications, e.g., plume temperature. The relative differences sometimes show agreement, but may also show both under-prediction and over-prediction. These relative differences are affected by the capabilities of the models, the availability of accurate applicable experimental data, and the experimental uncertainty of this data. The relative differences were used, in combination with some engineering judgment as to the appropriateness of the model and the

agreement between model and experiment, to produce a graded characterization of the fire model's capability to predict attributes important to NPP fire modeling applications.

This report does not provide relative differences for all known fire scenarios in NPP applications. This incompleteness is due to a combination of model capability and lack of relevant experimental data. The first can be addressed by improving the fire models while the second needs more applicable fire experiments.

EPRI Perspective

The use of fire models to support fire protection decision-making requires that their limitations and confidence in their predictive capability is well understood. While this report makes considerable progress towards that goal, it also points to ranges of accuracies in the predictive capability of these fire models that could limit their use in fire modeling applications. Use of these fire models present challenges that should be addressed if the fire protection community is to realize the full benefit of fire modeling and performance-based fire protection. This requires both short term and long term solutions. In the short term a methodology will be to educate the users on how the results of this work may affect known applications of fire modeling. This may be accomplished through pilot application of the findings of this report and documentation of the insights as they may influence decision-making. Note that the intent is not to describe how a decision is to be made, but rather to offer insights as to where and how these results may, or may not be used as the technical basis for a decision. In the long term, additional work on improving the models and performing additional experiments should be considered.

Keywords

Fire	Fire Modeling	Verification and Validation (V&V)
Performance-based	Risk-informed regulation	Fire Hazard Analysis (FHA)
Fire safety	Fire protection	Nuclear Power Plant
Fire Probabilistic Risk Assessment (PRA)		Fire Probabilistic Safety Assessment (PSA)

PREFACE

This report is presented in seven volumes. Volume 1, the Main Report, provides general background information, programmatic and technical overviews, and project insights and conclusions. Volumes 2 through 6 provide detailed discussions of the verification and validation (V&V) of the following five fire models:

Volume 2 Fire Dynamics Tools (FDT^S)

Volume 3 Fire-Induced Vulnerability Evaluation, Revision 1 (FIVE-Rev1)

Volume 4 Consolidated Model of Fire Growth and Smoke Transport (CFAST)

Volume 5 MAGIC

Volume 6 Fire Dynamics Simulator (FDS)

Finally, Volume 7 quantifies the uncertainty of the experiments used in the V&V study of these five fire models.

FOREWORD

Fire modeling and fire dynamics calculations are used in a number of fire hazards analysis (FHA) studies and documents, including fire risk analysis (FRA) calculations; compliance with, and exemptions to the regulatory requirements for fire protection in 10 CFR Part 50; "Specific Exemptions"; the Significance Determination Process (SDP) used in the inspection program conducted by the U.S. Nuclear Regulatory Commission (NRC); and, most recently, the risk-informed performance-based (RI/PB) voluntary fire protection licensing basis established under 10 CFR 50.48(c). The RI/PB method is based on the National Fire Protection Association (NFPA) Standard 805, "Performance-Based Standard for Fire Protection for Light-Water Reactor Generating Plants."

The seven volumes of this NUREG-series report provide technical documentation concerning the predictive capabilities of a specific set of fire dynamics calculation tools and fire models for the analysis of fire hazards in nuclear power plant (NPP) scenarios. Under a joint memorandum of understanding (MOU), the NRC Office of Nuclear Regulatory Research (RES) and the Electric Power Research Institute (EPRI) agreed to develop this technical document for NPP application of these fire modeling tools. The objectives of this agreement include creating a library of typical NPP fire scenarios and providing information on the ability of specific fire models to predict the consequences of those typical NPP fire scenarios. To meet these objectives, RES and EPRI initiated this collaborative project to provide an evaluation, in the form of verification and validation (V&V), for a set of five commonly available fire modeling tools.

The road map for this project was derived from NFPA 805 and the American Society for Testing and Materials (ASTM) Standard E1355-04, "Evaluating the Predictive Capability of Deterministic Fire Models." These industry standards form the methodology and process used to perform this study. Technical review of fire models is also necessary to ensure that those using the models can accurately assess the adequacy of the scientific and technical bases for the models, select models that are appropriate for a desired use, and understand the levels of confidence that can be attributed to the results predicted by the models. This work was performed using state-of-the-art fire dynamics calculation methods/models and the most applicable fire test data. Future improvements in the fire dynamics calculation methods/models and additional fire test data may impact the results presented in the seven volumes of this report.

This document does not constitute regulatory requirements, and RES participation in this study neither constitutes nor implies regulatory approval of applications based on the analysis contained in this text. The analyses documented in this report represent the combined efforts of individuals from RES and EPRI, both of which provided specialists in the use of fire models and other FHA tools. The results from this combined effort do not constitute either a regulatory position or regulatory guidance. Rather, these results are intended to provide technical analysis, and they may also help to identify areas where further research and analysis are needed.

Carl J. Paperiello, Director
Office of Nuclear Regulatory Research
U.S. Nuclear Regulatory Commission

ACKNOWLEDGMENTS

The work documented in this report benefited from contributions and considerable technical support from several organizations.

The verification and validation (V&V) studies for FDT^S (Volume 2), CFAST (Volume 4), and FDS (Volume 6) were conducted in collaboration with the U.S. Department of Commerce, National Institute of Standards and Technology (NIST), Building and Fire Research Laboratory (BFRL). Since the inception of this project in 1999, the NRC has collaborated with NIST through an interagency memorandum of understanding (MOU) and conducted research to provide the necessary technical data and tools to support the use of fire models in nuclear power plant fire hazard analysis (FHA).

We appreciate the efforts of Doug Carpenter and Rob Schmidt of Combustion Science Engineers, Inc. for their comments and contribution to Volume 2.

In addition, we acknowledge and appreciate the extensive contributions of Electricité de France (EdF) in preparing Volume 5 for MAGIC.

We also appreciate the efforts of organizations participating in the International Collaborative Fire Model Project (ICFMP) to Evaluate Fire Models for Nuclear Power Plant Applications, which provided experimental data, problem specifications, and insights and peer comment for the international fire model benchmarking and validation exercises, and jointly prepared the panel reports used and referred to in this study. We specifically appreciate the efforts of the Building Research Establishment (BRE) and the Nuclear Installations Inspectorate in the United Kingdom, which provided leadership for ICFMP Benchmark Exercise (BE) #2, as well as Gesellschaft fuer Anlagen-und Reaktorsicherheit (GRS) and Institut fuer Baustoffe, Massivbau und Brandschutz (iBMB) in Germany, which provided leadership and valuable experimental data for ICFMP BE #4 and BE #5. In particular, ICFMP BE #2 was led by Stewart Miles at BRE; ICFMP BE #4 was led by Walter Klein-Hessling and Marina Rowekamp at GRS, and R. Dobbernack and Olaf Riese at iBMB; and ICFMP BE #5 was led by Olaf Riese and D. Hosser at iBMB, and Marina Rowekamp at GRS. We acknowledge and sincerely appreciate all of their efforts.

We greatly appreciate Paula Garrity, Technical Editor for the Office of Nuclear Regulatory Research, and Linda Stevenson, agency Publication Specialist, for providing editorial and publishing support for this report. We also greatly appreciate Dariusz Szwarc, Nuclear Safety Professional Development Program participant, for his assistance finalizing this report.

LIST OF ACRONYMS

AGA	American Gas Association
AHJ	Authority Having Jurisdiction
ASME	American Society of Mechanical Engineers
ASTM	American Society for Testing and Materials
BE	Benchmark Exercise
BFRL	Building and Fire Research Laboratory
BRE	Building Research Establishment
CFAST	Consolidated Fire Growth and Smoke Transport Model
CFR	*Code of Federal Regulations*
EdF	Electricité de France
EPRI	Electric Power Research Institute
FDS	Fire Dynamics Simulator
FDT^S	Fire Dynamics Tools (NUREG-1805)
FHA	Fire Hazard Analysis
FIVE-Rev1	Fire-Induced Vulnerability Evaluation, Revision 1
FM-SNL	Factory Mutual & Sandia National Laboratories
FPA	Foote, Pagni, and Alvares
FRA	Fire Risk Analysis
GRS	Gesellschaft fuer Anlagen-und Reaktorsicherheit (Germany)
HRR	Heat Release Rate
IAFSS	International Association of Fire Safety Science
iBMB	Institut für Baustoffe, Massivbau und Brandschutz
ICFMP	International Collaborative Fire Model Project
IEEE	Institute of Electrical and Electronics Engineers
MCC	Motor Control Center
MQH	McCaffrey, Quintiere, and Harkleroad

MOU	Memorandum of Understanding
NBS	National Bureau of Standards (now NIST)
NFPA	National Fire Protection Association
NIST	National Institute of Standards and Technology
NPP	Nuclear Power Plant
NRC	U.S. Nuclear Regulatory Commission
NRR	Office of Nuclear Reactor Regulation (NRC)
RES	Office of Nuclear Regulatory Research (NRC)
RI/PB	Risk-Informed, Performance-Based
SDP	Significance Determination Process
SFPE	Society of Fire Protection Engineers
V&V	Verification & Validation

1
INTRODUCTION

As the use of fire modeling tools increases in support of day-to-day nuclear power plant (NPP) applications including fire risk studies, the importance of verification and validation (V&V) studies for these tools also increases. V&V studies afford fire modeling analysts confidence in applying analytical tools by quantifying and discussing the performance of the given model in predicting the fire conditions measured in a particular experiment. The underlying assumptions, capabilities, and limitations of the model are discussed and evaluated as part of the V&V study.

This volume documents the V&V study of the library of quantitative fire hazards analysis (FHA) models known as Fire Dynamics Tools (FDT^S). Quantitative FHA tools can be useful in predicting the risks of fire hazards in various settings within an NPP. Consequently, a number of quantitative FHA tools (including the FDT^S library) have been developed — with varying capabilities and levels of complexity — to serve this purpose.

The U.S. Nuclear Regulatory Commission (NRC), Office of Nuclear Reactor Regulation (NRR), Division of Systems Safety and Analysis (DSSA), Plant Systems Branch (SPLB), Fire Protection Engineering and Special Projects Section developed the FDT^S [Ref. 1] library using state-of-the-art principles of fire dynamics to assist fire protection inspectors in performing risk-informed evaluations of credible fires that may cause critical damage to essential safe-shutdown equipment. Toward that end, the FDT^S library comprises a series of Microsoft® Excel® spreadsheets, which are pre-programmed with fire dynamics equations and correlations to assist inspectors in performing quick, first-order calculations for potential fire scenarios. The technical bases for the models included in the FDT^S library were primarily derived from the *Society of Fire Protection Engineers (SFPE) Handbook of Fire Protection Engineering*, the *National Fire Protection Association (NFPA) Fire Protection Handbook*, and other fire science literature. This report describes the equations included in the spreadsheets that have been subjected to V&V, the technical bases of those equations, and evaluation of the sensitivities and predictive capabilities of the component spreadsheets.

The V&V methodology employed in this report generally follows the guidelines outlined in ASTM E1355, "Standard Guide for Evaluating the Predictive Capability of Deterministic Fire Models" [Ref. 2]. These guidelines were put into effect by the American Society for Testing and Materials (ASTM). As such, this report presents the fire model evaluation methodology in terms of the following basic focuses of evaluation:
Define the model and scenarios for which the evaluation is to be conducted.

- Assess the appropriateness of the theoretical basis and assumptions used in the model.
- Assess the mathematical and numerical robustness of the model.
- Quantify the uncertainty and accuracy of the model results in predicting the course of events in similar fire scenarios.

In accordance with ASTM E1355, it is critical to evaluate fire models to establish their acceptable uses and limitations. Evaluation is also necessary to ensure that those using the models can assess the adequacy of their scientific and technical bases, select appropriate models for a desired use, and understand the levels of confidence that can be placed on the results predicted by the models. Adequate evaluation will also help to prevent unintended misuse of fire models.

Evaluation of a fire model includes model verification and validation, which are commonly defined as follows:

- Verification: The process of determining that the implementation of a calculation method accurately represents the developer's conceptual description of the calculation method and its solution. The fundamental strategy of verifying computational models involves identifying and quantifying error in the computational model and its solution.
- Validation: The process of determining the degree to which a calculation method accurately represents the real world from the perspective of its intended uses. The fundamental strategy of validating computational models involves identifying and quantifying error and uncertainty in the conceptual and computational models with respect to their intended uses.

It is not possible to evaluate a fire model in its entirety. Thus, guidance such as that provided in ASTM E1355 is intended to define a methodology for evaluating the predictive capabilities for a specific use. Validation for one application does not indicate validation for a different scenario.

In accordance with ASTM E1355, this report is structured as follows:

- Chapter 2 provides qualitative background information about FDT^S and the V&V process.
- Chapter 3 describes the technical and theoretical bases of the FDT^S models that were included in this V&V study. This chapter also discusses the assumptions and limitations associated with each of the evaluated models.
- Chapter 4 discusses the mathematical and numerical robustness of the FDT^S models.
- Chapter 5 presents a sensitivity analysis, for which the researchers defined a base case scenario and varied selected input parameters in order to test each model's response to changes in the input parameters.
- Chapter 6 presents the results of the V&V study in the form of accuracies classified according to NPP configuration and relevant attributes of enclosure fires in NPPs. The calculated accuracies are based on both "blind" and "open" calculations. Blind calculations refer to those conducted before the experimental data were available. In contrast, open calculations refer to those conducted with the experimental data available.
- Appendix A presents the technical details supporting the calculated accuracies discussed in Chapter 6.

2
MODEL DEFINITION

This chapter provides qualitative background information about FDT^S and the V&V process, as required by ASTM E1355. Sufficient documentation of calculation models is necessary to assess the adequacy of their scientific and technical bases, as well as the accuracy of the computational procedures for the scenarios of interest. In addition, adequate documentation will help to prevent the unintentional misuse of the models.

This chapter briefly describes the FDT^S library, following the framework suggested by ASTM E1355. As such, this chapter identifies the version of the library that was evaluated in this study; identifies its type, developers, and relevant publications; discusses its governing equations and assumptions, as well as the required input data, property data, and results; and outlines the uses and limitations of the library. Chapter 3 presents more detailed information concerning the equations and correlations that comprise each of the library's component spreadsheets.

2.1 Name and Version of the Model

This study evaluated Version 1805.0 of the Fire Dynamics Tools (FDT^S), which the NRC released in January 2005.

2.2 Type of Model

The FDT^{Ss} library comprises a series of Microsoft® Excel® spreadsheets, which are pre-programmed with fire dynamics equations and correlations to assist inspectors in performing quick, first-order calculations for potential fire scenarios. Each spreadsheet also contains a list of the physical and thermal properties of the materials commonly encountered in NPPs.

2.3 Model Developers

The FDT^S library was developed by the U.S. Nuclear Regulatory Commission (NRC), Office of Nuclear Reactor Regulation (NRR), Division of Systems Safety and Analysis (DSSA), Plant Systems Branch (SPLB), Fire Protection Engineering and Special Projects Section.

2.4 Relevant Publications

The FDT^S library is documented in NUREG-1805, "Fire Dynamics Tools (FDT^S): Quantitative Fire Hazard Analysis Methods for the U.S. Nuclear Regulatory Commission Fire Protection Inspection Program." NUREG-1805 comprises the FDT^S Excel worksheet package and a detailed narrative describing the technical and theoretical bases for each of the fire dynamics tools included in the package. The narrative also discusses the uses and limitations of the spreadsheets and includes sample applications for each.

Other relevant texts include the *SFPE Handbook of Fire Protection Engineering* and the *NFPA Fire Protection Handbook*.

2.5 Governing Equations and Assumptions

The governing equations and assumptions used in the FDT^S spreadsheets come primarily from the principles described in the *SFPE Handbook of Fire Protection Engineering*, the *NFPA Fire Protection Handbook*, and other fire science literature. Those governing equations and assumptions are generally accepted within the fire science community as the state-of-the-art in calculation methods for fire phenomena. Chapter 3 provides detailed descriptions of the equations programmed into the spreadsheets included in this V&V study.

2.6 Input Data Required to Run the Model

Each FDT^S spreadsheet requires the user to input certain fire parameters that are necessary for the equations to compute the output of interest. For example, a spreadsheet may require information about the dimensions of the fire enclosure, the fire size, the ambient room conditions, and so forth. To reduce the chance of user error, the spreadsheets include drop-down selection menus for pre-programmed properties of various materials that are commonly found in NPPs.

2.7 Property Data

Some of the models in the FDT^S library require the following property data:

- thermal properties of enclosure surfaces:
  - thermal inertia
  - thermal conductivity
  - specific heat
  - density
- fuel properties:
  - mass burning rate
  - effective heat of combustion
  - density
  - fuel vapor mass
  - fuel vapor density
- target properties:
  - material thermal inertia
  - material ignition temperature
  - material critical heat flux for ignition

2.8 Model Results

The FDT^S spreadsheets use simple algebraic calculations that require little or no computation time to produce first order results. The output generated by each FDT^S spreadsheet is presented as either a single point value numerical result or a series of point values accompanied by a plot showing the trend in the results within the Excel spreadsheet.

2.9 Uses and Limitations of the Model

The primary objective of the FDT^S library and the accompanying documentation (NUREG-1805) is to provide a methodology for NRC fire protection inspectors to use in assessing potential fire hazards in NRC-licensed NPPs. The methodology uses simplified, quantitative FHA techniques to evaluate the potential for credible fire scenarios. One purpose of these evaluations is to determine whether a potential fire can cause critical damage to safe-shutdown components. Its intent is to provide insights into fire dynamics, without using the sophisticated mathematics that are normally associated with the study of fire dynamics. Inspectors using these tools need a working knowledge of algebra, graphical interpretation, scientific notation, formulas, and use of some simple mathematics functions to understand the quantitative aspects of fire phenomena.

Chapter 3 discusses the limitations and assumptions associated with each of the fire dynamics tools, within the context of its technical basis.

3
THEORETICAL BASIS FOR FDT^S

This chapter presents a technical description of the FDT^S library, including theoretical background and the underlying physics and chemistry inherent in the component models. The discussion includes assumptions and approximations, an assessment of whether the open literature provides sufficient scientific evidence to justify the approaches and assumptions used, and an assessment of empirical or reference data used for constant or default values in the context of the model. In so doing, this chapter addresses the ASTM E1355 requirement to "verify the appropriateness of the theoretical basis and assumptions used in the model."

FDT^S is not a model per se, but a set of algebraic hand calculations pre-programmed into Microsoft Excel spreadsheets and compiled into a package. The FDT^S library includes 23 distinct spreadsheets that can be used to calculate various fire parameters under varying conditions. Documentation of the theoretical bases underlying the equations used in the FDT^S spreadsheets will help to ensure that users understand the significance of the inputs that each spreadsheet requires, and why a particular spreadsheet should (or should not) be selected for a particular analysis. This chapter explains the predictive equations used in the FDT^S spreadsheets that were subjected to V&V in this study, as listed in Table 3-1. Note that some spreadsheets in the FDT^S library have not been subjected to V&V in this study because of a lack of applicable experimental data for comparison. NUREG-1805 provides complete documentation of the equations and theoretical bases for the FDT^S library.

Table 3-1: Spreadsheets included in the V&V Study

Spreadsheet Name	Excel File Name
Predicting Hot Gas Layer Temperature and Smoke Layer Height in a Room Fire With Natural Ventilation Compartment	02.1_Temperature_NV.xls
Predicting Hot Gas Layer Temperature in a Room Fire With Forced Ventilation Compartment	02.2_Temperature_FV.xls
Predicting Hot Gas Layer Temperature in a Fire Room With Door Closed	02.3_Temperature_CC.xls
Estimating Radiant Heat Flux From Fire to a Target Fuel at Ground Level Under Wind-Free Condition (Point Source Radiation Model)	05.1_Heat_Flux_Calculations_Wind_Free.xls
Estimating Centerline Temperature of a Buoyant Fire Plume	09_Plume_Temperature_Calculations.xls
Estimating Burning Characteristics of Liquid Pool Fire, Heat Release Rate, Burning Duration, and Flame Height (Flame Height Only)	03_HRR_Flame_Height_Burning_Duration_Calculations.xls

3.1 Estimating Hot Gas Layer Temperature

The various FDT^S spreadsheets include a number of correlations for estimating the hot gas layer temperature under varying conditions. The spreadsheet for calculating hot gas layer temperature in a compartment with natural ventilation also includes a calculation for hot gas layer or smoke layer height. This section discusses the predictive equations for each of the correlations for estimating hot gas layer temperature, while Section 3.2 discusses the correlations for smoke layer height. Section 3.3 augments this discussion by listing the assumptions and limitations that must be employed when using these spreadsheets. Chapter 2 of NUREG-1805 provides the following discussion on estimating hot gas layer temperature and smoke layer height.

3.1.1 Natural Ventilation: Method of McCaffrey, Quintiere, and Harkleroad (MQH)

The temperatures throughout a compartment in which a fire is burning are affected by the amount of air supplied to the fire and the location at which the air enters the compartment. Ventilation-limited fires produce different temperature profiles in a compartment than well-ventilated fires.

A compartment with a single rectangular wall opening (such as a door or window) is commonly used for room fire experiments. Such compartments are also commonly involved in real fire scenarios, in which a single door or vent opening serves as the only path for fire-induced natural ventilation to the compartment. The hot gas layer that forms in compartment fires descends within the opening until a quasi-steady balance is struck between the rate of mass inflow to the layer and the rate of mass outflow from the layer.

A complete solution of the mass flow rate in this scenario requires equating and solving two nonlinear equations describing the vent flow rate and the plume entrainment rate as a function of the layer interface height (the layer in a compartment that separates the smoke layer from the clear layer). If it is non-vented, the smoke layer gradually descends as the fire increases, thereby lowering the smoke interface and (possibly) eventually filling the compartment.

McCaffrey, Quintiere, and Harkleroad (MQH) [Ref. 5] have developed a simple statistical dimensionless correlation for evaluating fire growth (hot gas layer temperature) in a compartment with natural ventilation (also reported by Walton and Thomas [Ref. 14]). This MQH correlation is based on 100 experimental fires (from 8 test series involving several types of fuel) in conventional-sized rooms with openings. The temperature differences varied from $\Delta T = 20$ ˚C (68 ˚F) to 600 ˚C (1,112 ˚F). The fire source was away from walls (i.e., data was obtained from fires set in the center of the compartment). The larger the heat release rate (HRR) and the smaller the vent, the higher we expect the upper-layer gas temperature to increase.

The approximate formula for the hot gas layer temperature increase, ΔT_g, above ambient (T_g - T_a) is as follows:

$$\Delta T_g = 6.85\left[\frac{\dot{Q}^2}{\left(A_v\sqrt{h_v}\right)\left(A_T h_k\right)}\right]^{\frac{1}{3}} \qquad (3\text{-}1)$$

Where:
ΔT_g = upper layer gas temperature rise above ambient (T_g - T_a) (K)
$\dot{Q}$ = heat release rate of the fire (kW)
A_v = total area of ventilation opening(s) (m^2)
h_v = height of ventilation opening (m)
h_k = heat transfer coefficient (kW/m^2-K)
A_T = total area of the compartment enclosing surfaces (m^2), excluding area of vent opening(s).

The above equation can be used for multiple vents by summing the values, as follows:

$$\frac{A_v\sqrt{h_v}}{\left(\sum_{i=1}^{n}\left(A_v\sqrt{h_v}\right)\right)_i}$$

Where n is the number of vents, and can be used for different construction materials by summing the A_T values for the various wall, ceiling, and floor elements.

The compartment interior surface area is calculated as follows:

A_T = ceiling + floor = 2 (w_c x l_c)
+ 2 large walls = 2 (h_c x w_c)
+ 2 small walls = 2 (h_c x l_c)
- total area of vent opening(s) = (A_v)

$$A_T = [2\ (w_c \times l_c) + 2\ (h_c \times w_c) + 2\ (h_c \times l_c)] - A_v \qquad (3\text{-}2)$$

Where:
A_T = total compartment interior surface area (m^2), excluding area of vent opening(s)
w_c = compartment width (m)
l_c = compartment length (m)
h_c = compartment height (m)
A_v = total area of ventilation opening(s) (m^2)

For very thin solids, or for conduction through a solid that continues for a long time, the process of conduction becomes stationary (steady-state). The heat transfer coefficient, h_k, after long heating times, can be written as follows:

$$h_k = \frac{k}{\delta} \qquad (3\text{-}3)$$

Where:
k = thermal conductivity (kW/m-K) of the interior lining
δ = thickness of the interior lining (m)

This equation is useful for steady-state applications in which the fire burns longer than the time required for the heat to be transferred through the material until it begins to be lost out the back (cold) side. This time is referred to as the thermal penetration time, t_p, which can be calculated as follows:

$$t_p = \left(\frac{\rho c_p}{k}\right)\left(\frac{\delta}{2}\right)^2 \qquad (3\text{-}4)$$

Where:
ρ = density of the interior lining (kg/m^3)
c_p = thermal capacity of the interior lining (kJ/kg-K)
k = thermal conductivity of the interior lining (kW/m-K)
δ = thickness of the interior lining (m)

However, if the burning time is less than the thermal penetration time, t_p, the boundary material retains most of the energy transferred to it and little will be lost out the non-fire (cold) side. In this case, the heat transfer coefficient, h_k, can be estimated using the following equation for $t < t_p$:

$$h_k = \sqrt{\frac{k\rho c}{t}} \qquad (3\text{-}5)$$

Where:
$k\rho c$ = interior construction thermal inertia [(kW/m^2-K)^2-sec]
(thermal property of the material responsible for the rate of temperature increase)

t = time after ignition in seconds (characteristic burning time)

By contrast, for $t \geq t_p$, the heat transfer coefficient is estimated using Equation 3-3.As indicated above, the $k\rho c$ parameter is a thermal property of the material responsible for the rate of temperature increase. This is the product of the material thermal conductivity (k), material density (ρ), and heat capacity (c). Collectively, $k\rho c$ is known as the material thermal inertia. For most materials, c does not vary significantly, and the thermal conductivity is largely a function of material density. This means that density tends to be the most important material property.

Low-density materials are excellent thermal insulators. Since heat does not pass through such materials, the surface of the material actually heats more rapidly and, as a result, can ignite more quickly. Good insulators (low-density materials), therefore, typically ignite more quickly than poor insulators (high-density materials). This is the primary reason that foamed plastics are so dangerous in fires; they heat rapidly and ignite in situations in which a poor insulator would be slower to ignite because of its slower response to the incident heat flux. The thermal response properties ($k\rho c$), for a variety of generic materials have been reported in the literature. These values have been derived from measurements in the small-scale lateral ignition and flame spread test (LIFT) apparatus [Ref. 4].

3.1.2 Natural Ventilation (Compartment Closed): Method of Beyler

Beyler [Ref. 12] developed a correlation based on a non-steady energy balance to the closed compartment, by assuming that the compartment has sufficient leaks to prevent pressure buildup (also reported by Walton and Thomas [Ref. 14]).For constant HRR, the compartment hot gas layer temperature increase, ΔT_g, above ambient (T_g - T_a) is given by the following equation:

$$\Delta T_g = T_g - T_a = \frac{2K_2}{K_1^2}\left(K_1\sqrt{t} - 1 + e^{-k_1\sqrt{t}}\right) \qquad (3\text{-}6)$$

Where:

$$K_1 = \frac{2\left(0.4\sqrt{k\rho c}\right)}{mc_p} \qquad K_2 = \frac{\dot{Q}}{mc_p}$$

And:

ΔT_g = upper layer gas temperature rise above ambient (T_g - T_a) (K)
k = thermal conductivity of the interior lining (kW/m-K)
ρ = density of the interior lining (kg/m^3)
c = thermal capacity of the interior lining (kJ/kg-K)
$\dot{Q}$ = heat release rate of the fire (kW)
m = mass of the gas in the compartment (kg)
c_p = specific heat of air (kJ/kg-k)
t = exposure time (sec)

3.1.3 Forced Ventilation: Method of Foote, Pagni, and Alvares (FPA)

Foote, Pagni, and Alvares [Ref. 16] developed another method that follows the basic correlations of the MQH method, but adds components for forced-ventilation fires (also reported in Refs. [13], [14]). This method is based on temperature data that were obtained from a series of tests conducted at Lawrence Livermore National Laboratory (LLNL), in which fresh air was introduced at the floor and pulled out the ceiling by an axial fan. Test fires from 150 to 490 kW were used, producing ceiling jet temperatures from 100 to 300 °C. The approximate constant

HRR and ventilation rates were roughly between 200 and 575 cfm, which were chosen to be representative of possible fires in ventilation-controlled rooms with seven room air changes per hour.

The upper-layer gas temperature increase above ambient is given as a function of the fire HRR, compartment ventilation flow rate, gas-specific heat capacity, compartment surface area, and effective heat transfer coefficient. The non-dimensional form of the resulting temperature correlation is as follows:

$$\frac{\Delta T_g}{T_a} = 0.63 \left(\frac{\dot{Q}}{\dot{m} c_p T_a} \right)^{0.72} \left(\frac{h_k A_T}{\dot{m} c_p} \right)^{-0.36} \qquad (3\text{-}7)$$

Where:
ΔT_g = hot gas layer temperature rise above ambient (T_g - T_a) (K)
T_a = ambient air temperature (K)
$\dot{Q}$ = HRR of the fire (kW)
$\dot{m}$ = compartment mass ventilation flow rate (kg/sec)
c_p = specific heat of air (kJ/kg-K)
h_k = heat transfer coefficient (kW/m^2-K)
A_T = total area of compartment enclosing surfaces (m^2)

The above correlation for forced-ventilation fires can be used for different construction materials by summing the A_T values for the various wall, ceiling, and floor elements.

3.1.4 Forced Ventilation: Method of Deal and Beyler

Deal and Beyler [Ref. 15] developed a simple model of forced-ventilation compartment fires (also reported in Ref. [14]). The model is based on a quasi-steady simplified energy equation with a simple wall heat loss model. The model is only valid for times up to 2,000 seconds. The approximate compartment hot gas layer temperature increase, ΔT_g, above ambient (T_g - T_a) is given by the following equation:

$$\Delta T_g = T_g - T_a = \frac{\dot{Q}}{\dot{m} c_p + h_k A_T} \qquad (3\text{-}8)$$

Where:
ΔT_g = hot gas layer temperature rise above ambient (T_g - T_a) (K)
T_a = ambient air temperature (K)
$\dot{Q}$ = HRR of the fire (kW)
$\dot{m}$ = compartment mass ventilation flow rate (kg/sec)
c_p = specific heat of air (kJ/kg-K)
h_k = convective heat transfer coefficient (kW/m^2-K)
A_T = total area of compartment enclosing surfaces (m^2)

The convective heat transfer coefficient is given by the following expression:

$$h_k = 0.4 \max\left(\sqrt{\frac{k\rho c}{t}},\ \frac{k}{\delta}\right) \tag{3-9}$$

Where:
k = thermal conductivity of the interior lining (kW/m-K)
ρ = density of the interior lining (kg/m^3)
c = thermal capacity of the interior lining (kJ/kg-K)
t = exposure time (sec)
δ = thickness of the interior lining (m)

3.2 Estimating Smoke Layer Height

The smoke layer can be described as the accumulated thickness of smoke below a physical or thermal barrier (e.g., ceiling). The smoke layer is typically not a homogeneous mixture, and it does not typically have a uniform temperature. However, for first-order approximations, the calculation methods presented below assume homogeneous conditions. The smoke layer includes a transition zone that is non-homogeneous and separates the hot upper layer from the smoke-free air (i.e., two zones).

3.2.1 Natural Ventilation (Smoke Filling): The Non-Steady State Yamana and Tanaka Method

In a compartment with larger openings (windows or doors), there will be little or no buildup of pressure attributed to the volumetric expansion of hot gases, with the exception of rapid accumulation of mass or energy. Thus, for first-order approximations, pressure is assumed to remain at the ambient pressure. The opening flows are thus determined by the hydrostatic pressure differences across the openings, and mass flows out of and into the compartment. We also assume that the upper layer density (ρ_g) is some average constant value at all times throughout the smoke-filling process.

Assuming a constant average density in the upper hot gas layer has the advantage that we can form an analytical solution of the smoke-filling rate, where the HRR does not need to be constant (that is, it can be allowed to change with time), and we can use the conservation of mass to arrive at the expression for the smoke-filling rate. When this is done, the height of the smoke layer as a function of time is known, and we can use the conservation of energy to check the stipulated value of ρ_g.

Yamana and Tanaka [Ref. 19] developed an expression for the height of the smoke layer interface, z, in terms of time, as follows (also reported in Ref. [17]):

$$z = \left(\frac{2 \quad k \quad \dot{Q}^{\frac{1}{3}} \quad t}{3 \quad A_c} + \frac{1}{h_c^{\frac{2}{3}}} \right)^{-\frac{3}{2}} \qquad (3\text{-}10)$$

Where:
z = height (m) of the smoke layer interface above the floor
$\dot{Q}$ = heat release rate of the fire (kW)
t = time after ignition (sec)
A_c = compartment floor area (m^2)
h_c = compartment height (m)

And:
k = a constant given by the following equation:

$$k = \frac{0.21}{\rho_g} \left(\frac{\rho_a^2 g}{c_p T_a} \right)^{\frac{1}{3}} \qquad (3\text{-}11)$$

Where:
ρ_g = hot gas density kg/m^3
ρ_a = ambient density = 1.20 kg/m^3
g = acceleration of gravity = 9.81 m/sec^2
c_p = specific heat of air = 1.0 kJ/kg-K
T_a = ambient air temperature = 298 K

Substituting the above numerical values in Equation 3-11, we get the following expression:

$$k = \frac{0.076}{\rho_g} \qquad (3\text{-}12)$$

Where density of the hot gas layer (ρ_g) is given by:

$$\rho_g = \frac{353}{T_g} \qquad (3\text{-}13)$$

Where:
T_g = hot gas layer temperature (K) calculated from Equation 3-1

Calculation Procedure

- Calculate ρ_g from Equation 3-13.
- Calculate the constant k from Equation 3-12.
- Calculate the smoke layer height (z) at the some time (t) from Equation 3-10 given HRR.

3.3 Assumptions and Limitations for Hot Gas Layer Calculations

The methods discussed in this chapter have several underlying assumptions and limitations.

*The following assumptions and limitations apply to **all** forced and natural convection situations:*

(1) These methods best apply to conventional-sized compartments; they should be used with caution for large compartments.

(2) These methods apply to both transient and steady-state fire growth.

(3) The HRR must be known; it does not need to be constant, and can be allowed to change with time.

(4) Compartment geometry assumes that a given space can be analyzed as a rectangular space with no beam pockets. This assumption affects the smoke filling rate within a space if the space has beam pockets. For irregularly shaped compartments, equivalent compartment dimensions (length, width, and height) must be calculated and should yield slightly higher layer temperatures than would actually be expected from a fire in the given compartment.

(5) These methods predict average temperatures and do not apply to cases in which prediction of local temperature is desired. For example, this method should not be used to predict detector or sprinkler actuation or the material temperatures resulting from direct flame impingement.

(6) Caution should be exercised when the compartment overhead are highly congested with obstructions such as cable trays, conduits, ducts, and so forth.

(7) A single heat transfer coefficient may be used for the entire inner surface of the compartment.

(8) The heat flow to and through the compartment boundaries is unidimensional (i.e., corners and edges are ignored, and the boundaries are assumed to be infinite slabs).

(9) These methods assume that heat loss occurs as a result of mass flowing out through openings. Consequently, these methods do not apply to situations in which significant time passes before hot gases begin leaving the compartment through openings. This may occur in large enclosures (e.g., turbine building), where it may take considerable time for the smoke layer to reach the height of the opening.

*The following assumptions and limitations apply only to **natural convection** situations:*

(1) The correlations hold for compartment upper-layer gas temperatures up to approximately 600 °C (1,112 °F) only for naturally ventilated spaces in which a quasi-steady balance develops between the rates of mass inflow and outflow from the hot gas layer.

(2) These correlations assume that the fire is located in the center of the compartment or away from the walls. If the fire is flush with a wall or in a corner of the compartment, the MQH correlation is not valid with coefficient 6.85. The smoke layer height correlation assumes an average constant value of upper-layer density throughout the smoke-filling process. At the EPRI Fire Modeling Workshop in Seattle, Washington on August 26, 2002, Mark Salley asked Professor James G. Quintiere (one of the authors of the MQH method) what limits apply to compartment size when using the MQH equation. Professor Quintiere replied that the correlation will work for ***any*** size compartment, since it is a dimensionless equation, but $\dot{Q}$ should be limited by the following expressions:

$$\dot{m}_f \Delta H_c \leq 3000 \frac{kJ}{kg} \quad \text{or} \quad 0.5 A_v \sqrt{h_v} \leq 3000 \frac{kJ}{kg}$$

Where:
$\dot{m}_f$ = mass loss rate of fuel (kg/sec)
ΔH_c = heat of combustion (kJ/kg)
A_v = area of ventilation opening (m^2)
h_v = Height of ventilation opening (m)

*The following assumptions and limitations apply only to **forced convection** situations:*

(1) These correlations assume that the test compartment is open to the outside at the inlet, and its pressure is fixed near 1 atmosphere.

(2) These correlations do not explicitly account for evaluation of the fire source, and they assume that the fire is located in the center of the compartment or away from the walls. If the fire is flush with a wall or in a corner of the compartment, the FPA correlation is not valid with coefficient 0.63.

3.4 Flame Height

As documented in Chapter 3 of NUREG-1805, the height of a flame is a significant indicator of the hazard posed by the flame. Flame height directly relates to flame heat transfer and the propensity of the flame to impact surrounding objects. As a plume of hot gases rises above a flame, the temperature, velocity, and width of the plume changes as the plume mixes with its surroundings. The size (height) and temperature of the flame are important in estimating the ignition of adjacent combustibles. Figure 3-1 shows a characteristic sketch of the flame height fluctuations associated with the highly intermittent pulsing structure of a flame, particularly along its perimeter and near its top. This intermittence is driven largely by the turbulent mixing of air and subsequent combustion, and the pulsing behavior, in turn, affects the temperature of the flame. Thus, the temperature at a fixed position fluctuates widely, particularly around the edges and near the top of the flame. This is why flame temperature is usually reported in terms of the centerline temperature or average flame temperature.

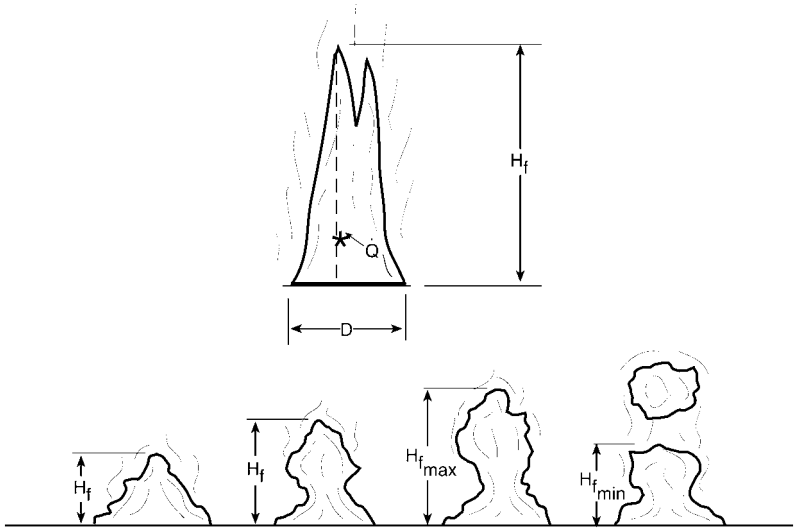

Figure 3-1: Characteristics of Flame Height Fluctuations

Researchers define flame height as the height at which the flame is observed at least 50 percent of the time. Above the fuel source, the flaming region is characterized by high temperature and is generally luminous. Flames from pool fires fluctuate periodically so that the tip of the flame is significantly different from the length of the continuous combustion (or luminous) region. Consequently, flame height has been defined by various criteria in order to correlate data.

The flame height is an important quantitative characteristic of a fire and may affect fire detection and suppression system design, fire heating of building structures, smoke filling rates, and fire ventilation. Flame height typically depends on whether the flame is laminar or turbulent. In general, laminar flames are short, while turbulent flames are tall. The following two correlations are widely used to determine the flame height of pool fires (Heskestad [Ref. 9] and Thomas [Ref. 11]), respectively:

$$H_f = 0.235\dot{Q}^{\frac{2}{5}} - 1.02D \qquad (3\text{-}14)$$

Where:

H_f = flame height (m)

$\dot{Q}$ = heat release rate of the fire (kW)

D = diameter of the fire (m)

$$H_f = 42D\left(\frac{\dot{m}''}{\rho_a\sqrt{gD}}\right)^{0.61} \qquad (3\text{-}15)$$

Where:

H_f = flame height (m)

D = diameter of the fire (m)

$\dot{m}''$ = burning or mass loss rate per unit area per unit time (kg/m^2-sec)

ρ_a = ambient air density (kg/m^3)

g = gravitational acceleration (m/sec^2)

The above correlations can also be used to determine the length of the flame extension along the ceiling and to estimate radiative heat transfer to objects in the enclosure.

The HRR of the fire can be determined by laboratory or field testing. In the absence of experimental data, the maximum HRR for the fire is given by the following equation:

$$\dot{Q} = \dot{m}'' \Delta H_{c,eff} A_f \qquad (3\text{-}16)$$

Where:

$\dot{m}''$ = burning or mass loss rate per unit area per unit time (kg/m^2-sec)

$\Delta H_{c,eff}$ = effective heat of combustion (kJ/kg)

A_f = horizontal burning area of the fuel (m^2)

For non-circular pools, the effective diameter is defined as the diameter of a circular pool with an area equal to the actual pool area given by the following equation:

$$D = \sqrt{\frac{4 A_f}{\pi}} \qquad (3\text{-}17)$$

Where:

A_f is the surface area of the non-circular pool

3.4.1 Assumptions and Limitations

(1) The flame height correlation described in this chapter was developed for horizontal pool fire sources in the center or away from the center of the compartment. The turbulent diffusion flames produced by fires burning near or close to a wall or in a corner configuration of a compartment affect the spread of the fire. Chapter 4 presents the flame height correlations for fires burning near walls and corners.

(2) The size of the fire (flame height) depends on the diameter of the fuel and the HRR attributable to the combustion.

(3) This correlation is developed for two-dimensional sources (primarily pool fires), and this method assumes that the pool is circular or nearly circular.

(4) There is no fire growth period. (As stated above, real liquid pool fires grow very quickly, and it is realistic to assume that the pool fire instantaneously reaches its maximum HRR.)

3.5 Estimating Radiant Heat Flux from Fire to a Target

Chapter 5 of NUREG-1805 provides a complete discussion on the methods FDT^S uses to estimate radiant heat flux from fire to a target. The method used in this V&V study is summarized below.

3.5.1 Point Source Radiation Model

A point source estimate of radiant flux is conceptually the simplest configurational model of a radiant source used in calculating the heat flux from a flame to target located outside the flame. To predict the thermal radiation field of flames, it is customary to model the flame based on the point source located at the center of a flame[1]. The point source model provides a simple relationship that varies as the inverse square of the distance, R. For an actual point source of radiation or a spherical source of radiation, the distance, R, is simply the distance from the point or from the center of the sphere to the target.

The thermal radiation hazard from a fire depends on a number of parameters, including the composition of the fuel, size and shape of the fire, its duration, proximity to the object at risk, and thermal characteristics of the object exposed to the fire. The point source method may be used for either fixed or transient combustibles. They may involve an electrical cabinet, pump, liquid spill, or intervening combustible at some elevation above the floor. For example, the top of a switchgear or motor control center (MCC) cabinet is a potential location for the point source of a postulated fire in this type of equipment. By contrast, the point source of a transient combustible liquid spill or pump fire is at the floor.

The point source model assumes that radiant energy is released at a point located at the center of the fire. The radiant heat flux at any distance from the source fire is inversely related to the horizontal separation distance (R), by the following equation [Ref. 7]:

$$\dot{q}'' = \frac{\chi_r \dot{Q}}{4\pi R^2} \qquad (3\text{-}18)$$

Where:

$\dot{q}''$ = radiant heat flux (kW/m$^{2)}$

$\dot{Q}$ = heat release rate of the fire (kW)

R = radial distance from the center of the flame to the edge of the target (m)

χ_r = fraction of total energy radiated

In general, χ_r depends on the fuel, flame size, and flame configuration, and can vary from approximately 0.15 for low-sooting fuels (e.g., alcohol) to 0.60 for high sooting fuels (e.g., hydrocarbons). For large fires (several meters in diameter), cold soot enveloping the luminous flames can reduce χ_r considerably.

[1] More realistic radiator shapes give rise to very complex configuration factor equations.

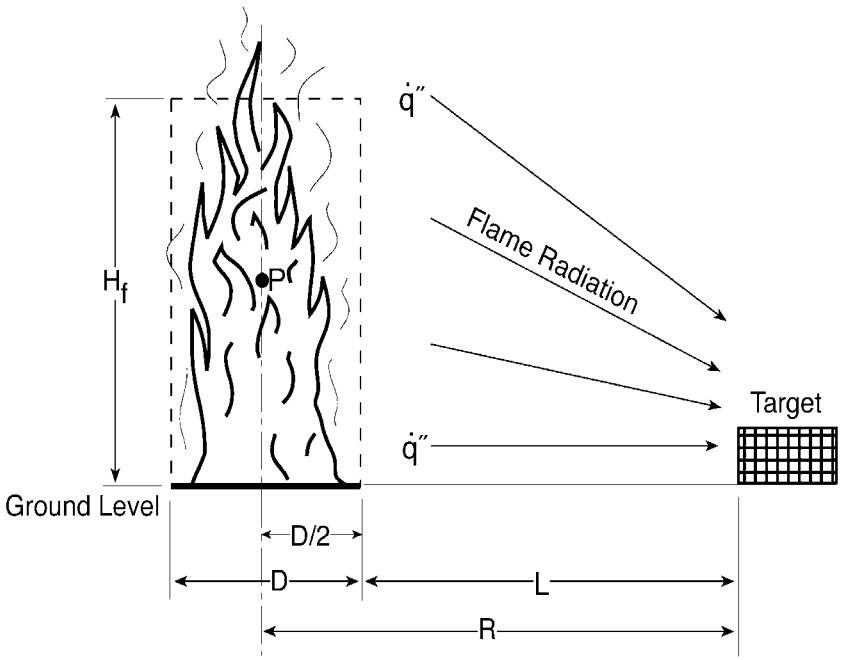

Figure 3-2: Radiant Heat Flux from a Pool Fire to a Floor-Based Target Fuel (Point Source Model)

The HRR of a fire can be determined by laboratory or field testing. In the absence of experimental data, the maximum HRR for the fire $(\dot{Q})$, is given by the following equation [Ref. 6]:

$$\dot{Q} = \dot{m}''\Delta H_{c,eff} A_f \qquad (3\text{-}19)$$

Where:

$\dot{Q}$ = heat release rate of the fire (kW)
$\dot{m}''$ = burning or mass loss rate per unit area per unit time (kg/m^2-sec)
$\Delta H_{c,eff}$ = effective heat of combustion (kJ/kg)
A_f = horizontal burning area of the fuel (m^2)

For non-circular pools, the effective diameter is defined as the diameter of a circular pool with an area equal to the actual pool area, given by the following equation:

$$D = \sqrt{\frac{4A_f}{\pi}} \qquad (3\text{-}20)$$

Where:
A_f = surface area of the non-circular pool (m^2)
D = diameter of the fire (m)

3.5.2 Solid Flame Radiation Model with Target at and Above Ground Level

The solid flame spreadsheet associated with this chapter provides a detailed method for assessing the impact of radiation from pool fires to potential targets using configuration factor algebra. This method covers a range of detailed calculations, some of which are most appropriate for first-order initial hazard assessments, while others are capable of more accurate predictions.

The solid flame model assumes that (1) the fire can be represented by a solid body of a simple geometrical shape, (2) thermal radiation is emitted from its surface, and (3) non-visible gases do not emit much radiation. (See Figures 3-3 and 3-4 for general nomenclature.) To ensure that the fire volume is not neglected, the model must account for the volume, because a portion of the fire may be obscured as seen from the target. The intensity of thermal radiation from the pool fire to an element outside the flame envelope for no-wind conditions and windblown flames is given by the following equation [Ref. 8]:

$$\dot{q}'' = EF_{1\to 2} \qquad (3\text{-}21)$$

Where:
$\dot{q}''$ = incident radiative heat flux (kW/m^2)
E = average emissive power at flame surface (kW/m^2)
$F_{1\to 2}$ = configuration factor

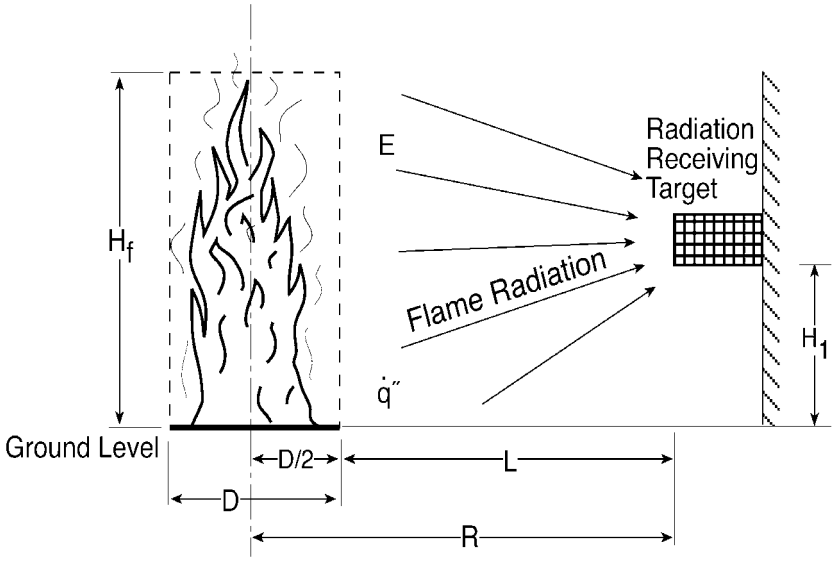

Figure 3-3: Radiant Heat Flux from a Pool Fire to a Floor-Based Target Fuel (Point Source Model)

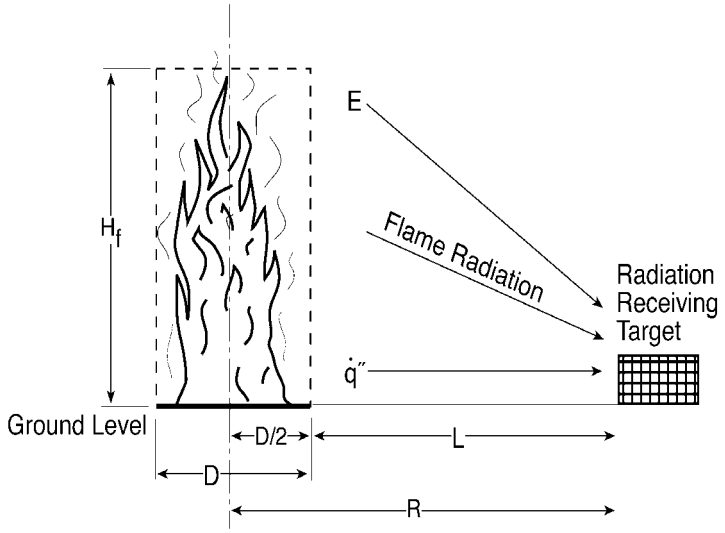

Figure 3-4: Solid Flame Radiation Model with No Wind and Target at Ground Level

3.5.3 Assumptions and Limitations

The methods discussed in this chapter are subject to several assumptions and limitations. For all radiation models, we assume that the pool is circular or nearly circular.

The following assumptions and limitations apply to point source radiation models:

(1) Except near the base of pool fires, radiation to the surroundings can be approximated as being isotropic or emanating from a point source.

(2) The point source model overestimates the intensity of thermal radiation at the observer's (target) locations close to the fire. This is primarily because the near-field radiation is greatly influenced by the flame size, shape, and tilt, as well as the relative orientation of the observer (target).

(3) A theoretical analysis of radiation from small pool fire by Modak [Ref. 10] indicated that the point source model is within 5 percent of the correct incident heat flux when L/D > 2.5.

(4) The energy radiated from the flame is a specified fraction of the energy released during combustion.

(5) The model can be used to determine thermal radiation hazards in scenarios for which a conservative estimate of the hazard is generally acceptable.

The following limitation applies to solid flame radiation models at and above ground level:

- The correlation of emissive power was developed on the basis of data from experiments that included kerosene, fuel oil, gasoline, JP-4, JP-5[2], and liquified natural gas (LNG). With the exception of the LNG, these are quite luminous flames, so the correlation should be suitable for most fuels. The pool diameters ranged from 1 to 50 m.

3.6 Estimating the Centerline Temperature of a Buoyant Plume

As discussed in Chapter 9 of NUREG-1805, the peak temperature is found in the plume centerline, and decreases toward the edge of the plume where more ambient air is entrained to cool the plume. The centerline temperature, denoted as $T_{p(centerline)}$, varies with height. In the continuous flame region, for example, the centerline temperature is roughly constant and represents the mean flame temperature. By contrast, the temperature decreases sharply above the flames as an increasing amount of ambient air is entrained into the plume. The symbol $\Delta T_{p(centerline)}$ describes the increase in centerline plume temperature above the ambient temperature, T_a, as shown in the following equation:

$$\Delta T_{p(centerline)} = T_{p(centerline)} - T_a \qquad (3\text{-}22)$$

Numerous correlations are available to estimate the plume centerline temperature. These correlations relate the temperature as a function of HRR and of height above the source. For example, consider a region of a ceiling jet at radial distance from the fire axis equal to the vertical distance from the fire source to the ceiling. In this region, the maximum velocity in the jet drops to half the value near the fire axis, and the temperature (relative to ambient) drops to about 40 percent of the value near the fire axis. The maximum velocity and temperature exist at a distance below the ceiling equal to about 1 percent of the distance from the fire source to the ceiling. If the walls are much farther away than this, the temperature and velocity of the ceiling jet decay to negligibly low values before the jet encounters the nearest wall. However, if the nearest wall is not far away, a reflection occurs when the jet reaches the wall, and the reflected jet moves back toward the fire axis just under the original jet. Thus, the hot layer under the ceiling becomes thicker.

If the compartment has an opening and fire continues, the hot layer ultimately becomes thick enough to extend below the top of the opening, after which the hot, smoke-laden gases begin to exit from the compartment.

[2] Common jet fuel.

Heskestad [Ref. 9] provided a simple correlation for estimating the maximum centerline temperature of a fire plume as a function of ceiling height and HRR:

$$T_{p(centerline)} - T_a = \frac{9.1 \left(\frac{T_a}{g c_p^2 \rho_a^2} \right)^{\frac{1}{3}} \dot{Q}_c^{\frac{2}{3}}}{(z - z_0)^{\frac{5}{3}}} \qquad (3\text{-}23)$$

Where:
$T_{p(centerline)}$ = plume centerline temperature (K)
T_a = ambient air temperature (K)
$\dot{Q}_c$ = convective HRR (kW)
g = acceleration of gravity (m/sec^2)
c_p = specific heat of air (kJ/Kg-K)
ρ_a = ambient air density (kg/m^3)
z = elevation above the fire source (m)
z_0 = hypothetical virtual origin of the fire (m)

The virtual origin is the equivalent point source height of a finite area fire (Figure 3-5). The location of the virtual origin is needed to calculate the thermal plume temperature for fires that originate in an area heat source. The thermal plume calculations are based on the assumption that the plume originates in a point heat source. Area heat sources include pool fires and burning three-dimensional objects such as cabinets and cable trays. The use of a point heat source model for area sources is accomplished by calculating the thermal plume parameters at the virtual point source elevation, rather than the actual area source elevation.

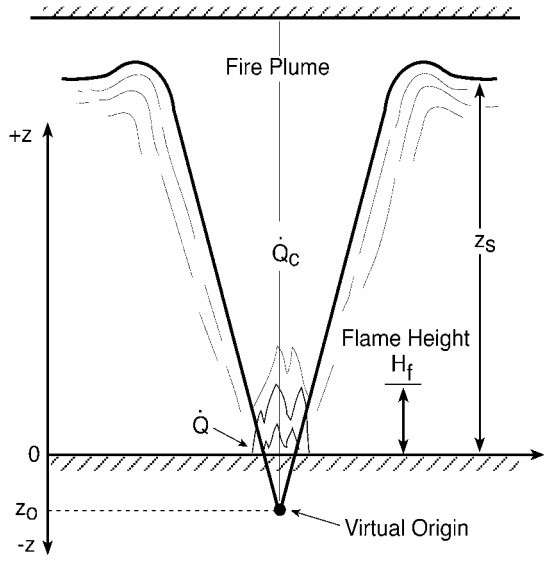

Figure 3-5: Point Source Fire Plume

The virtual origin, z_0, depends on the diameter of the fire source and the total energy released, as follows:

$$\frac{z_0}{D} = -1.02 + 0.083\frac{\dot{Q}^{\frac{2}{5}}}{D} \qquad (3\text{-}24)$$

Where:
z_0 = virtual origin (m)
D = diameter of fire source (m)
$\dot{Q}$ = total HRR (kW)

For non-circular pools, the effective diameter is defined as the diameter of a circular pool with an area equal to the actual area given by the following equation:

$$D = \sqrt{\frac{4A_f}{\pi}} \qquad (3\text{-}25)$$

Where:
D = diameter of the fire (m)
A_f = fuel spill area or curb area (m^2)

Total HRR $\dot{Q}$ is used when calculating the mean flame height and position of the virtual origin. However, the convective HRR $\dot{Q}_c$ is used when estimating other plume properties, since this is the part of the energy release rate that causes buoyancy. The energy losses attributable to radiation from the flame are typically on the order of 20 to 40 percent of the total HRR $\dot{Q}$. The higher of these values is valid for the sootier and more luminous flames, often from fuels

that burn with a low combustion efficiency. The convective HRR is, therefore, often in the range 0.6 $\dot{Q}$ to 0.8 $\dot{Q}$ where $\dot{Q}$ is the total HRR.

3.6.1 Assumptions and Limitations

The methods discussed in this chapter are subject to several assumptions and limitations:

(1) All heat energy is released at a point.

(2) The correlation was developed for two-dimensional area sources.

(3) If the surrounding air is at an elevated temperature, the temperature difference between the plume and the surrounding environment is small. In this situation, the thermal plume cools less effectively, so Equation 3-23 will underestimate the temperature.

(4) The thermal plume equation is not valid when the momentum forces in a plume are more significant than the buoyant forces, as in a jet fire. If this type of situation is encountered, specialized calculation approaches should be used.

4
MATHEMATICAL AND NUMERICAL ROBUSTNESS

This chapter documents the mathematical and numerical robustness of the FDT^S library, which involves verifying that the implementation of the model matches the stated documentation. A model's mathematical and numerical robustness refers to its stability and ability to reliably produce the results that the model developers intended it to produce. Specifically, ASTM E1355 requires the following analyses to address the mathematical and numerical robustness of models:

- Analytical tests involve testing the correct functioning of the model. In other words, these tests use the code to solve a problem with a known mathematical solution. However, analytical tests cannot be applied to FDT^S because there are no known mathematical solutions to which the results can be compared for the problems addressed by FDT^S.
- Code checking refers to verifying the computer code on a structural basis. This verification can be achieved manually or by using a code-checking program to detect irregularities and inconsistencies within the computer code. Code checking can increase the level of confidence in the program's ability to correctly process the data to the program; however, it does not give any indication of the likely adequacy or accuracy of the program in use. The FDT^S library comprises relatively simple closed form equations that are pre-programmed into Excel spreadsheets. Each function requires a set of inputs and returns either a single point value or a series of values showing a trend. Problems related to irregularities and inconsistencies within the computer code are not expected; therefore, code checking in this sense is not necessary for the FDT^S library. The calculations within each of the FDT^S spreadsheets have been verified by comparison with the results of hand calculations.
- Numerical tests investigate the magnitude of the residuals from the solution of a numerically solved system of equations employed in the model (as an indicator of numerical accuracy) and the reduction in residuals (as an indicator of numerical convergence). The models in the FDT^S library are closed form mathematical expressions that are not solved using numerical methods. As a result, there are no numerical instabilities or convergence issues associated with the solutions to the models.

In general, the analyses for numerical and mathematical robustness suggested by ASTM E1355 do not apply to the FDT^S library. Because the equations are generally solvable by hand calculations, there is little concern about model stability or program reliability. The equations used in the FDT^S spreadsheets are primarily derived from the principles described in the *SFPE Handbook of Fire Protection Engineering* [Ref. 20], the *NFPA Fire Protection Handbook* [Ref. 21], and other fire science literature. They are generally accepted within the fire science community as the state-of-the-art in calculation methods for fire phenomena.

In FDT^S version 1805.0, an error was identified in the algorithm for estimating the hot gas layer temperature in a closed compartment. The error was identified because it was found that the output for this algorithm was not consistent with the conceptual basis for this calculation. The

algorithm was subsequently corrected and re-released in version 1805.1 on the NRC fire protection website.

5
MODEL SENSITIVITY

This chapter discusses sensitivity analysis, which ASTM 1355 defines as a study of how changes in model parameters affect the results. In other words, sensitivity refers to the rate of change of the model output with respect to input variations. The standard also indicates that model predictions may be sensitive to (1) uncertainties in input data, (2) the level of rigor employed in modeling the relevant physics and chemistry, and (3) the accuracy of numerical treatments. Thus, the purpose of a sensitivity analysis is to assess the extent to which uncertainty in the model inputs is manifested as uncertainty in the model results of interest. The information obtained can be used to determine the dominant variables in the models, define the acceptable range of values for each input variable, quantify the sensitivity of output variables to variations in input data and inform and caution any potential users about the degree and level of care that should be taken in selecting inputs and running the model.

When an input parameter is changed there will also be a relative magnitude change in the output, a sensitivity analysis is conducted to determine and examine this relative magnitude change. These changes will vary with each input. Some might have a greater effect on the output then others.

The goal, when examining the results obtained from the sensitivity analysis, is to determine which inputs cause the greatest changes in the final output. In order to stay consistent, a base case must be established. The inputs for each base case will be set at a value, and then each input will be varied over a defined percentage change. If the percentage change in the output is greater than the percentage change in the input then the model is more sensitive to the input parameter. Conversely, if the relative change in output is less than the relative change in input, the model is not as sensitive to the parameter that was changed.

In the case of this study the inputs were varied by 10%, therefore if the output deviated by more than 10% from the base case output then the model has a higher sensitivity to that input. If the output deviates less than 10% then the model has a lower sensitivity to the input.

5.1 Definition of Base Case Scenario for Sensitivity Analysis

A sensitivity analysis involves defining a base case scenario, and varying selected input parameters. The resultant variations in the model output are then measured with respect to the base case scenario, in order to consider the extent to which uncertainty in model inputs influences model output. The inputs for the base case scenario used in this study are listed in the table that follows.

Table 5-1: Technical Details for Base Case

Room		**Material properties Interior Lining**	
Length	5 m	Specific heat	1.1 kJ/kg-K
Width	5 m	Thermal conductivity	0.00017 kW/m-K
Height	5 m	Density	960 kg/m^3
Vent Size	1 m x 2 m	**Target**	
Mech. ventilation	0.28 kg/s	Elevation	5 m
Top of Vent From Floor	2 m	**Fire (Heat release rate)**	
Ambient conditions		HRR	200 KW
Temperature	24.85 °C 298 K	Fuel Spill Area	1 m^2
Ambient Air Density	1.18 kg/m^3	Fuel Spill Volume	0.0189
Specific Heat of Air	1 kJ/kg-K	Heat of combustion	44600 kJ/kg

5.2 Sensitivity Analysis for FDT^S

FDT^S contains a number of algorithms, however, for this study, only the models included in the validation were analyzed. The models included were a natural ventilation compartment, a forced ventilation compartment via the FPA method, a forced ventilation via the method of Deal & Beyler, a closed compartment, the heat release rate from a pool fire, the burning duration of a pool fire, the flame height of a pool fire via the method of Heskestad, the flame height via the method of Thomas, and the center line plume temperature. The radiation model was not included in the sensitivity analysis. Most of the correlations are linear, therefore it is expected that a small change in input will not result in a large change in output. For this study each input was varied by +10% and -10% from the base case. The sensitivity ratio refers to the percentage change in output over the percentage change in the input. A ratio of greater than one (1.0) means that the model is sensitive to the input. Below are charts showing the inputs changed along with corresponding sensitivity ratio, the maximum, minimum, and average values for each ratio.

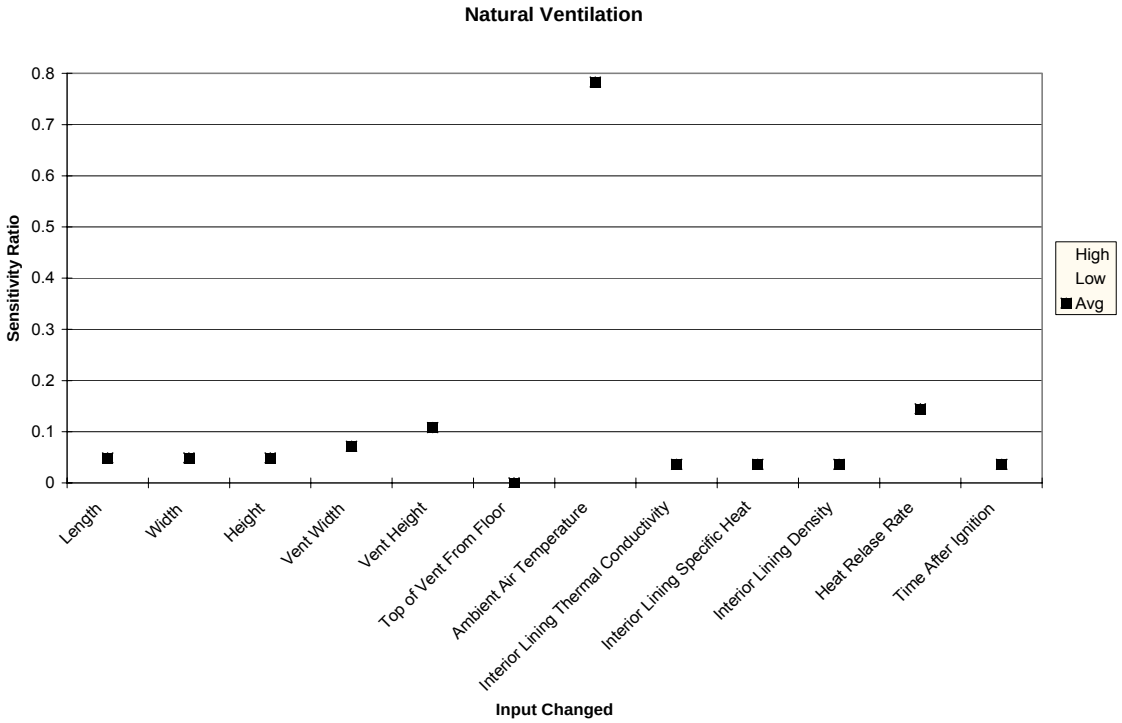

Figure 5-1: Sensitivity Ratios for inputs to HGL Temperature in a Compartment with Natural Ventilation

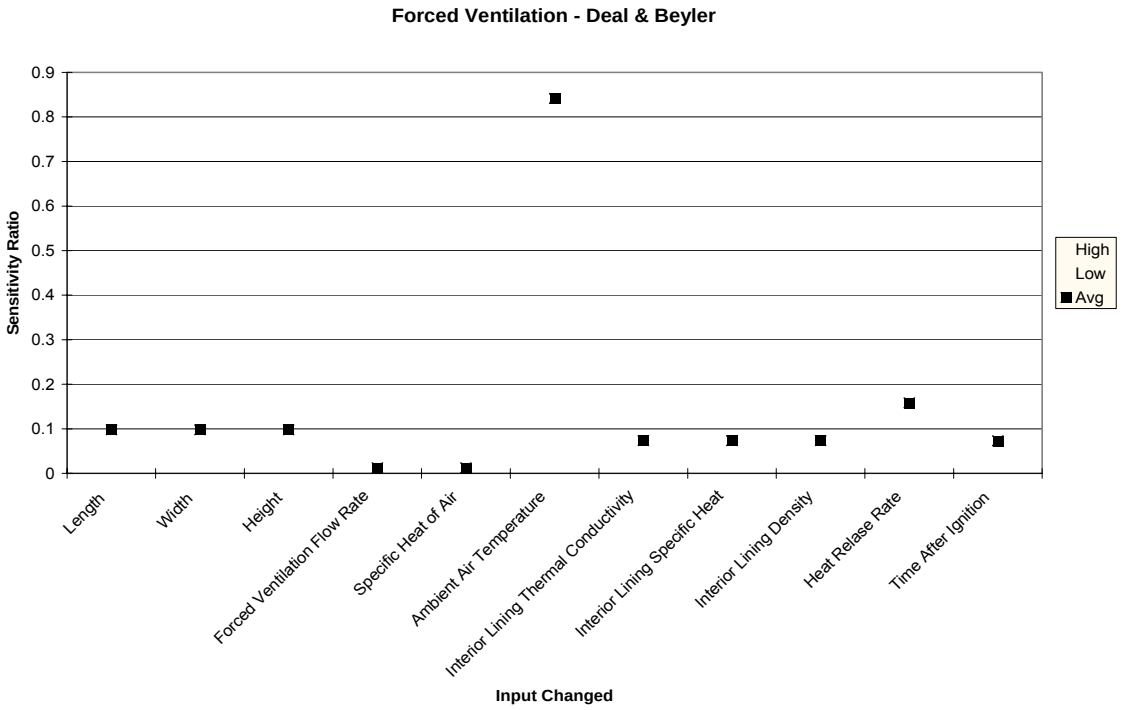

Figure 5-2: Sensitivity Ratios for Inputs to HGL Temperature in Compartment with Forced Ventilation

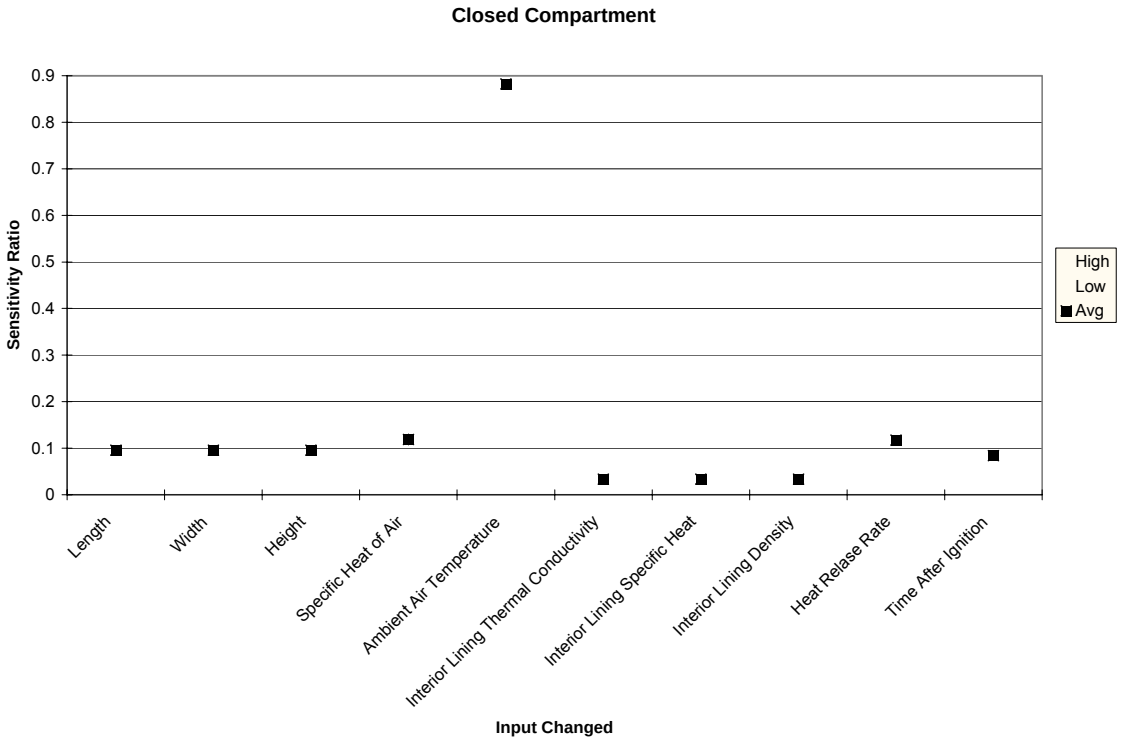

Figure 5-3: Sensitivity Ratios for Inputs to HGL Temperature in a Closed Compartment

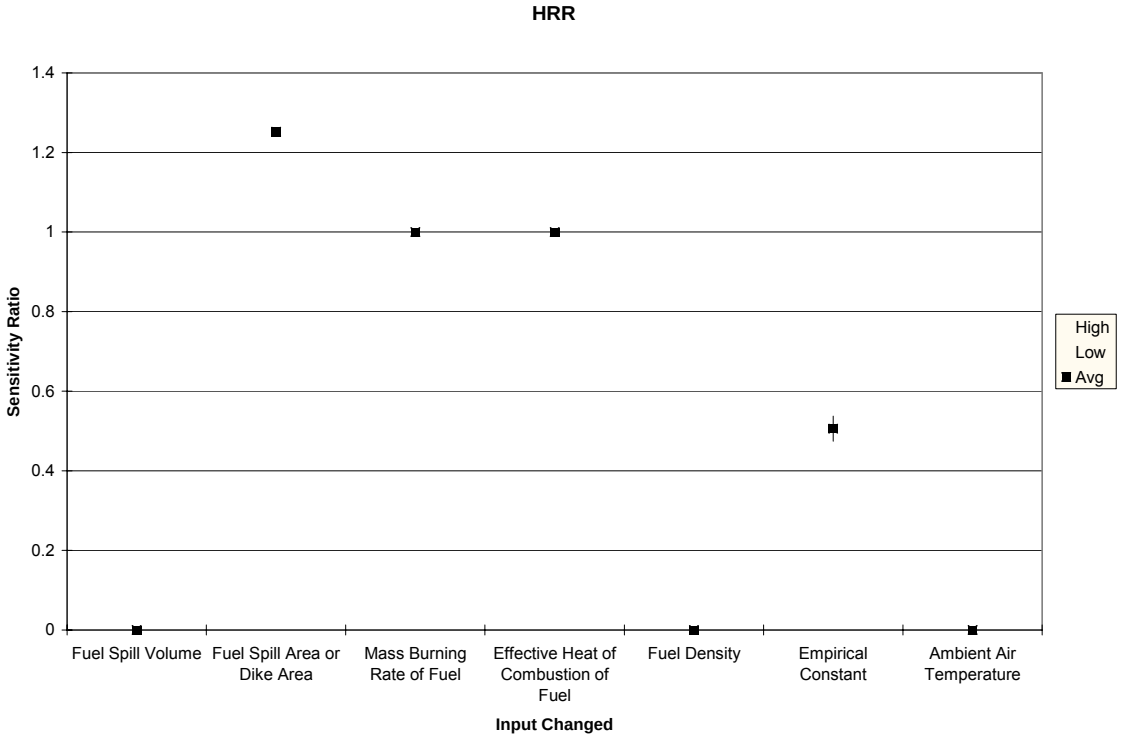

Figure 5-4: Sensitivity Ratios for Inputs to HRR Algorithm

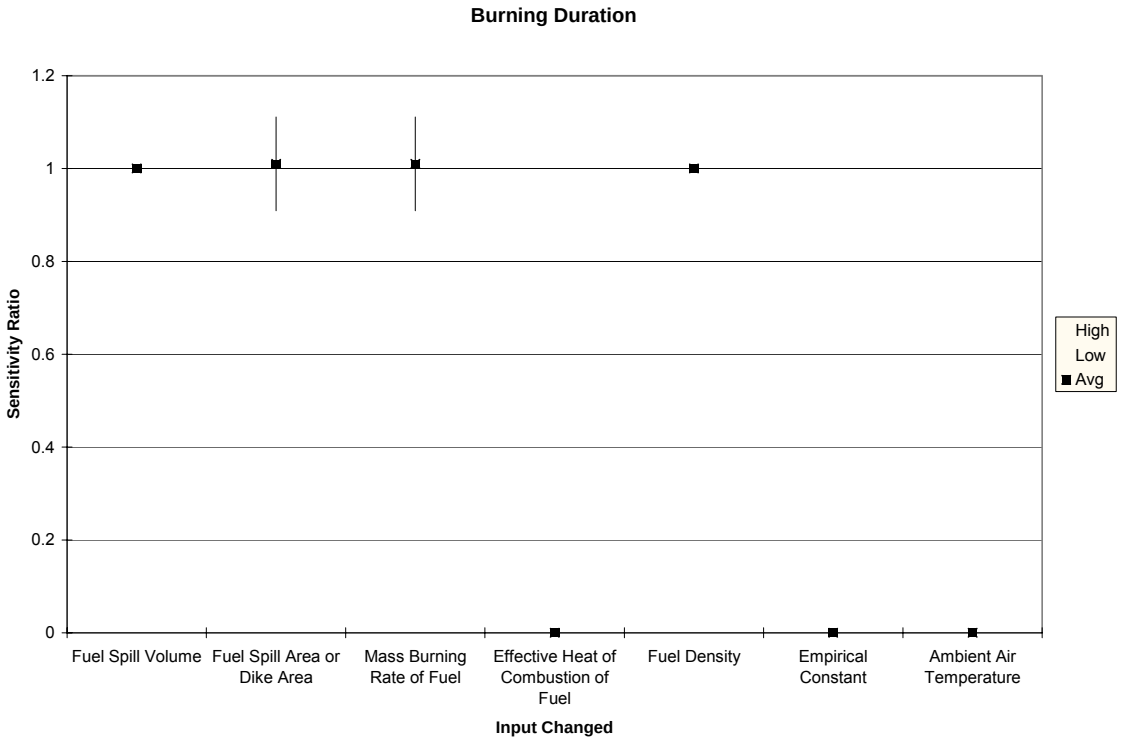

Figure 5-5: Sensitivity Ratios for Inputs to Burning Duration Algorithm

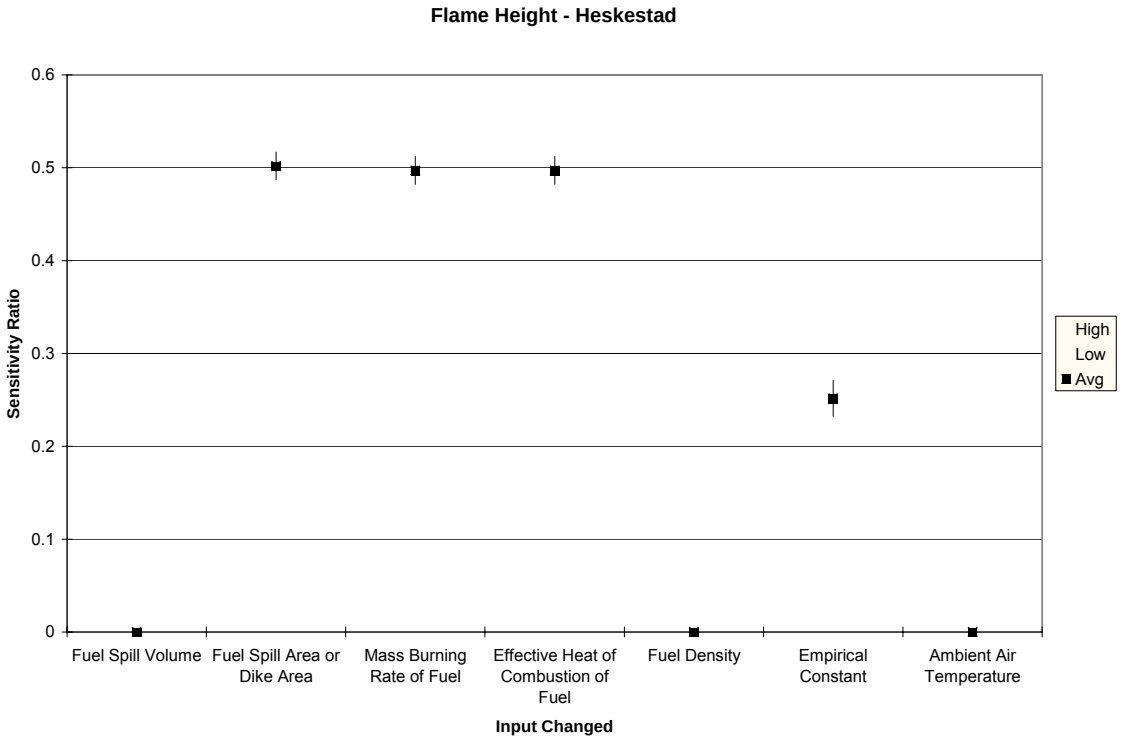

Figure 5-6: Sensitivity Ratios for Inputs to Heskestad's Flame Height Algorithm

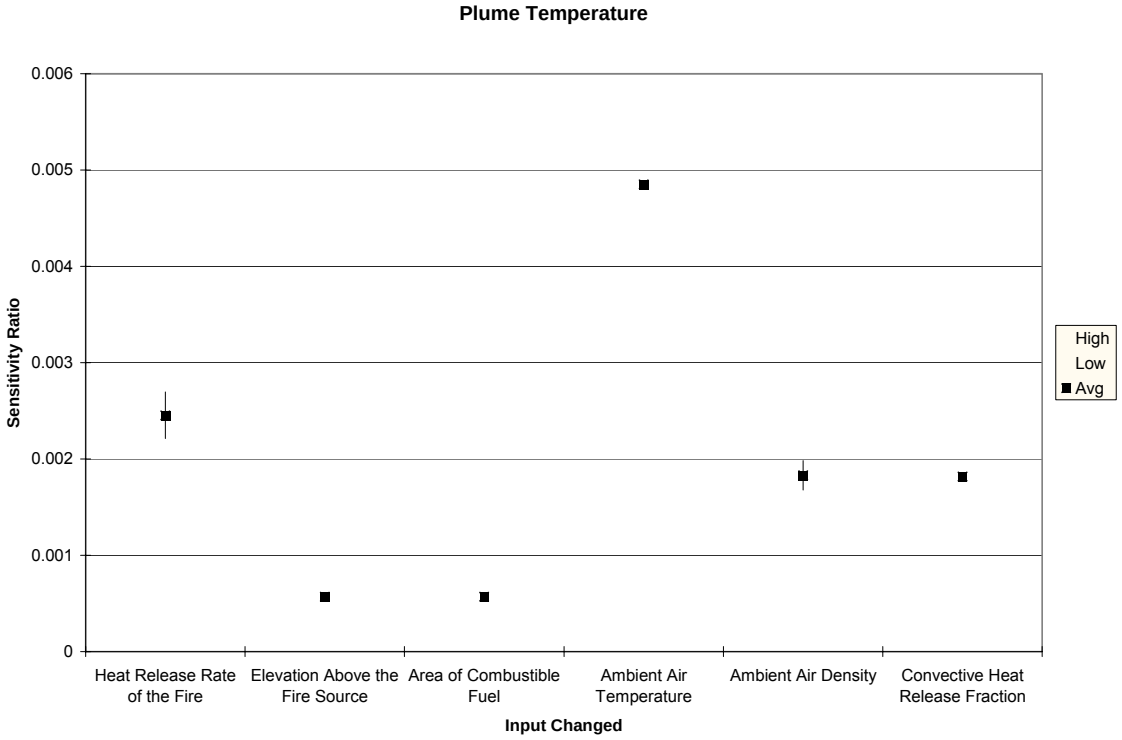

Figure 5-7: Sensitivity Ratios for Inputs to Plume Temperature Algorithm

5.3 Conclusions

As can be seen in the previous charts, the change in output is less than the change in input for the majority of the models. The only places where we see sensitivity ratio above one (1.0) is in the calculation of the heat release rate (HRR) and the burning duration of a pool fire.

The three inputs that bring the ratio above one (1.0) for the HRR are the fuel spill area, mass burning rate of the fuel, and the effective heat of combustion for the fuel. Both the mass burning rate and the effective heat of combustion keep the change in output very close to the change in input. On the other hand, a 10% change in fuel spill area results in a 12% change in output. It is easy to see how the mass burning rate and effective heat of combustion effect the change in output, if both these go up, then the total HRR should also go up with the same magnitude.

The burning duration output is sensitive to the fuel spill volume, fuel spill area, the mass burning rate, and the density of the fuel. All the averages of these sensitivity ratios fall very close to one (1.0). Therefore the relative change in the input variable will be very close to the relative change in the output. The effect the volume has on the burning duration is almost trivial, if you have 10% more fuel then it should take 10% longer to burn off completely. For the area if your area is 10% bigger then it should take around 10% less time to burn off. The same holds true for the burning rate, if the burning rate increases, then the burning duration should also fall respectively. Changing the density will in turn change the mass of fuel that occupies the volume being burned, therefore there is less mass in the same volume, resulting in a shorter burning duration.

Although there are some inputs that affect the model with a sensitivity ratio of greater than one (1.0), all in all, these results show that all the correlations are stable and their sensitivity to a particular input is typically low.

6
MODEL VALIDATION

Consistent with Section 11 of ASTM E1355, "Model Evaluation," this chapter summarizes the results of the validation study conducted for the FDT^S library. Appendix A presents the technical details supporting the validation, including model output and comparison with experimental data.

Six experimental test series have been used in the V&V study. A brief description of each is given here. Further details can be found in Volume 7 and in the individual test reports.

ICFMP BE #2: Benchmark Exercise #2 consists of 8 experiments, representing 3 sets of conditions, to study the movement of smoke in a large hall with a sloped ceiling. The results of the experiments were contributed to the International Collaborative Fire Model Project (ICFMP) for use in evaluating model predictions of fires in larger volumes representative of turbine halls in NPPs. The tests were conducted inside the VTT Fire Test Hall, which has dimensions of 19 m high by 27 m long by 14 m wide. Each case involved a single heptane pool fire, ranging from 2 MW to 4 MW.

ICFMP BE #3: Benchmark Exercise #3, conducted as part of the International Collaborative Fire Model Project (ICFMP) and sponsored by the US NRC, consists of 15 large-scale tests performed at NIST in June, 2003. The fire sizes range from 350 kW to 2.2 MW in a compartment with dimensions 21.7 m x 7.1 m x 3.8 m, designed to represent a variety of spaces in a NPP containing power and control cables. The walls and ceiling are covered with two layers of 25 mm thick marinate boards, while the floor is covered with two layers of 25 mm thick gypsum boards. The room has one 2 m x 2 m door and a mechanical air injection and extraction system. Ventilation conditions and fire size and location are varied, and the numerous experimental measurements include gas and surface temperatures, heat fluxes, and gas velocities.

ICFMP BE #4: Benchmark Exercise #4 consists of kerosene pool fire experiments conducted at the Institut für Baustoffe, Massivbau und Brandschutz (iBMB) of the Braunschweig University of Technology in Germany. The results of two experiments were contributed to the International Collaborative Fire Model Project (ICFMP). These fire experiments involve relatively large fires in a relatively small (3.6 m x 3.6 m x 5.7 m high) concrete enclosure. Only one of the two experiments was selected for the present V&V study (Test 1).

ICFMP BE #5: Benchmark Exercise #5 consists of fire experiments conducted with realistically routed cable trays in the same test compartment as BE #4. Only one test (Test 4) was selected for the present evaluation, and only the first 20 min during which time an ethanol pool fire pre-heats the compartment.

FM/SNL Series: The Factory Mutual & Sandia National Laboratories (FM/SNL) Test Series is a series of 25 fire tests conducted for the NRC by Factory Mutual Research Corporation (FMRC), under the direction of Sandia National Laboratories (SNL). The primary purpose of these tests was to provide data with which to validate computer models for various types of NPP

compartments. The experiments were conducted in an enclosure measuring 60 ft long x 40 ft wide x 20 ft high (18 m x 12 m x 6 m), constructed at the FMRC fire test facility in Rhode Island. All of the tests involved forced ventilation to simulate typical NPP installation practices. The fires consist of a simple gas burner, a heptane pool, a methanol pool, or a polymethyl-methacrylate (PMMA) solid fire. Four of these tests were conducted with a full-scale control room mockup in place. Parameters varied during testing were fire intensity, enclosure ventilation rate, and fire location. Only three of these tests have been used in the present evaluation (Tests 4, 5 and 21). Test 21 involves the full-scale mock-up. All are gas burner fires.

NBS Multi-Room Series: The National Bureau of Standards (NBS, now the National Institute of Standards and Technology, NIST) Multi-Compartment Test Series consists of 45 fire tests representing 9 different sets of conditions, with multiple replicates of each set, which were conducted in a three-room suite. The suite consists of two relatively small rooms, connected via a relatively long corridor. The fire source, a gas burner, is located against the rear wall of one of the small compartments. Fire tests of 100, 300 and 500 kW were conducted, but for the current V&V study, only three 100 kW fire experiments have been used (Test 100A, 100O, and 100Z).

The results for FDT^S comparisons are organized by the following quantities:

- Hot Gas Layer Temperature and Height
- Plume Temperature
- Flame Height
- Target/Radiant Heat Flux

As previously defined, validation is the process of determining the degree to which a calculation method accurately represents the real world from the perspective of its intended uses. To fulfill the need for validation, the experiments described above were modeled using the appropriate FDT^S spreadsheets, and the results from the FDT^S computations were then compared to the experimental measurements and presented in the form of relative differences. Peak values were compared from both the model predictions and the experimental data. For the comparison, the researchers used the following equation for relative difference between model and experiment:

$$\varepsilon = \frac{\Delta M - \Delta E}{\Delta E} = \frac{\left(M_p - M_o\right) - \left(E_p - E_o\right)}{\left(E_p - E_o\right)}$$

where ΔM is the difference between the modeled peak value (M_p) of the evaluated parameter and its original value (M_o), and ΔE is the difference between the experimental observation (E_p) and its original value (E_o). Appendix A lists the calculated relative differences for the fire modeling parameters listed above using FDT^S.

The measure of model "accuracy" used throughout this study is related to experimental uncertainty. Volume 7 discusses this issue in detail. In brief, the accuracy of a *measurement*, e.g. gas temperature, is related to the measurement device, e.g. a thermocouple. In addition, the accuracy of the *model prediction* of the gas temperature is related to the simplified physical description of the fire and to the accuracy of the input parameters, e.g. the *specified* heat release rate, which is based on experimental measurements. Ideally, the purpose of a validation study is to determine the accuracy of the model in the absence of any errors related to the measurement of both its inputs and outputs. Because it is impossible to eliminate experimental uncertainty, at

the very least a combination of the uncertainty in the measurement of model inputs and output can be used as a yard stick. If the numerical prediction falls within the range of uncertainty due to both the measurement of the input parameters and the output quantities, it is not possible to quantify its accuracy further. At this stage, it is said that the prediction is *within experimental uncertainty.*

Each section in this chapter contains a scatter plot that summarizes the relative difference results for all of the predictions and measurements of the quantity under consideration. Details of the calculations, the input assumptions, and the time histories of the predicted and measured output are included in Appendix A. Only a brief discussion of the results is included in this chapter. Included in the scatter plots are an estimate of the combined uncertainty for the experimental measurements and uncertainty in the model inputs. It is important to understand that these are simply estimates of the lower bounds of random uncertainty and do not include systematic uncertainty in either the experimental measurements or model predictions. Along with expert engineering judgment of the project team, these uncertainty bounds serve as guidelines to judge the predictive capability of the model.

At the end of each section, a color rating is assigned to each of the output categories, indicating, in a very broad sense, how well the model treats that particular quantity. A detailed discussion of this rating system is included in Volume 1. For FDT^S, the Green, Yellow+, and Yellow ratings have been assigned to 4 of the 13 quantities of interest because these quantities fall within the capability of the FDT^S library. The color Green indicates that the research team concluded the physics of the model accurately represent the experimental conditions and the calculated relative differences comparing the model and the experimental are consistent with the combined experimental and input uncertainty. The color Yellow+ indicates that the research team concluded the physics of the model accurately represent the experimental conditions and the model consistently over predicted the experimental measurements outside the combined experimental and input uncertainty. The user should take care and use caution when interpreting the results of the model for these parameters. The color Yellow suggests that one exercise caution when using the model to evaluate this quantity – consider carefully the assumptions made by the model, how the model has been applied, and the accuracy of its results. There is specific discussion of model limitations for the quantities assigned a Yellow rating. Parameters that are not given a color rating indicate that the model does not include output to be able to evaluate that parameter in its as-tested version.

6.1 Hot Gas Layer Temperature and Height

The single most important prediction a fire model can make is the temperature of the hot gas layer (HGL). After all, the impact of the fire is not so much a function of the heat release rate, but rather the temperature of the compartment. Following is a summary of the accuracy assessment for the HGL temperature predictions of the six test series. HGL Height calculations were not evaluated because FDT^S does not contain a method applicable to any of the test series.

ICFMP BE #2: FDT^S, using the methods of Beyler and Foote, Pagni, and Alvares, over-predicted the HGL temperature for all three cases. None of the predictions fell within the combined uncertainty bands. For the closed compartment predictions, the relative differences probably stem from an imprecise accounting of leakage in the model. The forced ventilation relative differences for case 3 might be a result of the fact that the spreadsheet used does not

account for natural flow through open doorways. The model calculations were performed with mineral wool as the wall material because it is much less conductive than steel and results in more realistic model results. In the actual experiment the walls were made up of a 1 mm (0.04 in) thick layer of sheet metal covering a 0.05 m (2 in) layer of mineral wool.

ICFMP BE #3: FDT^S over-predicted the HGL temperature for all fifteen tests. The open doors tests (Tests 3, 5, 9, 14, 15, and 18) using the method of McCaffrey, Quintiere, and Harkleroad are closer to experimental data than the closed door tests, with the exception of Test 5. In this test, the combination of open doors and mechanical ventilation (using the method of Foote, Pagni, and Alvares) led to experimental temperatures that were lower than similar tests without mechanical ventilation. None of the predictions fell within the combined uncertainty bands. For the closed compartment predictions where the method of Beyler was used, the relative differences probably stem may be the result of actual leakage. Beyler's correlation for closed compartments only assumes a small leakage rate that will prevent a pressure buildup in the compartment. Therefore, if significant leakage did exist during the actual tests it could have contributed to lower temperatures by allowing the hot gases inside the compartment to escape.

ICFMP BE #4: Using the Beyler method, FDT^S under-predicted the HGL temperature for this test, outside of the combined uncertainty bands. The assumptions in the natural ventilation spreadsheet may not be appropriate for this test configuration due to the relatively large fire in a relative small compartment. The compartment likely allowed more energy to build into the HGL and not as much to be lost out of the opening, thus creating an imbalance and a hotter HGL. The experimental temperature also reached levels outside the bounds where this correlation is applicable.

ICFMP BE #5: Test ICFMP BE #5 was conducted in the same compartment as test ICFMP BE #4 but utilized a smaller doorway and a smaller sized fire. As a result, the FDT^S prediction, using Beyler's method for a closed compartment with natural ventilation, fell within the combined experimental uncertainty. This is likely due to the smaller fire size.

FM/SNL: The Foote, Pagni, and Alvares method was used to predict the HGL temperatures in the FM/SNL tests. FDT^S over-predicted the HGL temperature for the three tests, well outside experimental uncertainty. Tests 4 and 21 had a ventilation rate of approximately 0.37 m^3/s (800 cfm), while Test 5 had a ventilation rate of approximately 3.7 m^3/s (8,000 cfm). As can be seen in Figure 6-1 the FM/SNL 5 test had the smallest relative difference (69%). The FPA model appears to work better with larger ventilation rates.

NBS Multi-Room: Using the method of McCaffrey, Quintiere, and Harkleroad FDT^S predicted the HGL temperature to within the experimental uncertainty for the three NBS tests. The model calculations were performed with a ceramic fiber as the wall material because it is less conductive than fire brick and results in more realistic model results. In the actual experiment the walls of the room of fire origin were made up of a 0.1 m (4 in) thick fire brick covered with a 0.05 m (2 in) thick ceramic fiber. It is also important to note that the standard reduction method was not used to compute the experimental HGL temperature or height for this test series. Rather, the test director reduced the layer information individually for the eight thermocouple arrays using an alternative method [Ref. 16].

Summary: **HGL Temperature—YELLOW+**

- The FDT^S models for HGL temperature capture the appropriate physics and are based on appropriate empirical data.
- FDT^S generally over-predicts HGL temperature, outside of uncertainty.

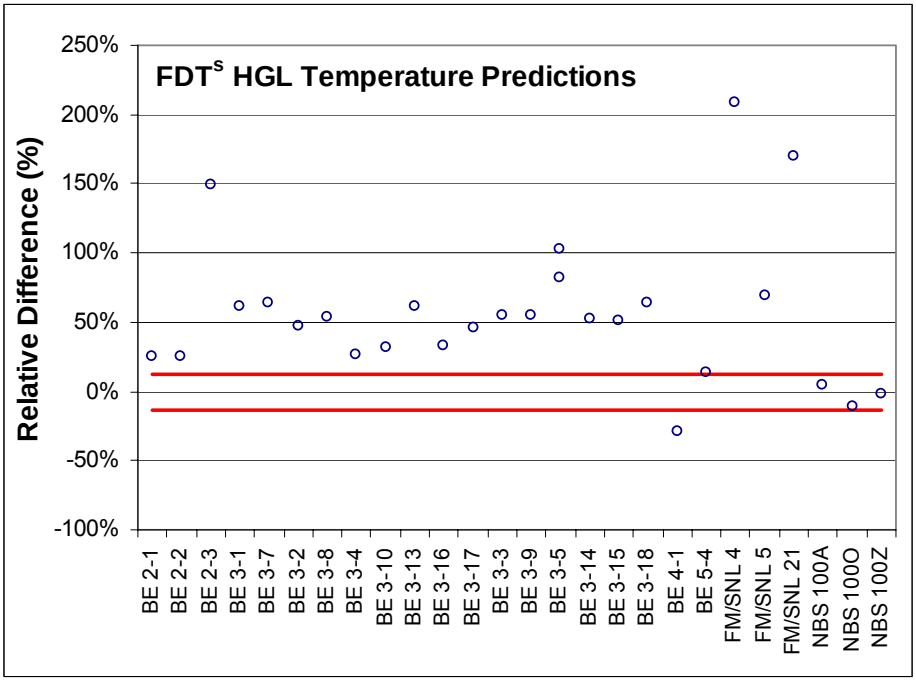

Figure 6-1: Relative Differences for HGL Temperature

6.2 Plume Temperature

Plume temperature data used to assess the accuracy of FDT^S predictions were taken from ICFMP Benchmark Exercise #2 at 7 and 13 meters above the fire source and in the FM/SNL test at 5.66 meters above the fire source. A total of 9 plume temperature data points were included in this study. The spreadsheet in the FDT^S library used to estimate the centerline temperature of a buoyant plume is 09_Plume_Temperature_Calculations.xls.

The primary user inputs to the plume temperature algorithm in FDT^S are HRR, the ambient air temperature of the enclosure, the elevation above the fuel source, and the area of combustible fuel. The inputs and assumptions required for the spreadsheet in FDT^S used to estimate the plume temperature are discussed in detail in Chapter 3, Section 3.7.

ICFMP BE #2: Heskestad's correlation in FDT^S under-predicts the plume temperature in five of the six cases in this test series. At 12 meters above the fire source FDTS under-predicts by around 40% in all 3 cases. At 6 meters above the fire source, FDT^S is more accurate, but it still under predicts in cases 1 and 2 and predicts within experimental uncertainty in case 3. However, upon observation of the plots in Figure A-9 in Appendix A, one can see that heat up of the plume is more closely modeled in cases 1 and 2. In cases 1 and 2 the doors to the compartment were closed, while in case 3, both natural and mechanical ventilation were present. The inaccurate FDT^S plume temperature calculations can be attributed to the fact that the Heskestad plume temperature correlation is not valid at elevations where the plume enters a smoke layer. The

HGL generally reached the 6 meter height within approximately two minutes for all three cases. This resulted in the inaccuracies of the model for the majority of each test.

FM/SNL: In this test series FDT^S, using Heskestad's correlation, under-predicts the plume temperature in tests 4 and 5 and predicts within experimental uncertainty in test 21. In tests 4 and 5 the fire was located in the center of the compartment, while in test 21 the fire was located inside an electrical cabinet. It is possible that the model predictions came closer to those observed in the experiment for test 21 because some of the heat generated by the fire was absorbed by the walls of the cabinet, thus reducing the temperatures in the plume during the experiment. The FDT^S algorithm has no way of taking this effect into account. The plots in Figure A-10 in Appendix A indicate that the transport lag effect is reduced somewhat, perhaps due to the shorter distance in question.

The scatter plot shown below depicts the relative differences between the peak plume temperature recorded in the experiments and the predictions made by the FDT^S algorithm. The red lines shown at -10% and 10% represent the approximate bounds to the combined uncertainty of the input values and the measurement of the experimental outputs. In these cases it appears that the maximum plume temperature estimates for the given conditions were always either under predicted or were predicted within experimental uncertainty. However, in both cases in which the temperature was predicted within experimental uncertainty it can be argued that the experimental temperatures were lowered due to test conditions that were not accounted for in the FDT^S prediction.

Summary: Plume Temperature – YELLOW

- The FDT^S model for plume temperature is based on appropriate empirical data and is physically appropriate.
- FDT^S generally under-predicts plume temperature, outside of uncertainty.
- The FDT^S model is not appropriate for predicting the plume temperatures at elevations within a hot gas layer.

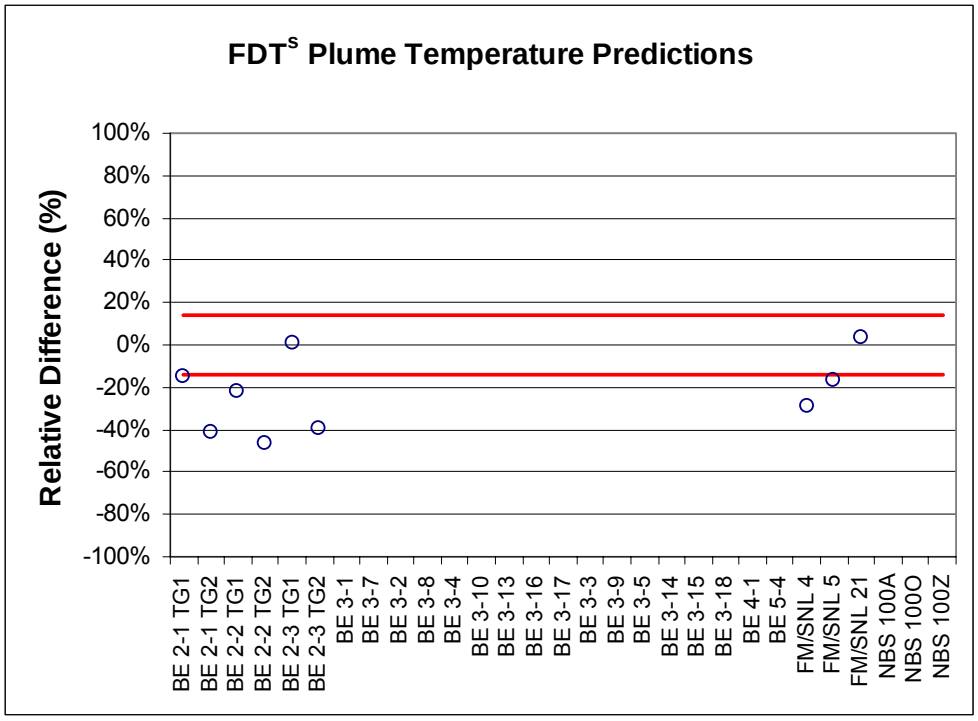

Figure 6-2: Relative Differences for Plume Temperature

6.3 Flame Height

Flame height is recorded by visual observations, photographs or video footage. Photographs from the ICFMP BE #2 test series and video from BE #3 test series are available. It is difficult to precisely measure the flame height, but the photos and videos allow one to make estimates accurate to within a pan diameter. Such observations can be compared with outputs from Heskestad's flame height correlation.

ICFMP BE #2: The height of the visible flame in these tests has been estimated to be between 2.4 and 3 pan diameters (3.8 m (12.5 ft) to 4.8 m (15.7 ft)). From Heskestad's flame height correlation in the FDT^S the estimated flame height is 4.3 m (14.1 ft).

ICFMP BE #3: During BE #3, Test 3, the peak flame height is estimated to be 2.8 m, roughly consistent with the view through the doorway in compartment. FDT^S results in a flame height of 3.0 m (9.8 ft) using Heskestad's flame height prediction.

Summary: Flame Height – GREEN

- The FDT^S model predicted flame heights consistent with visual test observations.

6.4 Target/Radiant Heat Flux

As described in Chapter 3, the FDT^S library of correlations includes a radiation heat flux model that estimates heat flux at a specific distance away from a fire. This model, called the point source radiation model, was compared to radiant heat flux data from the ICFMP BE #3 experiments.

ICFMP BE #3: The FDT^S spreadsheet used to calculate radiant heat flux is 05.1_Heat_Flux_Calculations_Wind_Free.xls. This spreadsheet uses Drysdale's equation for calculating the radiant heat flux. The graphs in Figures A-11 through A-18 in Appendix A and the scatterplot below do not indicate any specific trends about the accuracy of FDT^S in calculating radiant heat flux using the point source model. For a number of tests the model predicts the peak radiant heat flux at the gauge within the uncertainty of the input parameters and the experimental measurements. For other tests the model both under-predicts and over-predicts the radiant heat flux at a target, outside uncertainty bands. The reason that the model predictions varied so greatly can be attributed to the fact that the point source radiation model is not meant to be used for locations within a hot gas layer.

As can be seen in Figure 6-3 the majority of the under-predictions occurred at gauge 10, which was located at 1.8 m (5.9 ft) above the floor. Most of the over-predictions occurred at locations higher in the hot gas layer. Gauges 1, 3, and 7 were located at 2, 2.5, and 3 m (6.6, 8, and 9.8 ft) respectively above the floor. These gauges were immersed in smoke during all the tests by the time that the radiation measurements were selected for comparison.

Summary: Radiant Heat Flux – YELLOW

- The FDT^S point source radiation model in general is based on appropriate empirical data and is physically appropriate with consideration of the simplifying assumptions.
- The FDT^S point source radiation model is not valid for elevations within a hot gas layer.
- FDT^S predictions had no clear trend. The model under- and over-predicted, outside uncertainty.
- The point source radiation model is intended for predicting radiation from flames in an unobstructed and smoke-clear path between flames and targets.

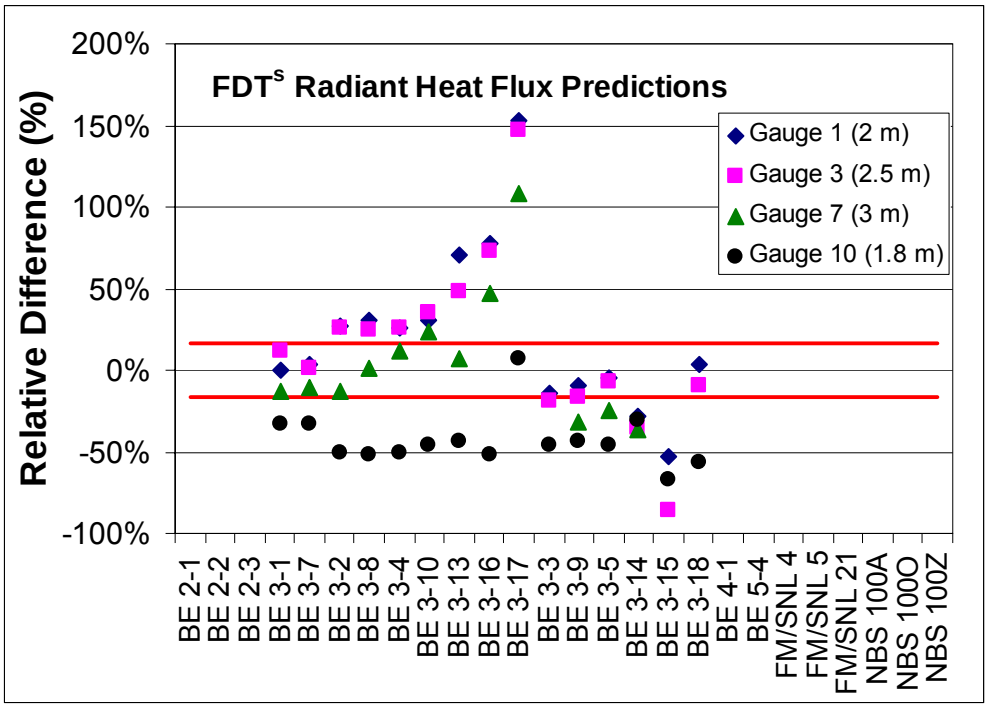

Figure 6-3: Relative Differences for Radiant Heat Flux

6.5 Summary

This chapter presents a summary of numerous comparisons of the FDT^S model with a range of experimental results conducted as part of this V&V effort. Four quantities were selected for comparison and a color rating assigned to each of the output categories, indicating, in a very broad sense, how well the model treats that particular quantity:

- Hot Gas Layer (HGL) Temperature: Yellow+
- Plume Temperature: Yellow
- Flame Height: Green
- Radiant Heat Flux: Yellow

One of the quantities (flame height) was assigned a green rating indicating that the research team concluded the physics of the model accurately represent the experimental conditions and the calculated relative differences comparing the model and the experimental are consistent with the combined experimental and input uncertainty.

- FDT^S predicts the flame height consistent with visual observations of flame height for the experiments.

One of the quantities (hot gas layer temperature) was assigned a yellow+ rating indicating that the research team concluded the physics of the model accurately represent the experimental conditions, but the calculated relative differences comparing the model and the experimental results are not consistent with the combined experimental and input uncertainty. The yellow+ rating indicates that most of the results outside the relative uncertainty resulted in over-

predictions of the HGL temperatures. The user should take caution when using the model to evaluate HGL temperatures and should not automatically assume that the model will always over predict these values.

Two of the quantities (plume temperature and radiant heat flux) were assigned a yellow rating indicating the user should take caution when using the model to evaluate that quantity. This typically indicates limitations in the use of the model. A few notes on the comparisons are appropriate:

- The FDT^S plume temperature and point source radiation models are not valid for elevations within a hot gas layer.
- The point source radiation model is only intended for predicting radiation from flames in an unobstructed and smoke-clear path between flames and targets.
- FDT^S predictions had no clear trend for either parameter. The model under- and over-predicted, outside uncertainty.

The FDT^S predictions in this validation study used physically appropriate models but often resulted in predictions outside of the relative uncertainty. As such, it is important for the user to exercise caution when using the FDT^S spreadsheets to model fire scenarios. Like all predictive models, the best predictions come with a clear understanding of the limitations of the model and of the inputs provided to do the calculations.

7
REFERENCES

1. U.S. Nuclear Regulatory Commission, "Fire Dynamics Tools (FDT^S) Quantitative Fire Hazard Analysis Methods for the U.S. Nuclear Regulatory Commission Fire Protection Inspection Program," NUREG-1805, November 2004.
2. National Fire Protection Association, NFPA 805, *Performance-Based Standard for Fire Protection for Light Water Reactor Electric Generating Plants*, Quincy, Massachusetts, 2001.
3. ASTM International, ASTM E1355-05a, *Standard Guide for Evaluating the Predictive Capability of Deterministic Fire Models*, 2005.
4. ASTM International, ASTM E1321-97a, *Standard Test Method for Determining Material Ignition and Flame Spread Properties*, 2002.
5. Quintiere, J.G., and B.J. McCaffrey, "The Burning of Wood and Plastic Cribs in an Enclosure: Volume 1," NBSIR 90-2054, National Bureau of Standards (NBS), U.S. Department of Commerce, Washington, DC, November 1980.
6. Babrauskas, V., "Burning Rates," Section 3, Chapter 3-1, *SFPE Handbook of Fire Protection Engineering*, 2nd Edition, P.J. DiNenno, Editor-in-Chief, National Fire Protection Association, Quincy, Massachusetts, 1995.
7. Drysdale, D.D., *An Introduction to Fire Dynamics*, Chapter 4, "Diffusion Flames and Fire Plumes," 2nd Edition, John Wiley and Sons, New York, pp.109–158, 1998.
8. Beyler, C.L., "Fire Hazard Calculations for Large Open Hydrogen Fires," Section 3, Chapter 1, *SFPE Handbook of Fire Protection Engineering*, 3rd Edition, P.J. DiNenno, Editor-in-Chief, National Fire Protection Association, Quincy, Massachusetts, 2002.
9. Heskestad, G., "Fire Plumes," Section 2, Chapter 2-2, *SFPE Handbook of Fire Protection Engineering*, 2nd Edition, P.J. DiNenno, Editor-in-Chief, National Fire Protection Association, Quincy, Massachusetts, 1995.
10. Modak, A., "Thermal Radiation from Pool Fires," *Combustion and Flames*, Volume 29, pp. 177–192, 1977.
11. Thomas, P.H., "The Size of Flames from Natural Fires," *Ninth Symposium (International) on Combustion*, The Combustion Institute, Pittsburgh, Pennsylvania, pp. 844–859, 1962.
12. Beyler, C.L., "Analysis of Compartment Fires with Overhead Forced Ventilation," *Proceedings of the 3rd International Symposium, International Association of Fire Safety Science (IAFSS)*, Cox and Langford, Editors, Elsevier Applied Science, New York, pp.291-300, 1991.

13. Walton, W.D., and P.H. Thomas, "Estimating Temperatures in Compartment Fires," Section 3, Chapter 3-6, *SFPE Handbook of Fire Protection Engineering*, 2nd Edition, P.J. DiNenno, Editor-in-Chief, National Fire Protection Association, Quincy, Massachusetts, 1995.

14. Walton, W.D., and P.H. Thomas, "Estimating Temperatures in Compartment Fires," Section 3, Chapter 6, *SFPE Handbook of Fire Protection Engineering*, 3rd Edition, P.J. DiNenno, Editor-in-Chief, National Fire Protection Association, Quincy, Massachusetts, 2002.

15. Deal, S., and C.L. Beyler, "Correlating Preflashover Room Fire Temperatures," *SFPE Journal of Fire Protection Engineering*, Volume 2, No. 2, pp. 33-48, 1990.

16. Foote, K.L, P.J. Pagni, and N.L. Alvares, "Temperature Correlations for Forced-Ventilated Compartment Fires," Fire Safety Science – Proceedings of the First International Symposium, International Association of Fire Safety Science (IAFSS), Grant and Pagni, Editors, Hemisphere Publishing Corporation, New York, pp. 139-148, 1985.

17. Karlsson, B., and J.G. Quintiere, *Enclosure Fire Dynamics*, Chapter 8, "Conservation Equations and Smoke Filling," CRC Press LLC, New York, p.206, 1999.

18. Peacock, R.D., S. Davis, and B.T. Lee, NBSIR 88-3752, "An Experimental Data Set for the Accuracy Assessment of Room Fire Models," U.S. Department of Commerce, Gaithersburg, MD, April 1988.

19. Yamana, T., and T. Tanaka, "Smoke Control in Large Spaces, Part 1: Analytical Theories for Simple Smoke Control Problems," *Fire Science and Technology*, Volume 5, No. 1, 1985.

20. *SFPE Handbook of Fire Protection Engineering, Third Edition*. P.J. DiNenno, Editor-in-Chief. National Fire Protection Association. Quincy, MA. 2002.

21. *NFPA Fire Protection Handbook, 18th Edition*. A.E. Cote, Editor-in-Chief. National Fire Protection Association. Quincy, MA. 1997.

Bibliography

U.S. Nuclear Regulatory Commission, "International Collaborative Project to Evaluate Fire Models for Nuclear Power Plant Applications: International Panel Report on Benchmark Exercise #1, Cable Tray Fires," Dey, M., NUREG-1758, June, 2002.

Budnick, E.K., D.D. Evans, and H.E. Nelson, "Simple Fire Growth Calculations," Section 11 Chapter 10, *NFPA Fire Protection Handbook*, 18th Edition, National Fire Protection Association, Quincy, Massachusetts, 1997.

Delichatsios, M.A., "Flame Heights of Turbulent Wall Fire with Significant Flame Radiation," *Combustion Science and Technology*, Volume 39, pp. 195–214, 1984.

Hasemi Y., and T.Tokunaga, "Modeling of Turbulent Diffusion Flames and Fire Plumes for the Analysis of Fire Growth," *Proceedings of the 21st National Heat Transfer Conference*, American Society of Mechanical Engineers (ASME), 1983.

Hasemi Y., and T.Tokunaga, "Some Experimental Aspects of Turbulent Diffusion Flames and Buoyant Plumes from Fire Sources Against a Wall and in Corner of Walls," *Combustion Science and Technology*, Volume 40, pp. 1–17, 1984.

Cote, A., and P. Bugbee, *Principle of Fire Protection*, 2nd Edition National Fire Protection Association, Quincy, Massachusetts, 1988.

Friedman, R., *Principles of Fire Protection Chemistry and Physics*, 3rd Edition, National Fire Protection Association, Quincy, Massachusetts, 1998.

Fire Dynamics Course Guide, Federal Emergency Management Agency (FEMA), United States Fire Administration (USFA), National Emergency Training Center, Emmitsburg, Maryland, 1995.

Icove, D.J., and J.D. DeHaan, *Forensic Fire Science Reconstruction*, 1st Edition, Pearson Education Inc., Upper Saddle River, New Jersey, 2004.

Quintiere, J.G., *Principles of Fire Behavior*, Chapter 9, "Compartment Fires,", Delmar Publishers, Albany, New York, pp. 169–195, 1997.

Quinitiere, J.G., "A Simple Correlation for Predicting Temperature in a Room Fire," NBSIR 83-2712, National Bureau of Standards (NBS), U.S. Department of Commerce, Washington, DC, June 1983.

American Gas Association (AGA), "LNG Safety Research Program," Report IS 3–1, 1974.

Barry, T.F., *Risk-Informed, Performance-Based Industrial Fire Protection*, T.F. Barry Publications and Tennessee Valley Publications, Knoxville, Tennessee, 2002.

EPRI TR-100370, "Fire-Induced Vulnerability Evaluation (FIVE)," Final Report, Electrical Power Research Institute, Palo Alto, California, April 1992.

Fay, J.A., and D.H. Lewis, "Unsteady Burning of Unconfined Fuel Vapor Clouds," *Sixteenth Symposium (International) on Combustion*, The Combustion Institute, Pittsburgh, Pennsylvania, pp. 1397–1404, 1977.

Hasegawa, K., and K. Sato, "Study on the Fireball Following Steam Explosion of n-Pentane," *Second Symposium on Loss Prevention and Safety Promotion in the Process Industries*, Heidelberg, pp. 297–304, 1977.

Nolan, D.P., *Handbook of Fire and Explosion Protection Engineering Principles for Oil, Gas, Chemical and Related Facilities*, Noyes Publications, Westwood, New Jersey, 1996.

Roberts, A., "Thermal Radiation Hazards from Release of LPG Fires from Pressurized Storage," *Fire Safety Journal*, Volume 4, pp. 197–212, 1982.

SFPE Engineering Guide, "Assessing Flame Radiation to External Targets from Pool Fires," Society of Fire Protection Engineers (SFPE), Bethesda, Maryland, June 1999.

Shokri, M., and C.L. Beyler, "Radiation from Large Pool Fires," *SFPE Journal of Fire Protection Engineering*, Volume 1, No. 4, pp.141–150, 1989.

Alpert, R.L., and E.J. Ward, "Evaluation of Unsprinklered Fire Hazard," *Fire Safety Journal*, Volume 7, No. 177, 1984.

Heskestad, G., "Fire Plumes," Section 2, Chapter 2, *SFPE Handbook of Fire Protection Engineering*, 2nd Edition, P.J. DiNenno, Editor-in-Chief, National Fire Protection Association, Quincy, Massachusetts, 1995.

George, W.K., R.L. Alpert, and F. Tamanini, "Turbulence Measurements in an Axisymmetric Buoyant Plume," *International Journal of Heat Mass Transfer*, Volume 20, pp.1145–1154, 1977.

A
TECHNICAL DETAILS OF THE FDT^S VALIDATION STUDY

This appendix provides technical basis for the relative difference values listed in Chapter 6 of Volume 2 for the output parameters in the compilation of quantitative fire hazard analysis tools, FDT^S. This appendix is organized into sections for the parameters that have been verified and validated in this study for this specific tool. Not all of the spreadsheets included in FDT^S have been subjected to verification and validation due to a lack of experimental data for comparison. Each section presents a graph of the experimental data and the model output and a table of relative differences at the peaks between experimental data and the model output. The sections also describe the process and the values selected for input to the model. Within each section, the graphs are grouped by experimental test series. Discussion and analysis of the relative differences can found in Chapter 6 of Volume 2. The Appendix is organized into four sections, as follows:

A.1 Hot Gas Layer Temperature and Height

A.2 Plume Temperature

A.3 Flame Height

A.4 Target Heat Flux

Volume 7 includes detailed discussion of the uncertainties associated with both the experimental data and model predictions presented in this Appendix.

A.1 Hot Gas Layer Temperature and Height

Hot gas layer (HGL) temperatures in the experiments were estimated using data from ICFMP benchmark exercises (BE) 2, 3, 4, and 5, the FM/SNL test series, and the NBS multi-compartment fire test series for the room of fire origin. Specifically, thermocouple tree data from those experiments was reduced to an instantaneous average temperature above the estimated layer interface height at a specific time step. The layer interface height is deduced from the continuous vertical profile of temperature indicated by the thermocouple tree data. Relative differences were calculated by comparing the peak HGL temperatures and heights estimated from the experiment to the peak predicted HGL temperatures calculated using FDT^S. Peak or, where available, steady-state heat release rates were used as inputs to the spreadsheets. The heat release rate values for the different experiments are located in tables in this volume.

A.1.1 ICFMP BE # 2

This test series consisted of three full-scale experiments with replicates. The experimental data reported here are averages of the replicate tests. In Cases 1 and 2 the test compartment was sealed with the exception of small openings incorporated as "infiltration ventilation," which amounted to approximately 2 m^2 (22 ft^2). Beyler's method for calculating HGL temperature in a closed compartment was used for Cases 1 and 2 (02.3_Temperature_CC.xls). The "infiltration ventilation" was considered small enough compared to the volume of the space so that a natural ventilation condition would not exist and Beyler's method would be appropriate.

In Case 3, mechanical exhaust ventilation (11 m^3/s [388 ft^3/s]) was employed, as well as two doorway openings (3.2 m^2 each [34 ft^3/s]). Although there is no specific correlation for the scenario with forced ventilation and open doorways, the method of Foote, Pagni, and Alvares for forced ventilation was used (0.2.2_Temperature_FV.xls).

A calculation method for HGL height is not found on the spreadsheets used for the predictions of BE #2. Also, the reduction method used to estimate experimental layer height from thermocouple trees does not apply to closed compartments. Therefore, no HGL height comparisons were made for BE #2.

For Cases 1 and 2, experimental HRR data at specific times was used as input to the spreadsheet. For Case 3, the spreadsheet requires a steady state HRR input. In this case, as a conservative assumption, the maximum HRR measured in the experiment was used as input. The interior wall material for all cases was assumed to be a 0.05 m layer of mineral wool. The experimental HRRs and wall thermal properties can be found in Table A-2.

Table A-1: Input Values for ICFMP BE # 2 Case 1 and 2

	Case 1	Case 2
Air		
Ambient Air Temperature (C)	20	20
Ambient Air Density (kg/m^3)	1.2	1.2
Room Size		
Compartment Width (m)	27	27
Compartment Length (m)	13.8	13.8
Compartment Height (m)	15.9	15.9
Wall Properties		
Interior Lining Thermal Inertia [$(kW/m^2\text{-}K)^2$-sec]	0.015	0.015
Interior Lining Thermal Conductivity (kW/m-K)	0.0002	0.0002
Interior Lining Specific Heat (kJ/kg-K)	0.15	0.15
Interior Lining Density (kg/m^3)	500	500
Interior Lining Thickness (m)	0.05	0.05

Table A-2: Input Values for ICFMP BE # 2 Case 3

Air	
Ambient Air Temperature (C)	20
Ambient Air Density (kg/m^3)	1.2
Room Size	
Compartment Width (m)	27
Compartment Length (m)	13.8
Compartment Height (m)	15.8
Wall Properties	
Interior Lining Thermal Inertia [(kW/m^2-K)^2-sec]	0.015
Interior Lining Thermal Conductivity (kW/m-K)	0.0002
Interior Lining Specific Heat (kJ/kg-K)	0.15
Interior Lining Density (kg/m^3)	500
Interior Lining Thickness (m)	0.05
Ventilation	
Forced Ventilation Flow Rate (cfm)	23500
Heat Release Rate	
Fire Heat Release Rate (kW)	3640

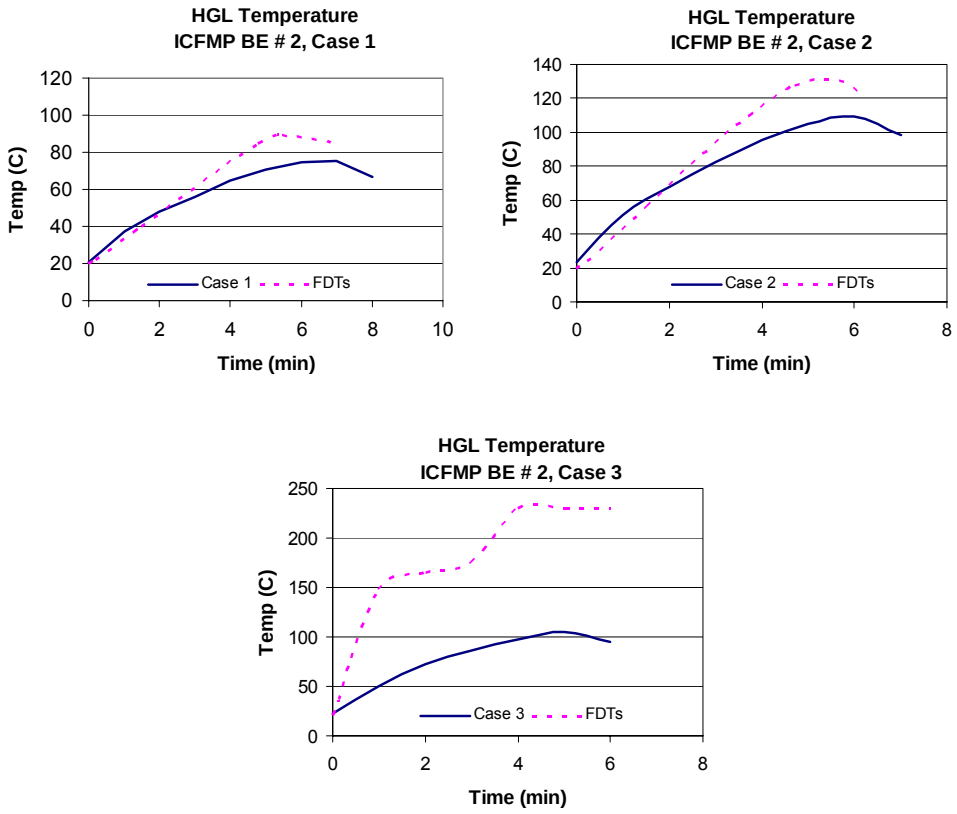

Figure A-1: Hot Gas Layer Temperature, ICFMP BE #2, Cases 1, 2, and 3

A.1.2 ICFMP BE # 3

The experiments in this test consisted of heptane and toluene spray fires varying nominally from 350 kW to 2 MW. There were 15 tests conducted with more than 370 channels of data for each test. Six of the 15 tests were conducted with open doors (3, 5, 9, 14, 15, 18) and 9 with closed doors (1, 2, 4, 7, 8, 10, 13, 16, 17). One of the open door tests (5) and 3 of the closed door tests (4, 10, 16) also had mechanical ventilation of approximately 0.81m^3/s (29 ft^3/s). The MQH model (02.1_Temperature_NV.xls) was used for open door tests without mechanical ventilation. The input values for these tests can be found in Table A-4. Beyler's method for calculating HGL temperature in closed compartments (02.3_Temperature_CC.xls) was used for closed door tests without mechanical ventilation. The input values for these tests can be found in Table A-3. The FPA model was used for all tests with forced ventilation (02.2_Temperature_FV.xls). The input values for these tests can be found in Table A-5. For Test 5, the combination of mechanical ventilation and open doors cannot be directly modeled using FDT^s, so there are two predictions reported—one using the forced ventilation model, and another using the natural ventilation model. The HRRs used for inputs were taken from the experimental report issued by NIST. The wall material was assumed to be Marinite I and the thermal properties were taken from manufacturer's data.

Table A-3: Input values for ICFMP BE#3 Closed Compartment Tests

	Test 1	Test 2	Test 7	Test 8	Test 13	Test 17
Air						
Ambient Air Temperature (C)	21.1	23.9	22.2	28.9	32.2	25.6
Ambient Air Density (kg/m^3)	1.2	1.19	1.2	1.17	1.16	1.18
Room Size						
Compartment Width (m)	7.04	7.04	7.04	7.04	7.04	7.04
Compartment Length (m)	21.7	21.7	21.7	21.7	21.7	21.7
Compartment Height (m)	3.82	3.82	3.82	3.82	3.82	3.82
Wall Properties						
Interior Lining Thermal Inertia [(kW/m^2-K)^2-sec]	0.11	0.111	0.11	0.11	0.11	0.11
Interior Lining Thermal Conductivity (kW/m-K)	0.00012	0.00012	0.00012	0.00012	0.00012	0.00012
Interior Lining Specific Heat (kJ/kg-K)	1.26	1.26	1.26	1.26	1.26	1.26
Interior Lining Density (kg/m^3)	737	737	737	737	737	737
Interior Lining Thickness (m)	0.0254	0.0254	0.0254	0.0254	0.0254	0.0254
Fire Heat Release Rate (kW)						
60 sec	410	1190	400	1190	2330	1160
120 sec	410	1190	400	1190	2330	1160
180 sec	410	1190	400	1190	2330	1160
240 sec	410	1190	400	1190	2330	1160
270 sec						1160
300 sec	410	1190	400	1190	2330	1160
360 sec					2330	
600 sec	410	1190	400	1190	2330	1160
900 sec	410		400		2330	1160
1200 sec	410		400			
1380 sec	410		400			

Table A-4: Input values for ICFMP BE # 3 No Ventilation Tests

	Test 3	Test 9	Test 14	Test 15	Test 18
Air					
Ambient Air Temperature (C)	27.8	28.9	25.6	23.3	24.4
Ambient Air Density (kg/m^3)	1.2	1.2	1.2	1.2	1.2
Room Size					
Compartment Width (m)	7.04	7.04	7.04	7.04	7.04
Compartment Length (m)	21.7	21.7	21.7	21.7	21.7
Compartment Height (m)	3.82	3.82	3.82	3.82	3.82
Wall Properties					
Interior Lining Thermal Inertia [(kW/m^2-K)^2-sec]	0.11	0.11	0.11	0.11	0.11
Interior Lining Thermal Conductivity (kW/m-K)	0.00012	0.00012	0.00012	0.00012	0.00012
Interior Lining Specific Heat (kJ/kg-K)	1.26	1.26	1.26	1.26	1.26
Interior Lining Density (kg/m^3)	737	737	737	737	737
Interior Lining Thickness (m)	0.0254	0.0254	0.0254	0.0254	0.0254
Ventilation					
Vent Width (m)	2	2	2	2	2
Vent Height (m)	2	2	2	2	2
Top of Vent from Floor (m)	2	2	2	2	2
Heat Release Rate					
Fire Heat Release Rate (kW)	1190	1170	1180	1180	1180

Table A-5: Input values for ICFMP BE # 3 Forced Ventilation Tests

	Test 4	Test 5	Test 10	Test 16
Air				
Ambient Air Temperature (C)	26.7	25	24.4	21.1
Ambient Air Density (kg/m^3)	1.2	1.2	1.2	1.2
Room Size				
Compartment Width (m)	7.04	7.04	7.04	7.04
Compartment Length (m)	21.7	21.7	21.7	21.7
Compartment Height (m)	3.82	3.82	3.82	3.82
Wall Properties				
Interior Lining Thermal Inertia [$(kW/m^2\text{-}K)^2$-sec]	0.11	0.11	0.11	0.11
Interior Lining Thermal Conductivity (kW/m-K)	0.00012	0.00012	0.00012	0.00012
Interior Lining Specific Heat (kJ/kg-K)	1.26	1.26	1.26	1.26
Interior Lining Density (kg/m^3)	737	737	737	737
Interior Lining Thickness (m)	0.0254	0.0254	0.0254	0.0254
Ventilation				
Forced Ventilation Flow Rate (cfm)	1907	1907	1907	1907
Heat Release Rate				
Fire Heat Release Rate (kW)	1200	1190	1190	2300

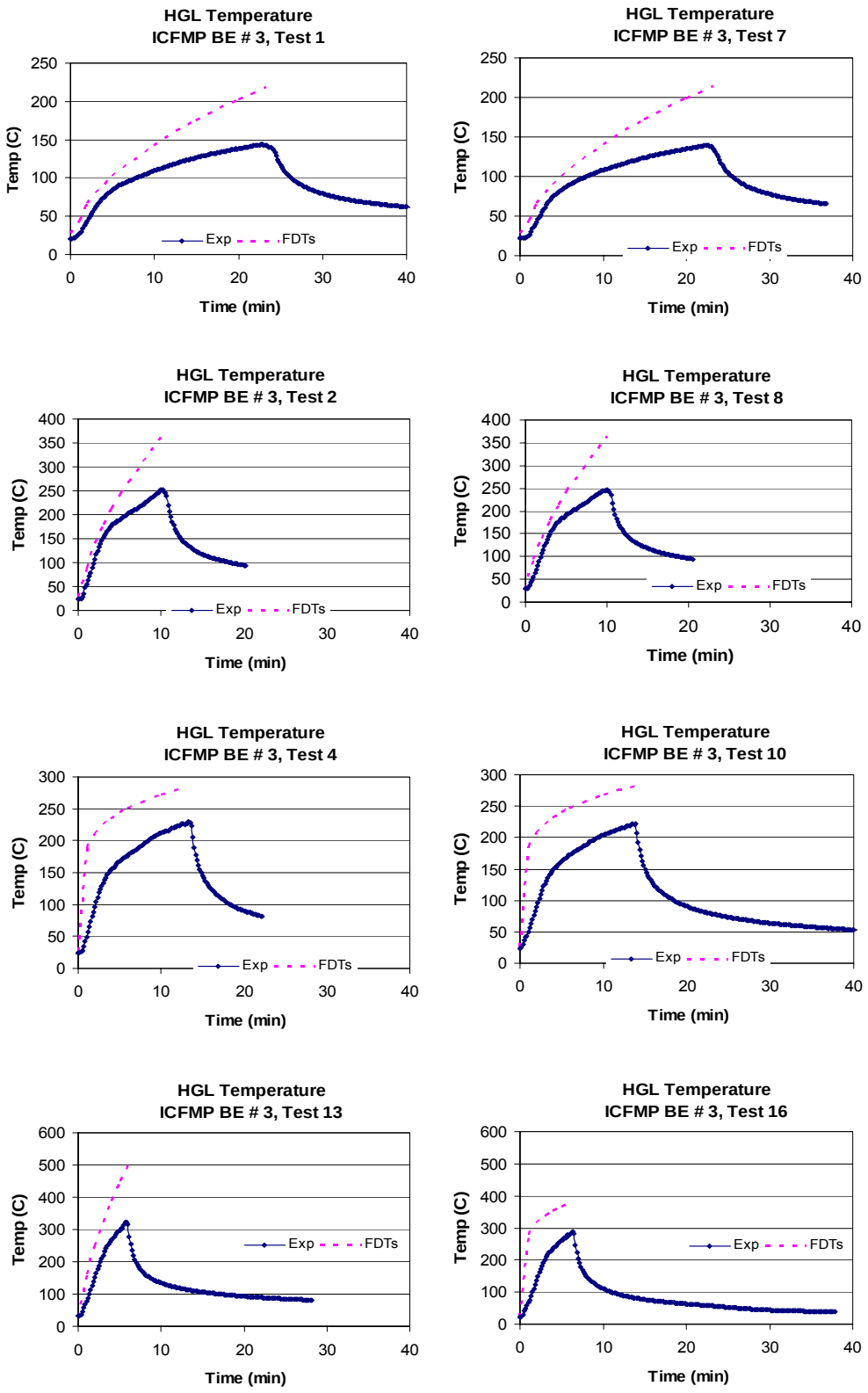

Figure A-2: Hot Gas Layer Temperature, ICFMP BE #3, closed door tests

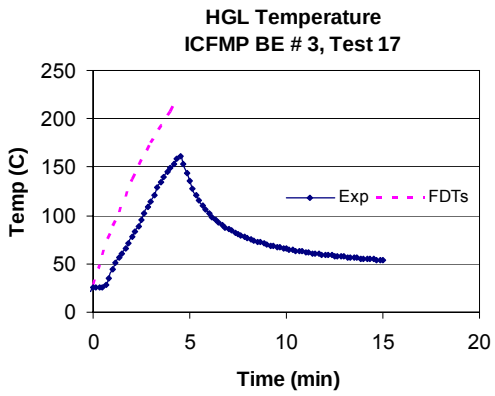

Figure A-3: Hot Gas Layer Temperature, ICFMP BE #3, closed door tests (cont.)

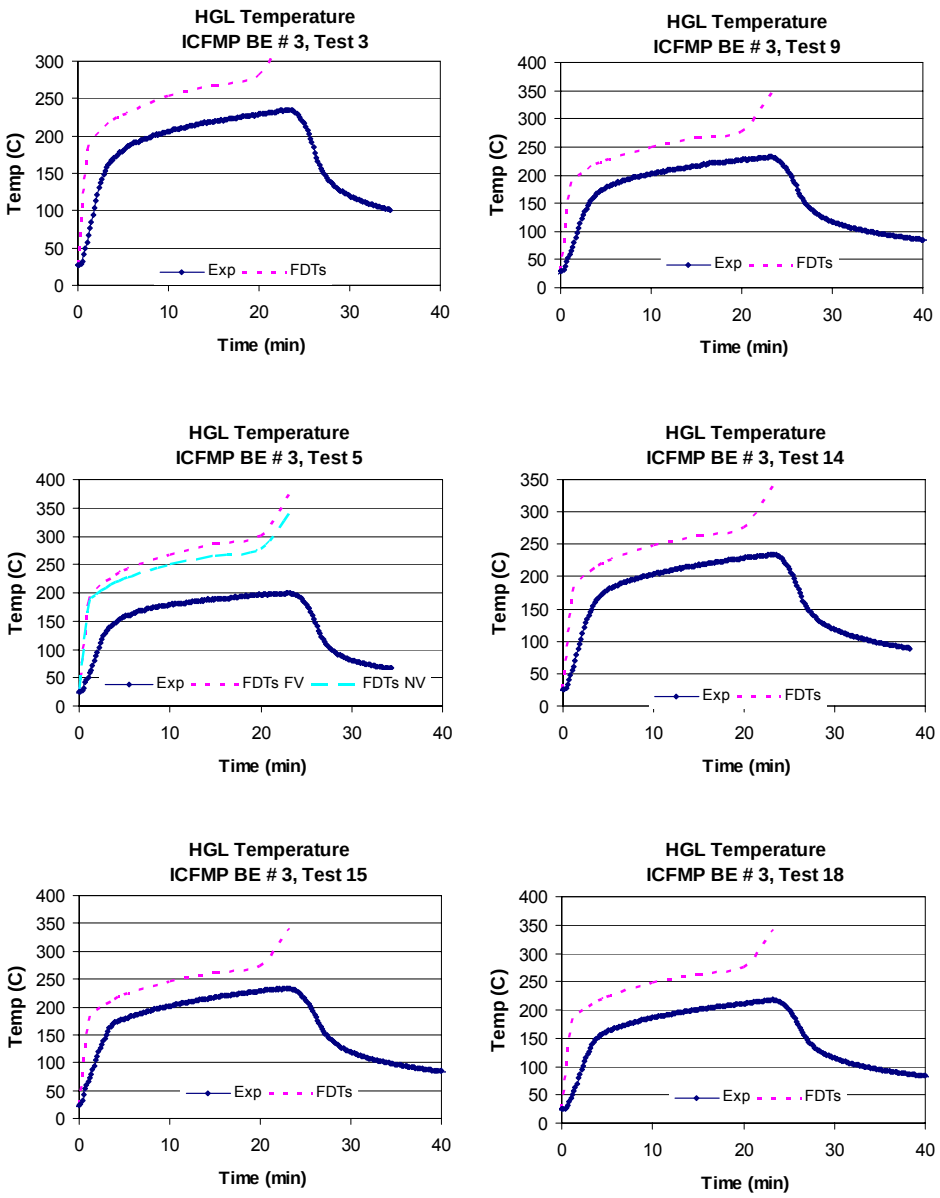

Figure A-4: Hot Gas Layer Temperature, ICFMP BE #3, open door tests

A calculation method for HGL height is only found on the spreadsheet for open door conditions. However, this calculation method is only valid before the layer descends to an opening and spills out of the fire room. The graphs for HGL height comparisons for open door rooms only depict the early times of the test, before the layer spills out of the room. A relative difference comparison is not made due to the restricted application of layer height calculation.

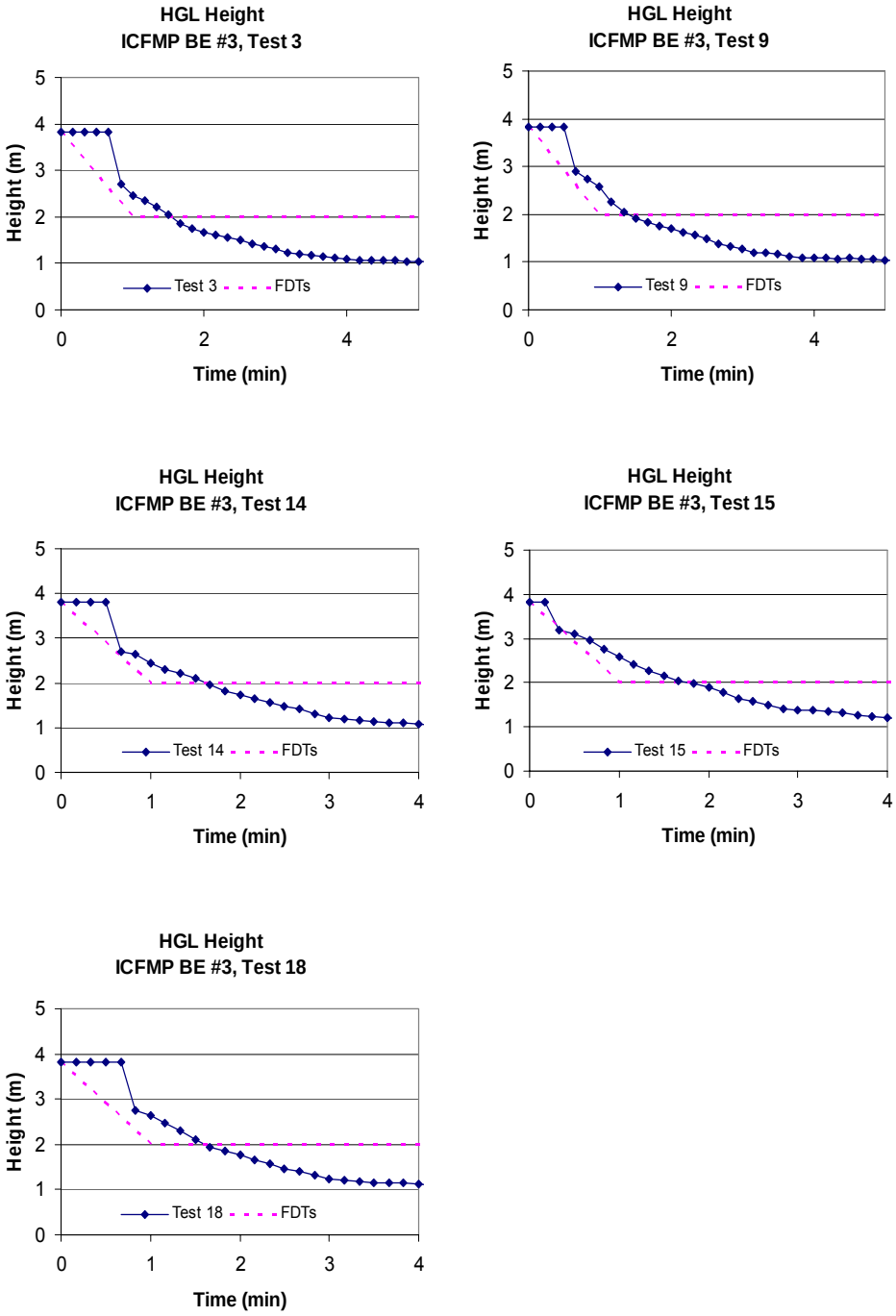

Figure A-5: Hot Gas Layer Height, ICFMP BE #3, open door tests w/o ventilation

A.1.3 ICFMP BE # 4

This experiment included a relatively large fire in a relatively small compartment. The compartment included a doorway of about 2.1m^2 (23 ft^2) and no mechanical ventilation. The spreadsheet in FDT^S used to estimate the HGL temperature for this exercise was 02.1_Temperature_NV.xls. The maximum experimental HRR was input as a steady-state value for the spreadsheet as a conservative assumption. The experimental HRR, thermal properties of the wall materials, and other input values can be found in Table A-6.

Experimental data for HGL Height during this test is not available for comparison.

Table A-6: Input Values for ICFMP BE # 4

Air	
Ambient Air Temperature (C)	20
Ambient Air Density (kg/m^3)	1.2
Room Size	
Compartment Width (m)	3.6
Compartment Length (m)	3.6
Compartment Height (m)	5.7
Wall Properties	
Interior Lining Thermal Inertia [(kW/m^2-K)^2-sec]	9.45
Interior Lining Thermal Conductivity (kW/m-K)	0.0075
Interior Lining Specific Heat (kJ/kg-K)	0.84
Interior Lining Density (kg/m^3)	1500
Interior Lining Thickness (m)	0.3
Ventilation	
Vent Width (m)	0.7
Vent Height (m)	3
Top of Vent from Floor (m)	3.6
Heat Release Rate	
Fire Heat Release Rate (kW)	3518

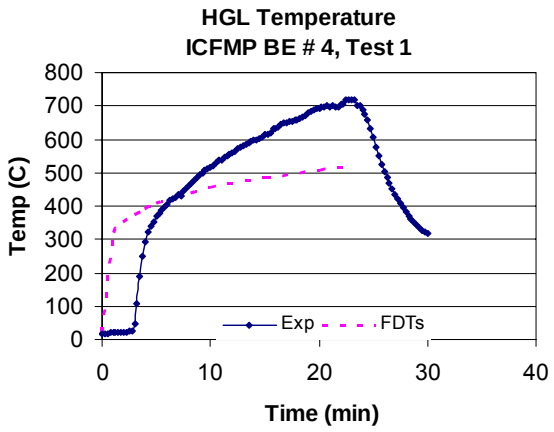

Figure A-6: Hot Gas Layer Temperature, ICFMP BE #4

A.1.4 ICFMP BE # 5

This experiment was conducted in the same compartment as ICFMP BE #4, except the doorway was small, about 1.5m^2 (16ft^2), again with no mechanical ventilation. The spreadsheet in FDT^S used to estimate the HGL temperature for this exercise is 02.1_Temperature_NV.xls. The maximum experimental HRR was input as a steady-state value for the spreadsheet as a conservative assumption. The HRR and other input values can be found in Table A-7.

Table A-7: Input Values for ICFMP BE # 5

Air	
Ambient Air Temperature (C)	20
Ambient Air Density (kg/m^3)	1.2
Room Size	
Compartment Width (m)	3.6
Compartment Length (m)	3.6
Compartment Height (m)	5.7
Wall Properties	
Interior Lining Thermal Inertia [(kW/m^2-K)^2-sec]	9.45
Interior Lining Thermal Conductivity (kW/m-K)	0.0075
Interior Lining Specific Heat (kJ/kg-K)	0.84
Interior Lining Density (kg/m^3)	1500
Interior Lining Thickness (m)	0.3
Ventilation	
Vent Width (m)	0.7
Vent Height (m)	2.2
Top of Vent from Floor (m)	3.6
Heat Release Rate	
Fire Heat Release Rate (kW)	716

Experimental data for HGL Height during this test is not available for comparison.

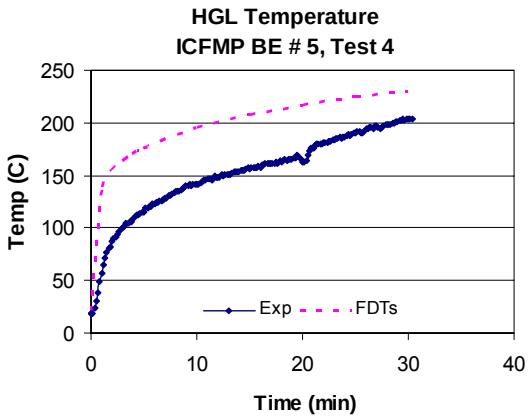

Figure A-7: Hot Gas Layer Temperature, ICFMP BE #5

A.1.5 The FM-SNL Test Series

This test series was conducted in a large closed room with mechanical ventilation. Tests 4 and 21 had a ventilation rate of approximately 0.37 m^3/s (13 ft^3/s), while Test 5 had a ventilation rate of approximately 3.7 m^3/s (131 ft^3/s). The FPA model was used for these tests with forced ventilation (02.2_Temperature_FV.xls). A steady-state HRR of 516 kW based on experimental data was used as input to the spreadsheets. The input values used for these three tests can be found in Table A-8.

Table A-8: Input values for FM/SNL Tests

	Test 4	Test 5	Test 21
Air			
Ambient Air Temperature (C)	20	20	20
Ambient Air Density (kg/m^3)	1.2	1.2	1.2
Room Size			
Compartment Width (m)	12.2	12.2	12.2
Compartment Length (m)	18.3	18.3	18.3
Compartment Height (m)	6.1	6.1	6.1
Wall Properties			
Interior Lining Thermal Inertia [(kW/m^2-K)^2-sec]	0.108	0.108	0.108
Interior Lining Thermal Conductivity (kW/m-K)	0.00012	0.00012	0.00012
Interior Lining Specific Heat (kJ/kg-K)	1.25	1.25	1.25
Interior Lining Density (kg/m^3)	720	720	720
Interior Lining Thickness (m)	0.0127	0.0127	0.0127
Ventilation			
Forced Ventilation Flow Rate (cfm)	800	8000	800
Heat Release Rate			
Fire Heat Release Rate (kW)	516	516	516

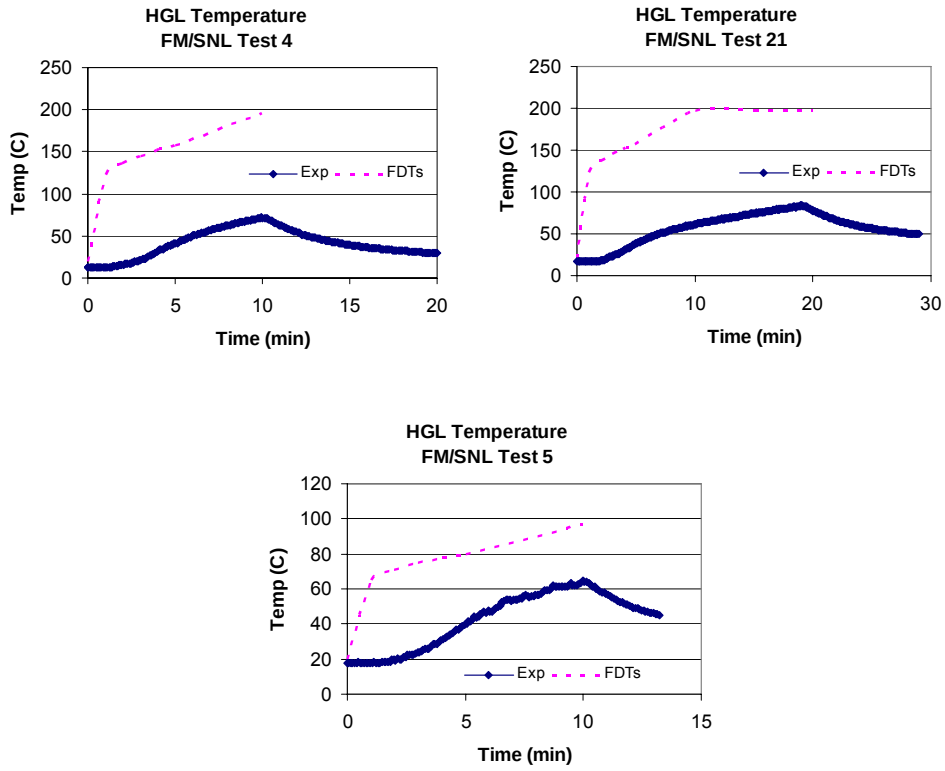

Figure A-8: Hot Gas Layer Temperature, FM/SNL tests

A.1.6 The NBS Test Series

This test series involved a three compartment configuration with two smaller rooms opening off of a long corridor. One of the smaller rooms contained the fire source. All experimental data used to compare with FDT^s came from the fire room because FDT^s does not have the capability to model conditions in rooms other than the fire room. The three tests considered are labeled 100A, 100O and 100Z, respectively. The differences between these three tests concerned ventilation conditions in the corridor. Test 100A involved closed doors from the corridor to the outside and from the corridor to the third room. Test 100O involved an open door from the corridor to the outside and a closed door from the corridor to the third room. Test 100Z involved open doors from the corridor to the outside and from the corridor to the third room. Since all tests involved an open door between the fire room and the corridor, the spreadsheet with the MQH model (02.1_Temperature_NV.xls) was used to estimate HGL temperature for the NBS tests. All three tests used a HRR of 110 kW, based on experimental HRR data. Material properties and other input values can be found in Table A-9.

Table A-9: Input Values for NBS Tests

Air	
Ambient Air Temperature (C)	22.8
Ambient Air Density (kg/m^3)	1.19
Room Size	
Compartment Width (m)	2.34
Compartment Length (m)	2.34
Compartment Height (m)	2.16
Wall Properties	
Interior Lining Thermal Inertia [(kW/m^2-K)^2-sec]	0.012
Interior Lining Thermal Conductivity (kW/m-K)	0.00009
Interior Lining Specific Heat (kJ/kg-K)	1.04
Interior Lining Density (kg/m^3)	128
Interior Lining Thickness (m)	0.05
Ventilation	
Vent Width (m)	0.8
Vent Height (m)	1.6
Top of Vent from Floor (m)	1.6
Heat Release Rate	
Fire Heat Release Rate (kW)	110

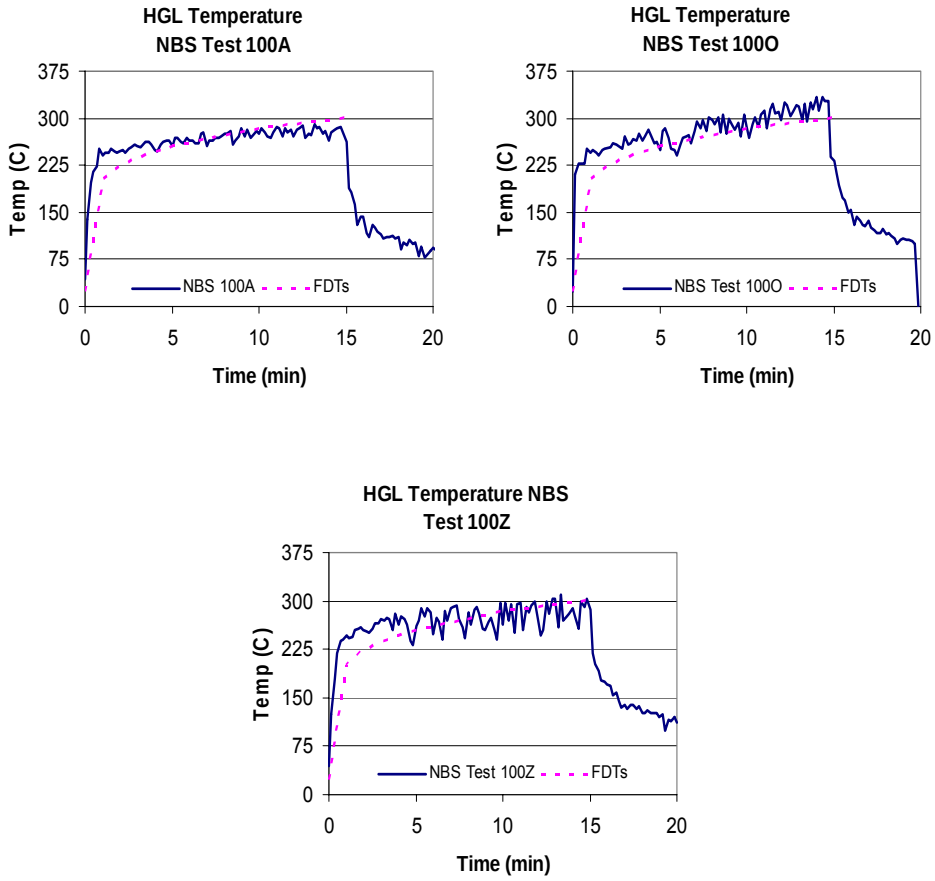

Figure A-9: Hot Gas Layer Temperature, NBS tests

A.1.7 Summary: Hot Gas Layer Temperature and Height

The following chart lists the relative differences between experimental data and model results for HGL temperature. "Δ E" is the difference between the experimental peak and the experimental initial condition. "Δ M" is the difference between model peak and experimental peak. Since FDT^{s} does not have an appropriate calculation method for layer height for the experimental conditions in these tests, no relative differences are given.

Table A-10: Hot Gas Layer Temperature Relative Differences

		Hot Gas Layer Temperature (C)		
		Δ E	Δ M	% Difference
ICFMP BE # 2	Case 1	55	14	**25%**
	Case 2	86	22	**25%**
	Case 3	83	124	**150%**
ICFMP BE # 3	Test 1	123	75	**61%**
	Test 2	229	108	**47%**
	Test 3	207	113	**54%**
	Test 4	204	56	**27%**
	Test 5	175	180 (144)	**103% (82%)**
	Test 7	117	75	**65%**
	Test 8	218	116	**53%**
	Test 9	204	111	**55%**
	Test 10	198	62	**31%**
	Test 13	290	178	**61%**
	Test 14	208	108	**52%**
	Test 15	211	107	**51%**
	Test 16	268	88	**33%**
	Test 17	135	61	**45%**
	Test 18	194	123	**64%**
BE # 4	Test 1	701	-201	**-29%**
BE # 5	Test 4	186	26	**14%**
FM/SNL	Test 4	60	124	**209%**
	Test 5	47	32	**69%**
	Test 21	66	113	**170%**
NBS	Test 1	248	12	**5%**
	Test 2	310	-32	**-10%**
	Test 4	284	-7	**-2%**

A.2 Plume Temperature

Plume temperatures are measured with thermocouple trees above the fire source. The test series that included an arrangement for collecting plume temperature data include ICFMP benchmark exercises number 2, 4, and 5, and FM-SNL. During benchmark exercises 4 and 5, the fire and the plume tilted away from the plume thermocouples, therefore, that data will not be used. The following figures present the experimental observations as well as FDT^S predictions for plume temperature using Heskestad's plume temperature correlation (FDT^S spreadsheet: 09_Plume_Temperature_Calculations.xls).

A.2.1 ICFMP BE # 2

In the experiment, the two thermocouples in the fire plume were located 7 m (23 ft) and 13 m (43 ft) above the fire source, respectively. Heat release rates were calculated from fuel mass loss rates during the experiments, modified by an efficiency factor of 0.85. The convective heat release fraction used was 0.65. The input values for this experiment can be found in Table A-11 while the heat release rates can be found in Table A-12.

Table A-11: Input values for ICFMP BE # 2 Plume Temperature Calculations

	TG1	TG2
Air		
Ambient Air Temperature (C)	20	20
Ambient Air Density (kg/m^3)	1.2	1.2
Fire Characteristics		
Elevation Above the Fire Source (m)	7	13
Area of Combustible Fuel (m^2)	0.5	0.5
Convective Heat Release Rate Fraction (x_c)	0.65	0.65

Table A-12: ICFMP BE #2 Heat Release Rates

Case 1		Case 2		Case 3	
Time (sec)	HRR (kW)	Time (sec)	HRR (kW)	Time (sec)	HRR (kW)
0	0	0	0	0	0
13.2	1251	13.8	2161	13.2	2426
90	1706	30	2540	63	3184
288	1858	91.2	3071	166.2	3601
327	1782	193.2	3260	256.2	3639
409.2	1365	282	3146	292.2	3450
438	0	340.2	2729	330	2654
		372	2275	345	0
		394.8	0		

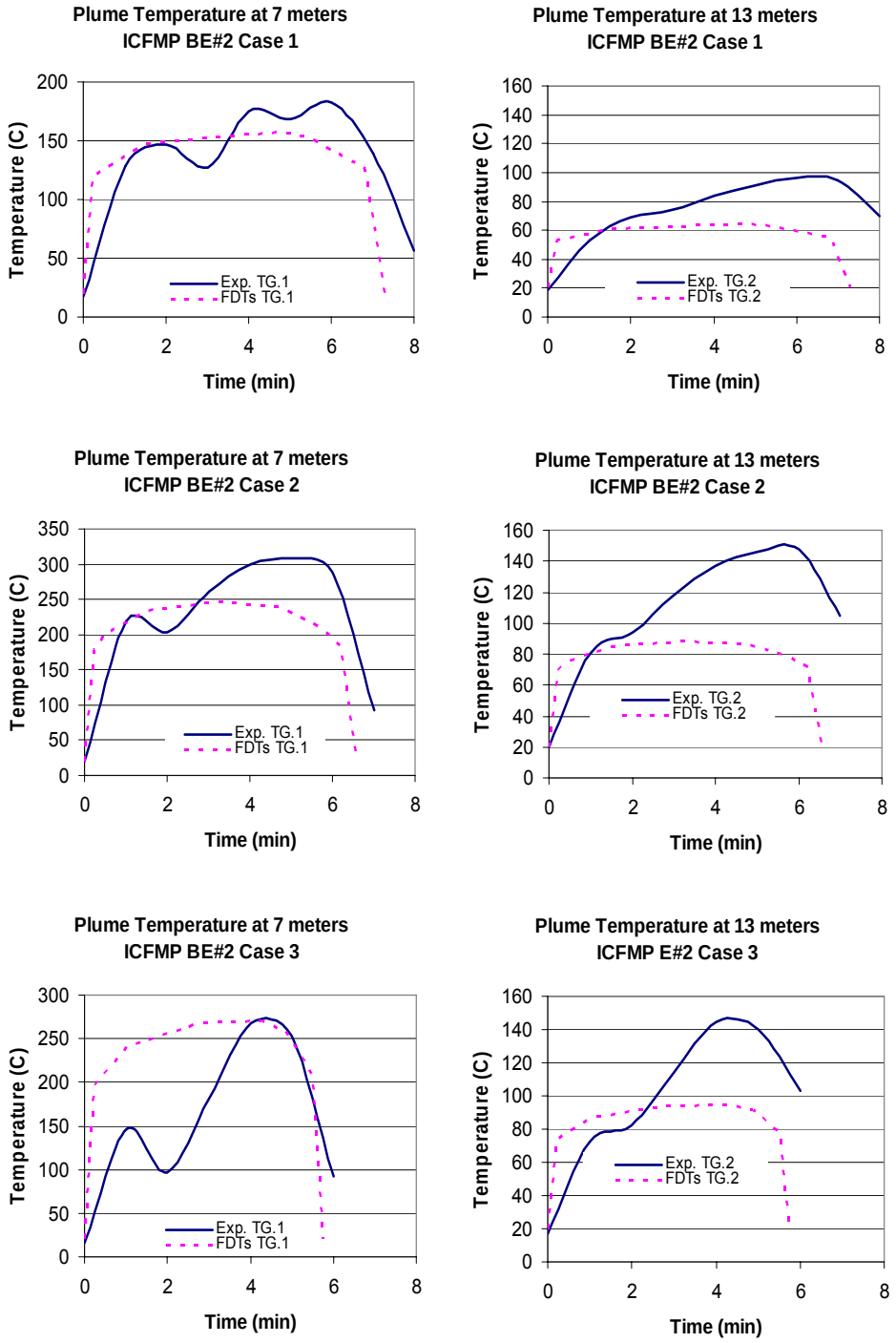

Figure A-10: Plume Temperature, ICFMP BE #2, Cases 1, 2, and 3

A.2.2 The FM-SNL Test Series

The thermocouple for measuring plume temperatures was located 5.66 m (18.6 ft) above the base of the fire, approximately 5.95 m (19.5 ft) above the floor. The HRRs used as inputs were calculated using a t^2 curve with a peak of 516 kW, which matches the experimental data. The

convective heat release fraction used was 0.65. Additional input values can be found in Table A-13.

Table A-13: Input values for FM/SNL Tests Plume Temperature Calculations

Air	
Ambient Air Temperature (C)	20
Ambient Air Density (kg/m^3)	1.2
Fire Characteristics	
Elevation Above the Fire Source (m)	5.66
Area of Combustible Fuel (m^2)	0.17
Convective Heat Release Rate Fraction (x_c)	0.65

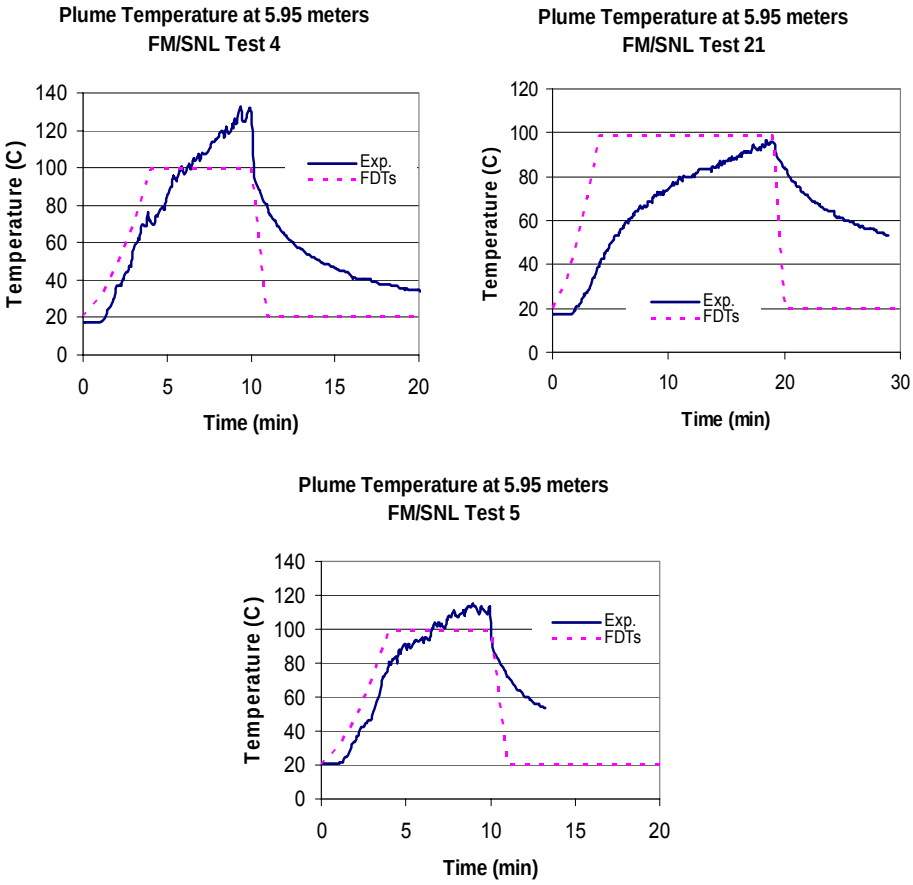

Figure A-11: Plume Temperature, FM/SNL tests

A.2.3 Summary: Plume Temperature

The following chart lists the relative differences between experimental data and model results for plume temperature. "Δ E" is the difference between the experimental peak and the experimental initial condition. "Δ M" is the difference between model peak and experimental peak.

Table A-14: Plume Temperature Relative Differences

			Plume Temperature (C)		
		Sensor	Δ E	Δ M	% Difference
ICFMP BE # 2	Case 1	TG1	166	-25	**-15%**
		TG2	77	-32	**-41%**
	Case 2	TG1	288	-62	**-22%**
		TG2	128	-60	**-47%**
	Case 3	TG1	252	2	**1%**
		TG2	128	-51	**-40%**
FM/SNL	Test 4	5.66 m above fire	116	-34	**-29%**
	Test 5	5.66 m above fire	94	-16	**-17%**
	Test 21	5.66 m above fire	79	3	**4%**

A.3 Flame Height

Flame height is recorded by visual observations, photographs or video footage. Photographs from the ICFMP BE #2 test series and video from BE #3 test series are available. It is difficult to precisely measure the flame height, but the photos and videos allow one to make estimates accurate to within a pan diameter. Such observations can be compared with outputs from Heskestad's flame height correlation. Although no accuracy can be calculated, this comparison may provide insights about the capabilities and limitations of the model. The spreadsheet in FDT^S used to calculate the flame height was 03_HRR_Flame_Height_Burning_Duration_Calculations.xls.

A.3.1 ICFMP BE # 2

Figure 1 contains photographs of the actual fire. The height of the visible flame in the photographs has been estimated to be between 2.4 and 3 pan diameters (3.8 m (12.5 ft) to 4.8 m (15.7 ft)). Using Heskestad's method for estimating the height of a pool fire flame FDTs estimated flame height to be 4.3 m (14.1 ft).

Figure A-12: Photographs of heptane pan fires, ICFMP BE #2, Case 2. Courtesy, Simo Hostikka, VTT Building and Transport, Espoo, Finland.

A.3.1 ICFMP BE # 3

No measurements were made of the flame height during BE #3, but numerous photographs were taken through the 2 m by 2 m doorway. Figure 2 is one of these photographs. During BE #3, Test 3, the peak flame height is estimated to be 2.8 m, roughly consistent with the view through the

doorway in the figure below. FDT^S results in a flame height of 3.0 m (9.8 ft) using Heskestad's flame height prediction.

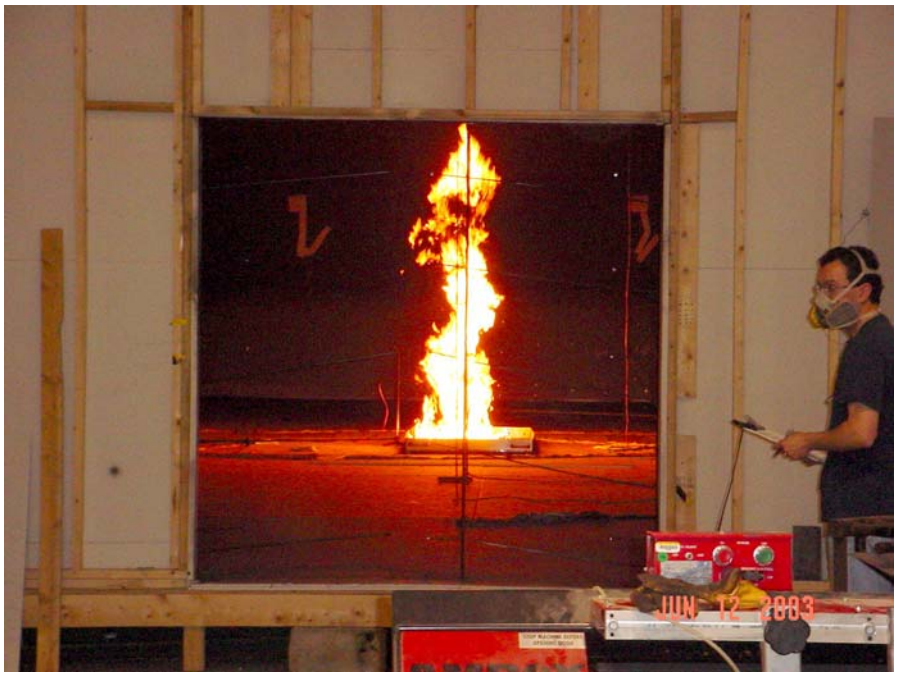

Figure A-13: Photograph and simulation of ICFMP BE #3, Test 3, as seen through the 2 m by 2 m doorway. Photo courtesy of Francisco Joglar, SAIC.

A.4 Target Heat Flux

A.4.1 ICFMP BE #3

The experimental results for radiant heat flux were obtained from Benchmark Exercise #3. The spreadsheet in FDT^S used to calculate the radiant heat flux is 05.1_Heat_Flux_Calculations_Wind_Free.xls. The Point Source Radiation model was used. The heat flux measurements were taken using ten different gauges located at varying distances from the fire. Five gauges measured total heat flux, and five measured radiant heat flux. Since FDT^s calculates radiant heat flux, just that data was compared. Also, one of the five radiant heat flux gauges was oriented in the horizontal direction and not with the proposed targets, so that data will not be compared.

The heat release rates used as inputs are listed in Table A-3, Table A-4, and Table A-5 and are consistent with the experimental measurements of HRR. The radiation fraction for all tests except test 17 was 0.44. The radiation fraction used for test 17 was 0.40. The following table lists the distances to targets for each test. The position of the fire was different for three of the fifteen tests in BE #3, so the distances to targets are different for those tests.

Table A-15: Distance from Fire to Radiant Heat Flux Gauges, meters

Gauge	Test 14	Test 15	Test 18	All Others
1	5.23	2.20	2.78	4.07
3	4.73	2.52	2.96	3.39
7	4.45	3.13	3.43	3.40
10	2.38	5.87	5.77	3.77

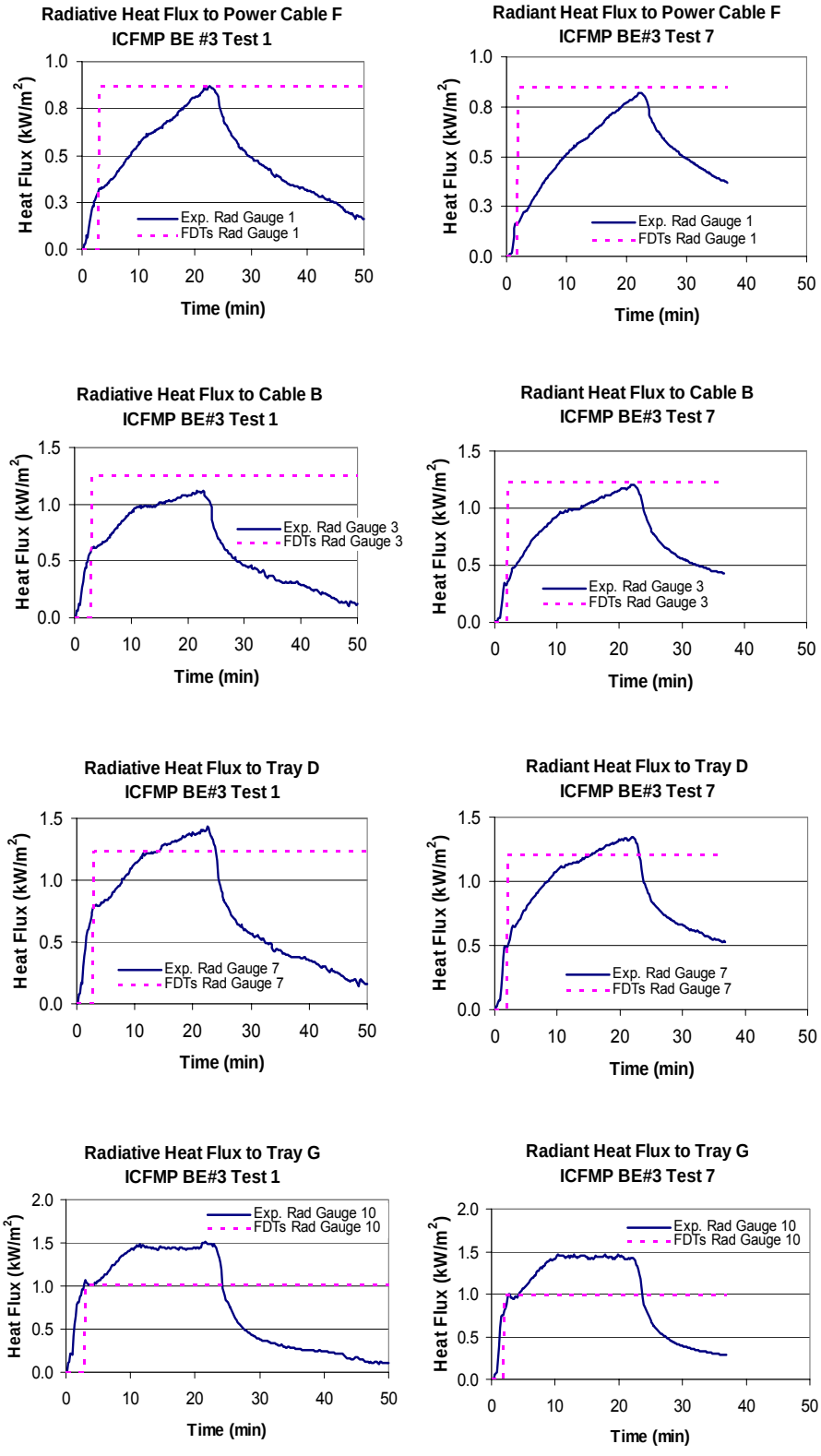

Figure A-14: Radiant Heat Flux, ICFMP BE #3, Tests 1 and 7

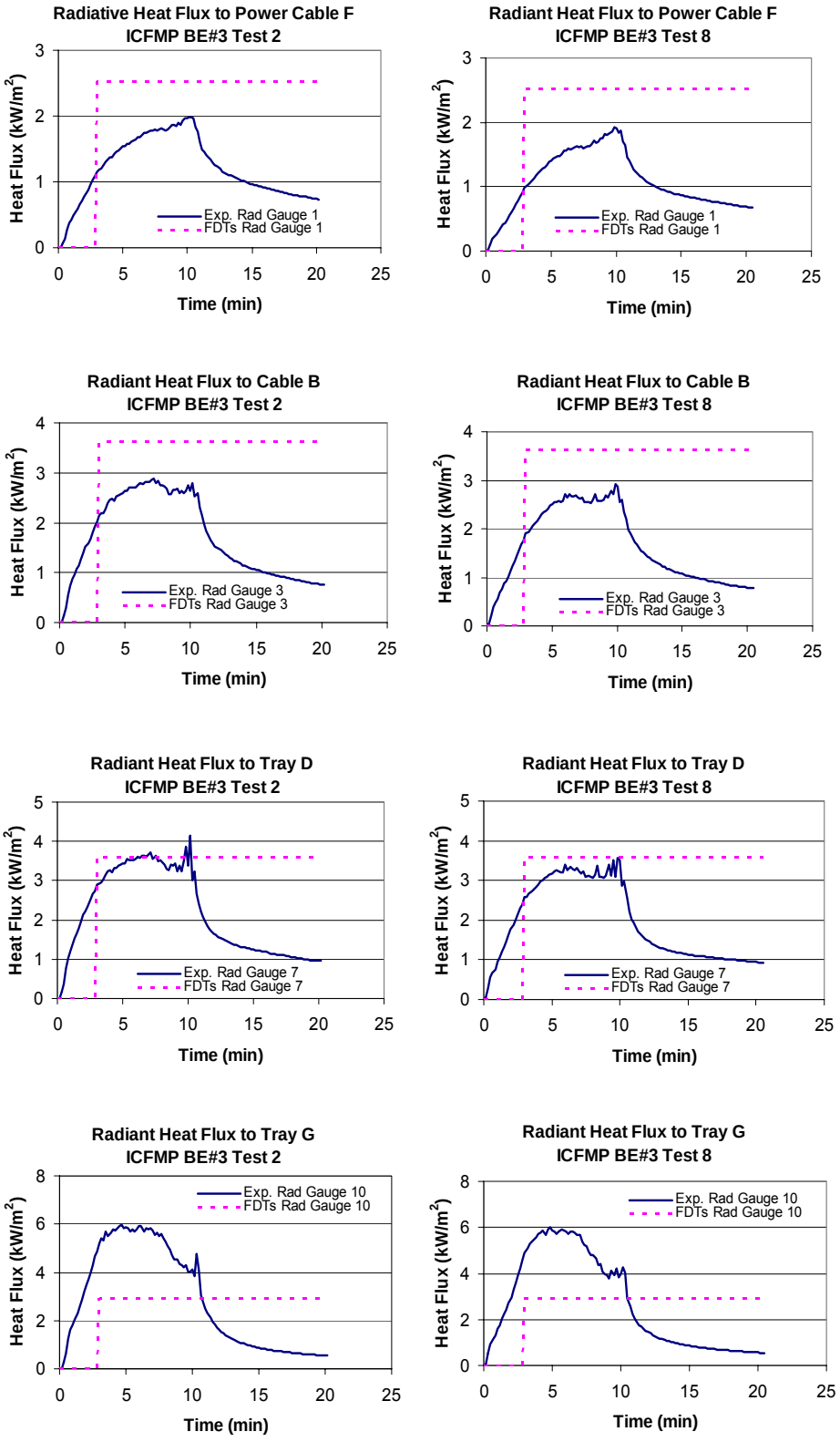

Figure A-15: Radiant Heat Flux, ICFMP BE #3, Tests 2 and 8

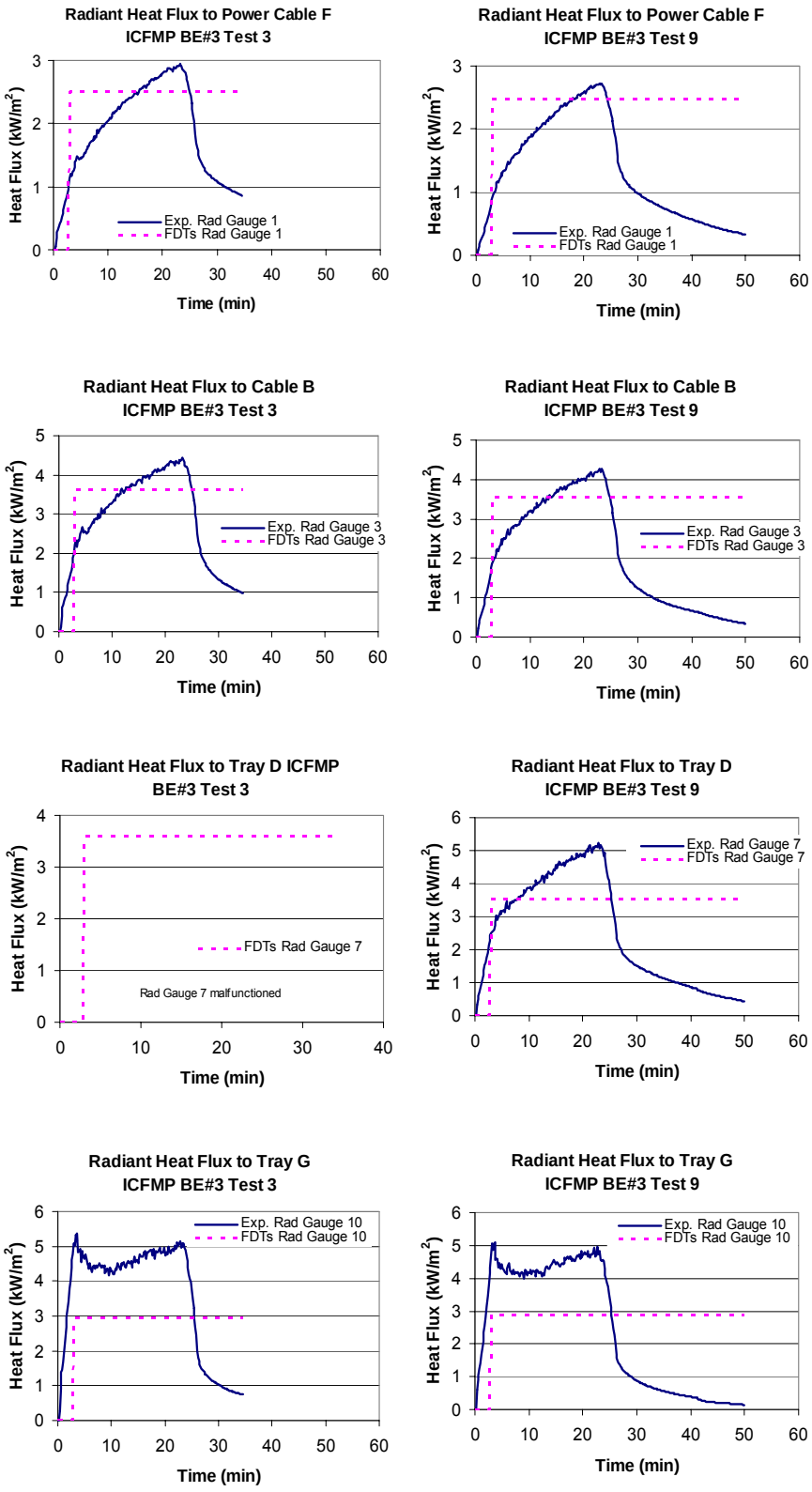

Figure A-16: Radiant Heat Flux, ICFMP BE #3, Tests 3 and 9

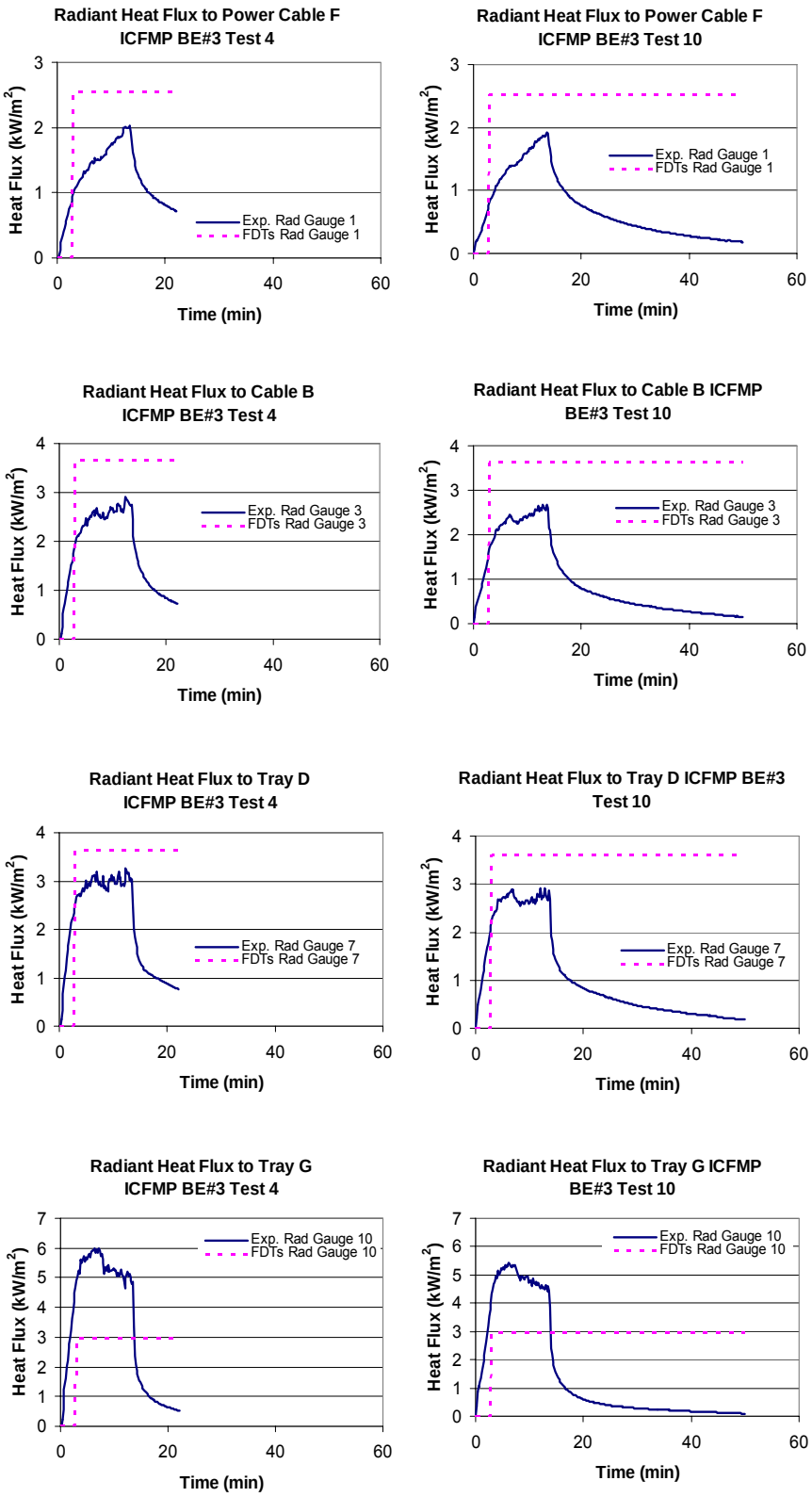

Figure A-17: Radiant Heat Flux, ICFMP BE #3, Tests 4 and 10

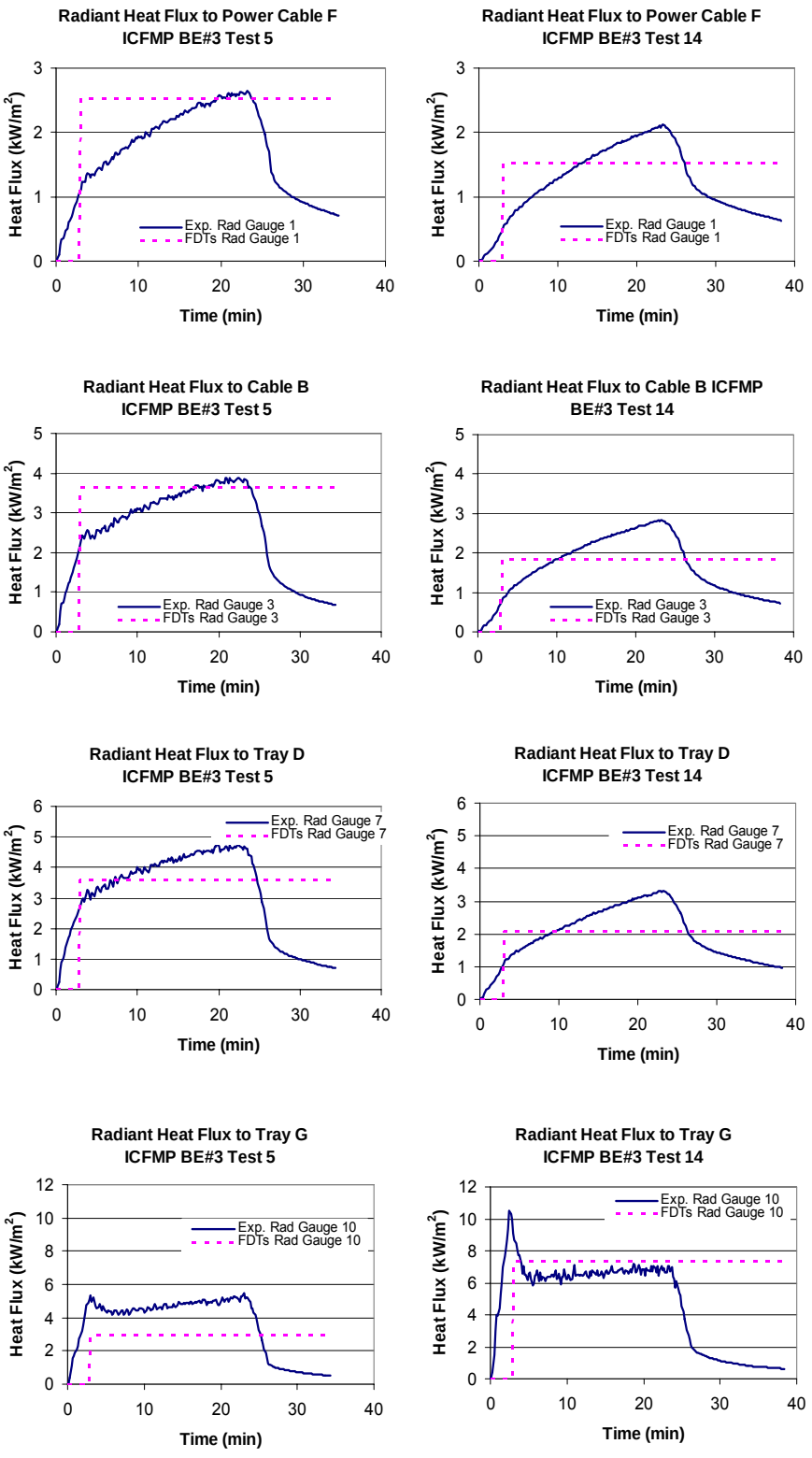

Figure A-18: Radiant Heat Flux, ICFMP BE #3, Tests 5 and 14

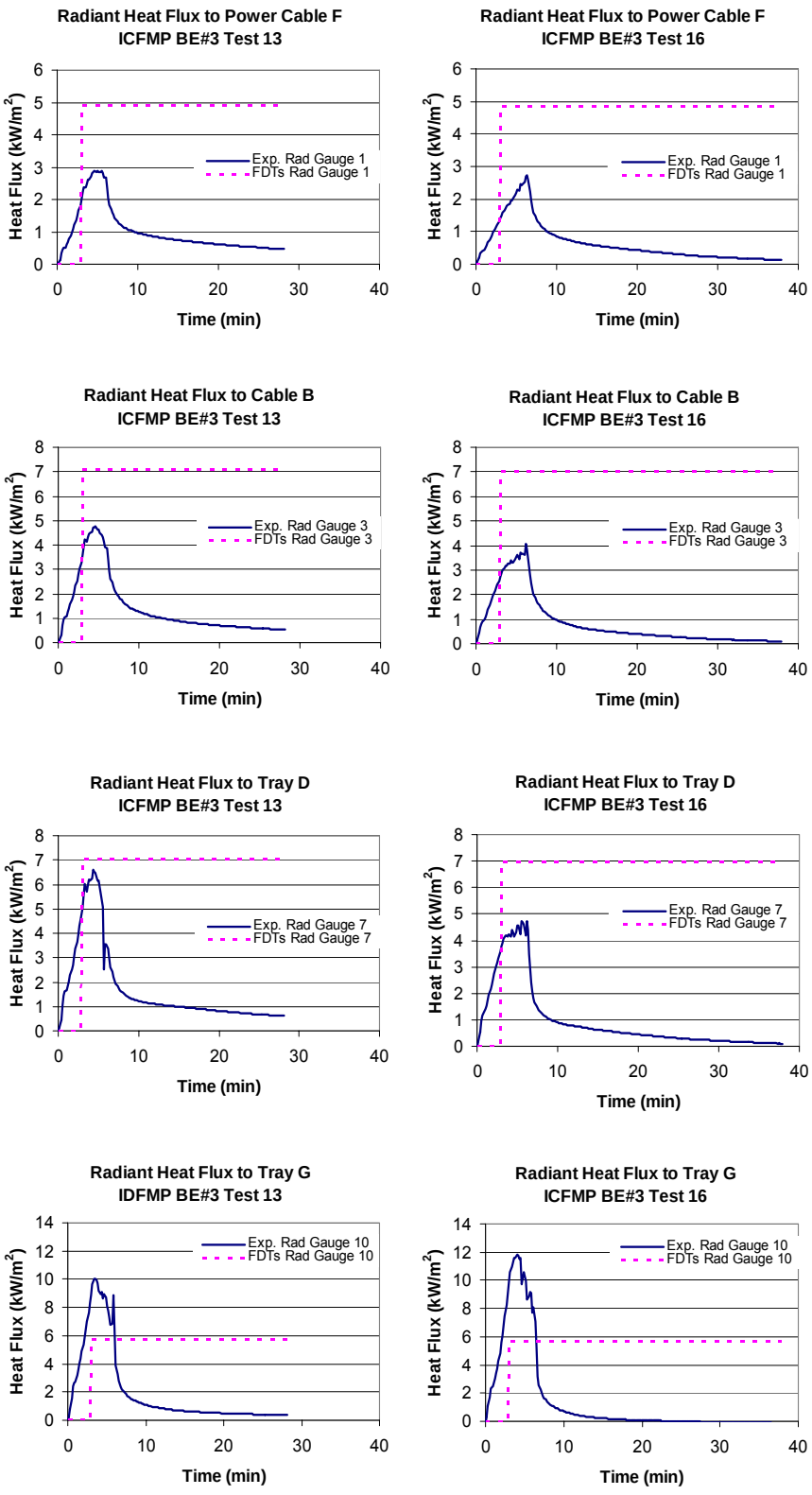

Figure A-19: Radiant Heat Flux, ICFMP BE #3, Tests 5 and 14

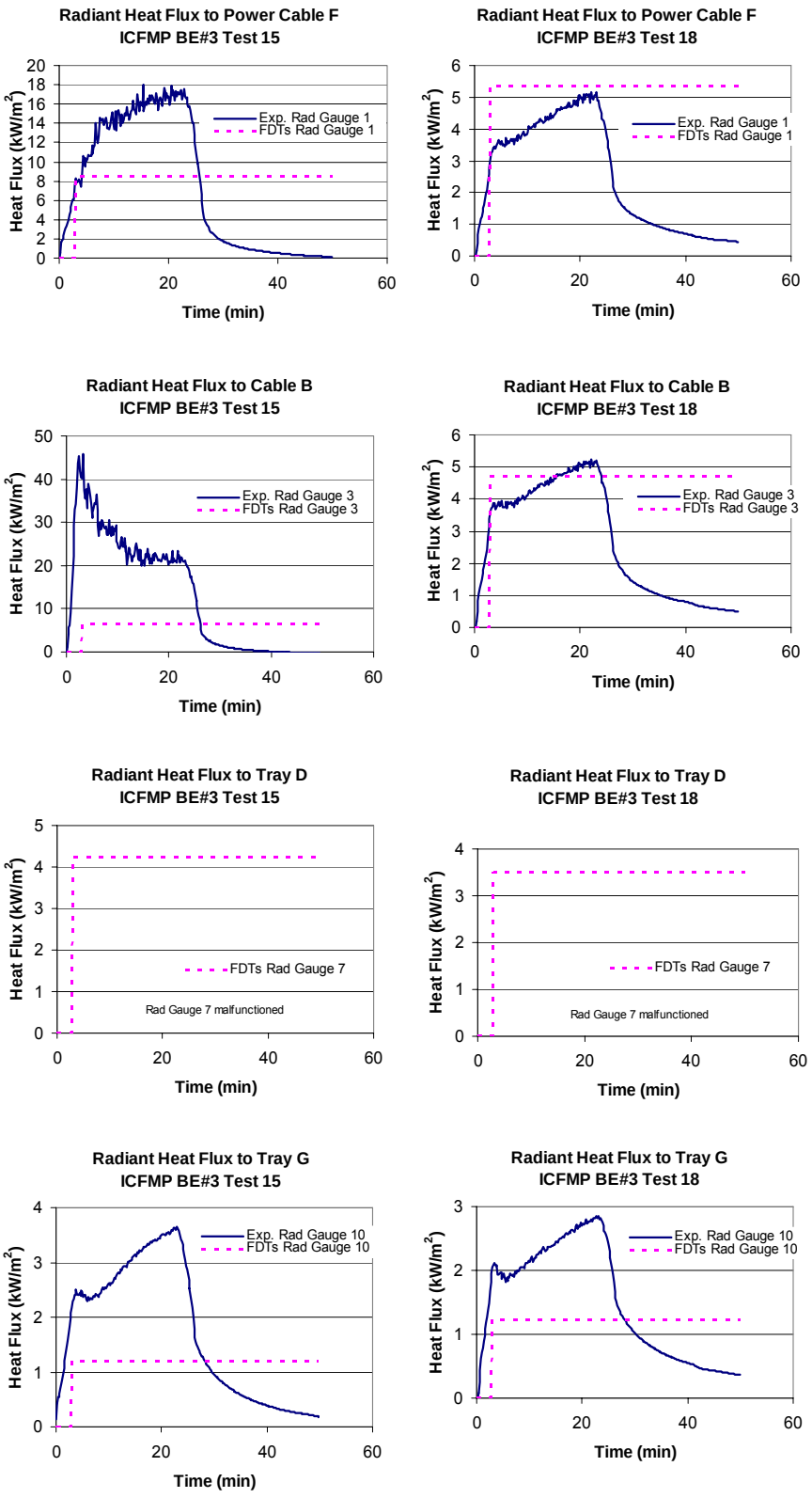

Figure A-20: Radiant Heat Flux, ICFMP BE #3, Tests 15 and 18

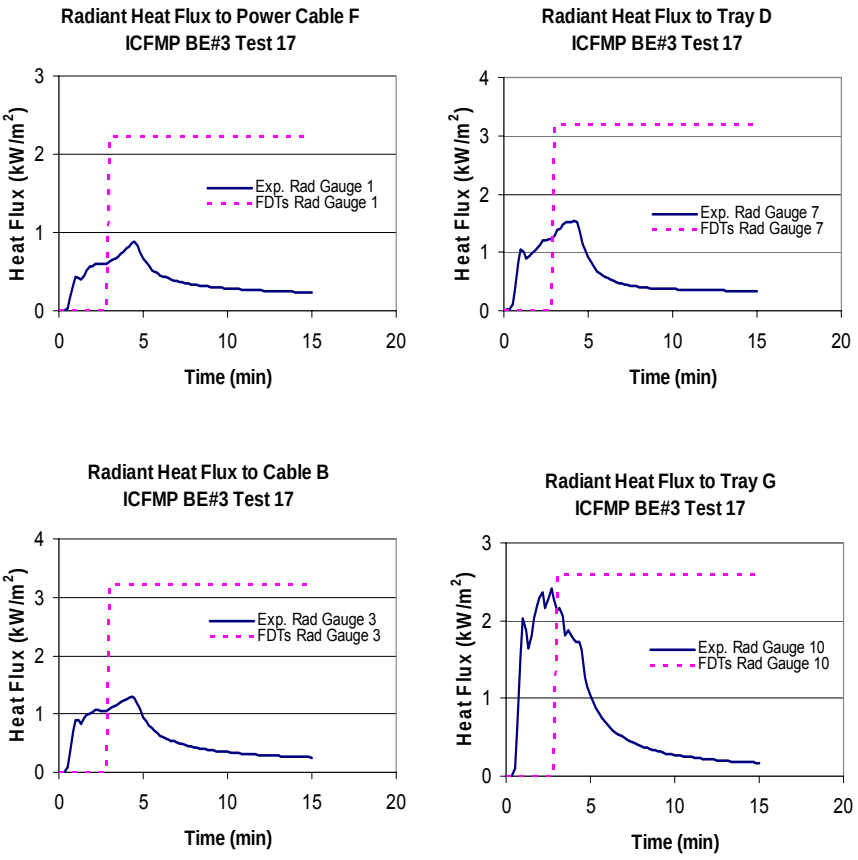

Figure A-21: Radiant Heat Flux, ICFMP BE #3, Test 17

A.4.2 Summary: Radiant Heat Flux

The following chart lists the relative differences between experimental data and model results for radiant heat flux. "Δ E" is the difference between the experimental peak and the experimental initial condition. "Δ M" is the difference between model peak and experimental peak.

Table A-16: Relative Differences, Radiant Heat Flux

BE # 3	Sensor	Radiant Heat Flux (kW/m^2)		
		Δ E	Δ M	% Difference
Test 1	Gauge 1	0.87	0.00	**0%**
	Gauge 3	1.12	0.13	**12%**
	Gauge 7	1.43	-0.19	**-13%**
	Gauge 10	1.51	-0.50	**-33%**
Test 2	Gauge 1	1.99	0.53	**27%**
	Gauge 3	2.88	0.75	**26%**
	Gauge 7	4.16	-0.56	**-13%**
	Gauge 10	5.97	-3.04	**-51%**
Test 3	Gauge 1	2.95	-0.43	**-15%**
	Gauge 3	4.45	-0.82	**-18%**
	Gauge 7			

BE # 3	Sensor	Radiant Heat Flux (kW/m^2)		
		Δ E	Δ M	% Difference
	Gauge 10	5.36	-2.43	**-45%**
	Gauge 1	2.02	0.52	**26%**
	Gauge 3	2.92	0.74	**25%**
	Gauge 7	3.26	0.37	**11%**
Test 4	Gauge 10	6.00	-3.04	**-51%**
	Gauge 1	2.65	-0.13	**-5%**
	Gauge 3	3.88	-0.25	**-7%**
	Gauge 7	4.78	-1.18	**-25%**
Test 5	Gauge 10	5.45	-2.52	**-46%**
	Gauge 1	0.82	0.03	**4%**
	Gauge 3	1.21	0.01	**1%**
	Gauge 7	1.35	-0.14	**-10%**
Test 7	Gauge 10	1.47	-0.48	**-33%**
	Gauge 1	1.93	0.59	**30%**
	Gauge 3	2.92	0.71	**25%**
	Gauge 7	3.56	0.04	**1%**
Test 8	Gauge 10	6.02	-3.09	**-51%**
	Gauge 1	2.72	-0.25	**-9%**
	Gauge 3	4.27	-0.71	**-17%**
	Gauge 7	5.23	-1.69	**-32%**
Test 9	Gauge 10	5.10	-2.22	**-44%**
	Gauge 1	1.92	0.60	**31%**
	Gauge 3	2.68	0.95	**36%**
	Gauge 7	2.91	0.69	**24%**
Test 10	Gauge 10	5.42	-2.49	**-46%**
	Gauge 1	2.90	2.03	**70%**
	Gauge 3	4.77	2.33	**49%**
	Gauge 7	6.58	0.48	**7%**
Test 13	Gauge 10	10.06	-4.32	**-43%**
	Gauge 1	2.12	-0.60	**-28%**
	Gauge 3	2.84	-0.99	**-35%**
	Gauge 7	3.32	-1.23	**-37%**
Test 14	Gauge 10	10.50	-3.21	**-31%**
	Gauge 1	18.02	-9.48	**-53%**
	Gauge 3	45.88	-39.37	**-86%**
	Gauge 7			
Test 15	Gauge 10	3.65	-2.45	**-67%**
	Gauge 1	2.73	2.13	**78%**
	Gauge 3	4.05	2.96	**73%**
	Gauge 7	4.74	2.23	**47%**
Test 16	Gauge 10	11.79	-6.12	**-52%**
	Gauge 1	0.88	1.35	**153%**
	Gauge 3	1.30	1.91	**147%**
	Gauge 7	1.53	1.66	**108%**
Test 17	Gauge 10	2.42	0.18	**8%**
Test 18	Gauge 1	5.18	0.17	**3%**

BE # 3	Sensor	Radiant Heat Flux (kW/m^2)		
		Δ E	Δ M	% Difference
	Gauge 3	5.24	-0.52	**-10%**
	Gauge 7			
	Gauge 10	2.84	-1.60	**-56%**